# UNIVERSITY OF AGDER

# Parametric study and optimization of turret and mooring line connections

## Detailed analyses of the connecting link including advanced numerical modeling

**Stine Gabestad Kristiansen**

**Supervisors**

Katalin Vértes

Kurt Jørgensen Furre

University of Agder, 2015

Faculty of Engineering and Science

Department of Engineering Sciences

Confidential

# Preface

This master's thesis concludes the Master Degree program of Civil Engineering at the University of Agder (UiA). The thesis has been carried out from January to May 2015 in cooperation with National Oilwell Varco (NOV). The topic for the thesis is optimization of turret and mooring connections performed by advanced numerical modeling.

First of all I would like to thank NOV for giving me the opportunity to write a thesis based on a real problem they wanted to look further into. Knowing that the thesis is useful and helpful for NOV have given me an extra "drive" when proceeding in the work with the thesis. I would also like to thank NOV for providing me with a computer and license to ANSYS and other relevant computer programs to conduct my master's thesis.

Second of all I would like to thank my supervisor Katalin Vértes. Apart from the scheduled appointments, the door has always been open for consultation regarding the master's thesis, especially with ANSYS. The modeling and analyses has been quite challenging, but thanks to Katalin the problems have been solved.

From NOV I would like to thank Kurt Jørgensen Furre for sending documentation and information, and the regular follow-up meetings, so that the master's thesis has been proceeding in the right direction. I would also like to thank Sankar Arughadhoss for the help regarding the fatigue analysis, and Knut Morten Johansen for discussions during our follow-up meetings.

Last but not least, I would like to thank Ketil Bingslien, Åge Bjørn Kristiansen, Britt Gabestad Kristiansen and fellow students for help and support during this period.


Grimstad, 26.05.2015

Stine Gabestad Kristiansen


*Stine Gabestad Kristiansen*
_____

# Abstract

The basis of the Submerged Turret Loading (STL) system is formed by a buoy moored to the seabed. The buoy is the connection between the vessel and the mooring system. An important component in the STL system is the connection between the mooring line and the buoy, and this is the connecting link.

The task given by NOV is an optimization of the connecting link. The problem statement leads to following research questions:

1. *How does an optimization affect the connecting link, regarding strength and fatigue analysis?*
2. *What benefits leads an optimization of the connecting link to?*
3. *Which rules and regulations should be taken into account when changing the connecting link from a structural component to a mooring component, and what are the differences in the requirements?*

The master's thesis is performed by using finite element software as well as analytical calculations. The final shape of the connecting link was approached through analyses in ANSYS, to find the stress distribution and deformation, and analytical calculations by performing design checks according to DNVs standards.

The optimized connecting link achieved higher utilization regarding the strength analysis, and it has sufficient strength with respect to fatigue. By reducing the size it is possible to save costs and weight since you will need smaller amounts of steel to produce a connecting link. When looking at the connecting link as a mooring component, DNV-OS-E302 and DNV-OS-E304 are the most relevant offshore standards. It seems like the requirement of 5% max allowable plastic strain is inevitable, and the connecting link must be checked according to this requirement.

# Table of Content

## List of Figures

# List of Tables

# Abbreviations

| | |
|---|---|
| ALS | Accidental Limit State |
| APL | Advanced Production and Loading |
| DNV | Det Norske Veritas |
| DFF | Design Fatigue Factor (PFL/TSL) |
| DOF | Degree of Freedom |
| FE | Finite Element |
| FSU | Floating Storage Unit |
| HS | Hot Spot |
| LRFD | Load and Resistance Factor Design |
| MBL | Minimum Breaking Load |
| MTF | Mechanical Transfer Function |
| PFL | Predicted Fatigue Life |
| OOP | Out of plane |
| SCF | Stress Concentration Factor |
| STL | Submerged Turret Loading |
| TSL | Target Service Life |
| ULS | Ultimate Limit State |

# 1 Introduction

## 1.1 Background

National Oilwell Varco (NOV) wanted to optimize an important component in the Submerged Turret Loading (STL) mooring system they are currently using, and this component is called a connecting link. The background for the master's thesis is therefore a wish for looking into the possibilities for optimizing the connecting link. In Figure 1.1 an illustration of the arrangement between the different parts in a mooring system is shown. The connecting link is the connection point between the "Diconnectable Turret" and "Mooring systems", which is pointed out in the illustration. More information about the connecting link will be presented in Chapter 2.
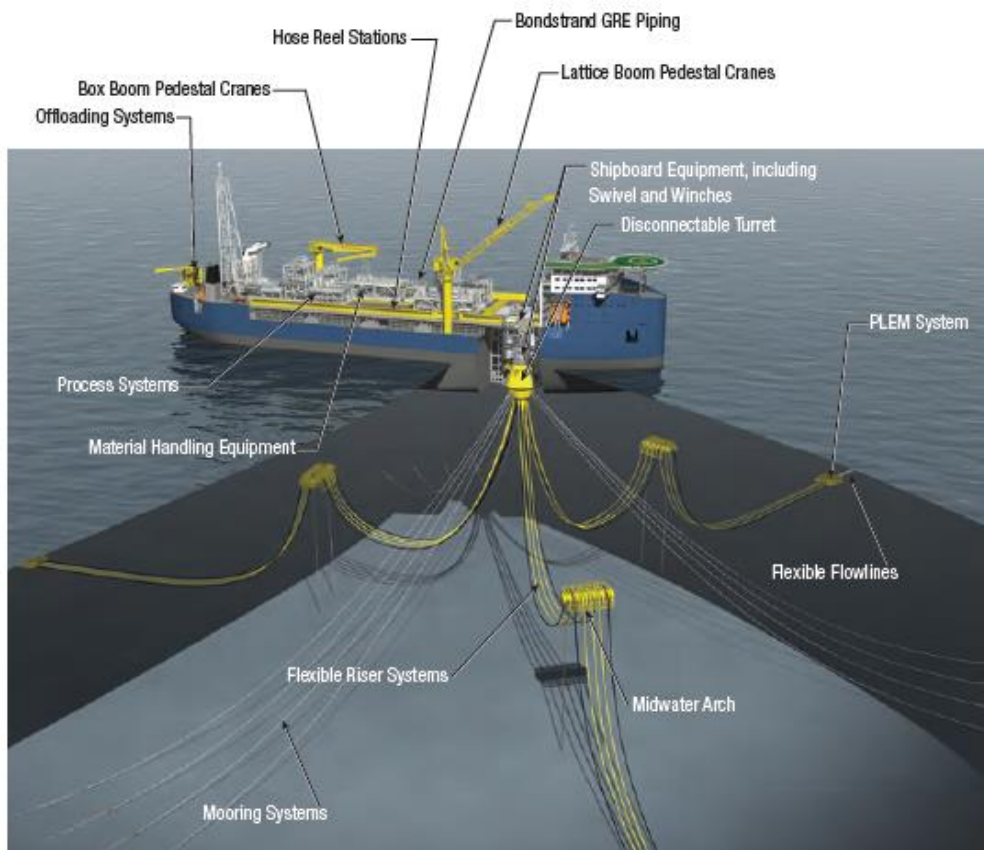


**Figure 1.1: The arrangement between the different parts in a mooring system.**

Three different oil and gas fields, called Heidrun, Gina Krog and Mariner will be of interest in this master's thesis, and the given documentation for the three projects will form the basis for the required data to conduct the optimization of the connecting link.

## 1.2 Approach to the Problem and Research Questions

According to the available calculations the connecting links are at the moment conservative, which is why the company thinks that an optimization of the connecting links is necessary.

The loads are given for the connecting link and by optimizing the geometry it might be possible to get a better utilization. By reducing the size it is possible to save costs and weight since you will need smaller amounts of steel to produce a connecting link. This will affect not only the connecting link, but all the main parts like the buoy, the locking mechanism located at the vessel and many other things related to the connecting link. The company now looks at the connecting link as a structural component, but they want to change it from a structural component to a mooring component. That implies the application of different standards and in that way different requirements may be considered. As pointed out earlier; in Chapter 2 the connecting link will be presented in detail. The approach to the problem leads to following research questions:

1. *How does an optimization affect the connecting link, regarding strength and fatigue analysis?*
2. *What benefits leads an optimization of the connecting link to?*
3. *Which rules and regulations should be taken into account when changing the connecting link from a structural component to a mooring component, and what are the differences in the requirements?*

## 1.3 The Company

Advanced Production and Loading (APL™) became a part of National Oilwell Varco (NOV) in December of 2010. The objective of establishing APL was to develop and exploit the Submerged Turret Loading (STL™) and Submerged Turret Production (STP™) mooring system. The technology from these mooring systems is still an essential part of APL's product offerings, but it has been extended to moor customer units in any situation. APL has therefore become one of the world's leading mooring providers for offshore oil and gas production and transfer. (National Oilwell Varco, 2014a).

NOV's company structure is divided into three: NOV Rig Systems, NOV Wellbore Technologies and NOV Completion & Production Solutions. APL is a part of NOV Completion & Production Solutions, and this master's thesis is based on a given task description from APL. NOV Completion & Production Solutions main expertise is to "[…] serve well intervention service providers and oil and gas producers, and pursue opportunities around hydraulic fracture stimulation, wellbore intervention equipment, composite tubulars, pumps, floating production systems and subsea production technologies" (National Oilwell Varco, 2015a).

## 1.4    The Master's Thesis Limitations

The optimization was done to connecting link type 1 shown in Figure 1.2 below. The loads and material grade was also given by NOV, see Chapter 6.
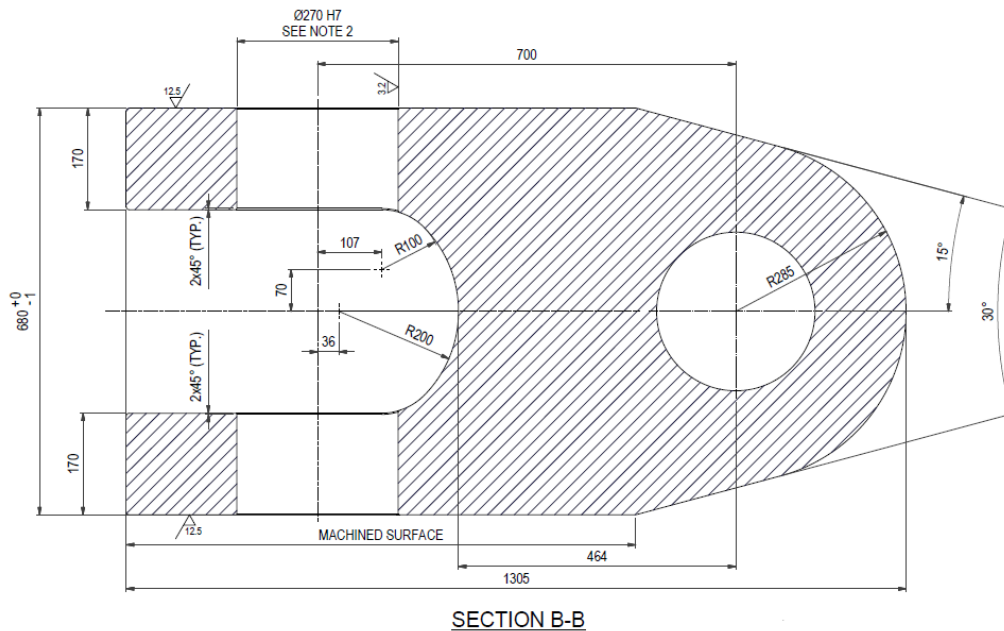


**Figure 1.2: The geometry of the original connecting link (National Oilwell Varco, 2014e), ref. Appendix A.**

The optimization was limited by several fixed geometrical data of the connecting link. The diameter of the three pin holes was fixed, and the length from pin hole to pin hole was fixed at 700 mm. The width between the endpoint on top of the two oval heads was also fixed at 680 mm. These measurements are shown in Figure 1.2 above. The two pin holes of the connecting link are connected to the turret, and the single hole is connected to the mooring line through a socket (ref. Figure 1.1). This is why the length and width limitations must be considered when optimizing the connecting link. Except for these limitations the rest of the geometry was changeable.

## 1.5    The Master's Thesis Structure

| Chapter | Overview |
|---|---|
| 1 Introduction | The master's thesis introduction with the background for the thesis, approach to the problem and research questions, about the company and the master's thesis limitations. |
| 2 The Connecting Link | About the connecting link in detail and the scope given by the company. |

| | |
|---|---|
| 3 Theory | The master's thesis is based on the basic theory regarding ANSYS, Finite Element Method, von Mises yield criterion, tension elements, stress concentrations, contact stresses, fatigue, design optimization, rules and regulations and LRFD method. |
| 4 Method | The approach of the master's thesis and how it has been conducted. |
| 5 Optimization of the Connecting Link | The five suggestions for the optimization of the connecting link is presented in tables, showing the different changes of the connecting link, both in figure and text. |
| 6 Initial Data | Material properties, design principles and mooring loads are given by NOV and presented in this chapter. |
| 7 ANSYS Model | The modeling in ANSYS is presented in different steps, with detailed information about how the modeling is performed in this master's thesis. |
| 8 Results and Analysis | The results from the suggestions for the optimization of the connecting link and combination of the five suggestions into one final model. The MBL, ULS, fatigue and bearing wear assessment of the new connecting link without lugs, washers and rings. Drawings of the new connecting link. Comparison between the MBL and ULS results for the new connecting link without lugs, with the new connecting link with lugs. Structural component vs. mooring component |
| 9 Conclusions | The conclusions are based on the approach to the problem and research questions given in the introduction. Further work is also presented. |

All of the results are shown in the appendices in the end of the master's thesis.

## 2 The Connecting Link

This chapter introduces the subject of the master's thesis, which is the connecting link. Details about the connecting link and the scope regarding the connecting link is in the following presented.

### 2.1 Introduction

A picture of a buoy and the attached connecting links (red ring) is shown in Figure 2.1 below. This illustrates where the connecting links are in proportion to the buoy. Comparing the connecting links to the men in the picture, they are bigger than imagined. The company has developed different kinds of buoys over the years. In Section 1.1, the disonnectable turret was highlighted. The disconnetable turret is a part of the buoy, which means that the buoy is located inside of the vessel, when it is connected.
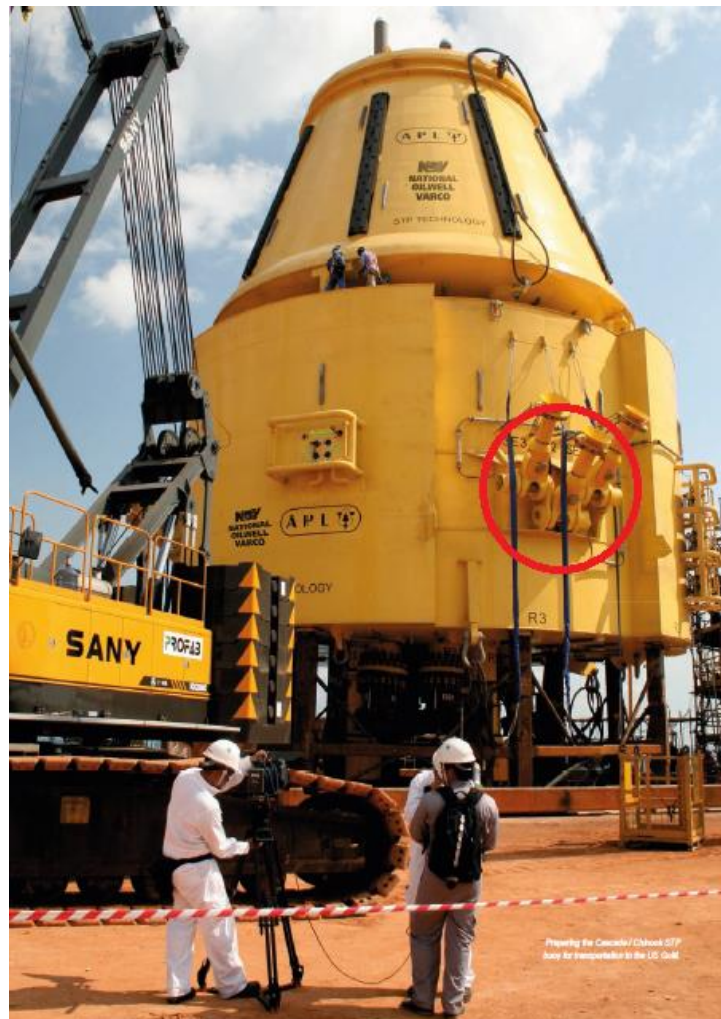


**Figure 2.1: A buoy and the attached connecting links.**

For this master's thesis the buoy of interest is the Submerged Turret Loading (STL) buoy. The basis of the STL system is formed by a buoy moored to the seabed. The buoy is the

connection between the vessel (Floating Storage Unit) and the mooring system. A turret structure is located in the middle of the buoy, which is connected to the mooring and the risers. This allows the vessel to weathervane. Gas and oil are transferred from the seabed to the vessel through the risers. Another important component in the STL system is the connection between the mooring line and the buoy, which is the connecting link. The mooring line contains the chain segment and wire segment as shown in Figure 2.2 below. The figure also shows that the connecting link is the component between the mooring line and the turret located inside the buoy.



**Figure 2.2: Flexible mooring system (National Oilwell Varco, 2014d, pp. 4-5).**

## 2.2 Details about the Connecting Link

The mooring lines are attached to the turret structure through the turret connections. The turret connections consist of the following main components and are shown in Figure 2.3 below:

- Connecting Link
- Link pin
- Locking Disc
- Locking Disc Bolts
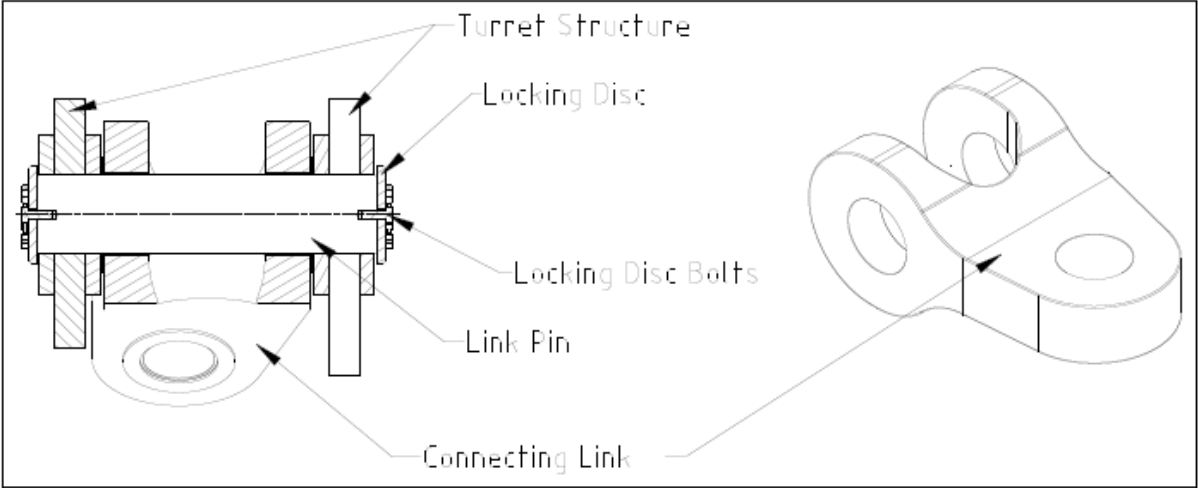


**Figure 2.3: Typical turret connection (National Oilwell Varco, 2014c, p. 10).**

The connecting link is the connecting point for the mooring lines to the turret. In this case, the turret connections consist of one type connecting link. The link allows the mooring line to

rotate in two planes, i.e. no severe moments are induced into the turret connections by the movement of the line. However, transverse forces from the mooring line tension will induce some bending moment due to distance between the bearings in the connecting link. Transverse forces will be induced if the mooring lines are acting on the turret with a horizontal angle. This angle is caused due to a static geometrical change (for large offsets), a dynamic part due to vessel motion and a part caused by friction in the turret bearings and the swivel system. This friction causes a "slip" angle of the turret, which is defined as the horizontal angle all mooring lines have relative to their nominal direction when the turret starts sliding. The maximum angle before the friction in the turret bearing is overcome and the turret rotates is called the "slip angle". For the purpose of documenting the connecting links, a 5° angle is considered. (National Oilwell Varco, 2014c, p. 9) (National Oilwell Varco, 2015b, p. 12). Figure 2.4 below shows the inside of a STL buoy. The location of the connecting link and the shape is also shown (red ring). The connecting link is the most important part of the thesis and this is the detail that is going to be investigated.
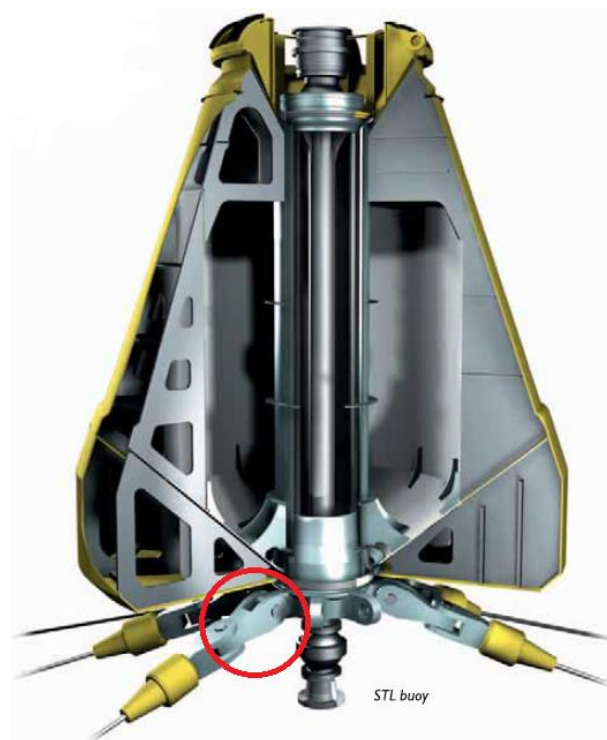


**Figure 2.4: Inside of a STL buoy (National Oilwell Varco, 2014d, p. 4).**

## 2.3   The Scope Regarding the Connecting Link

According to the available calculations the connecting links are at the moment conservative, which is why the company thinks that an optimization of the connecting links is necessary. The Minimum Breaking Load (MBL) and Ultimate Limit State (ULS) load are given for the

connecting link, and by optimizing the geometry it might be possible to get a better utilization. By reducing the size it is possible to save costs and weight since you will need smaller amounts of steel to produce a connecting link. This will affect not only the connecting link, but all the main parts like the buoy, the locking mechanism located at the vessel and many other things related to the connecting link. The company now looks at the connecting link as a structural component, but they want to change it from a structural component to a mooring component. That implies the application of different standards and in that way different requirements may be considered. The rules and regulations they have been using for the design of the STL Buoy are the following (National Oilwell Varco, 2014b, p. 8):

**DNV Offshore Standards and Recommended Practices:**

- DNV-OS-B101: Metallic Materials
- DNV-OS-C101: Design of Offshore Steel Structures, General (LRFD method)
- DNV-OS-C401: Fabrication of Offshore Structures
- DNV-OS-E301: Position Mooring
- DNV-RP-C201: Buckling Strength of Plated Structures
- DNV-RP-C202: Buckling Strength of Shells
- DNV-RP-C203: Fatigue Strength Analysis of Offshore Steel Structures
- Class Note 30.1: Buckling Strength Analysis of Bars and Frames and Spherical Shells
- DNV Rules for planning and execution of marine operations, Pt. 2, Ch. 5 LIFTING
- DNV-RP-B401: Cathodic Protection Design
- DNV Rules for planning and execution of marine operations

In this master's thesis, not all the rules and regulations will be relevant. To change the connecting link from a structural component to a mooring component, these following rules and regulations will be applied:

**DNV Offshore Standards and Recommended Practices:**

- DNV-OS-E302: Offshore Mooring Chain
- DNV-OS-E304: Offshore Mooring Steel Wire Ropes
- DNVGL-RP-0005: RP-C203: Fatigue design of offshore steel structures

# 3 Theory

This chapter presents the theory the thesis is based on.

## 3.1 ANSYS

For the numerical calculations ANSYS have been used. ANSYS is an finite element analysis (FEA) software and was released for the first time in 1971. For over 40 years, it has been a leading FEA program. ANSYS is characterized as a comprehensive general-purpose finite element computer program. ANSYS is capable of performing different kinds of analyses, such as static, dynamic, heat transfer, fluid flow, and electromagnetism analyses. Many engineering fields uses ANSYS, such as aerospace, automotive, electronics, and nuclear. (Moaveni, 2008, p. 6). ANSYS is relevant for the thesis, since NOV uses it when performing finite element analysis.

## 3.2 Finite Element Method

Finite element method is relevant for the thesis, since ANSYS is a FEA computer program.

### 3.2.1 Introduction

It is possible to use numerical solutions when dealing with practical engineering problems. When trying to solve a problem, the difficulties around the governing differential equations or the boundary and initial conditions can be the reason for why it is not possible to achieve exact solutions. Analytical solutions are used when you want to show the exact behavior of a system at any point within the system. On the other hand, numerical solutions approximate exact solutions only at discrete points, also called nodes. Discretization is the first step of any numerical procedure, and it is about dividing the part of interest into finite elements, often just called elements, connected by nodes. From this it is possible to obtain an approximate solution. (Moaveni, 2008, p. 5) (Fish & Belytschko, 2007, p. 1). There are two common classes of numerical methods: 1) Finite difference methods and 2) Finite element methods. "[…] the finite element method uses *integral formulations* rather than difference equations to create a system of algebraic equations. Moreover, a continuous function is assumed to represent the approximate solution for each element. The complete solution is then generated by connecting or assembling the individual solutions, allowing for continuity at the interelemental boundaries" (Moaveni, 2008, p. 5).

### 3.2.2 Definition

Since the research field on finite element method started, there has been developed a standard methodology when analyzing problems of a discrete nature. "The civil engineer, dealing with structures, first calculates force-displacement relationships for each element of the structure and then proceeds to assemble the whole by following a well-defined procedure of establishing local equilibrium at each "node" or connecting point of the structure. The resulting equations can be solved for the unknown displacements" (Zienkiewicz & Taylor, 2000, p. 2). This type of analyses and other types of analyses for other fields is adaptable to discrete systems, like a standard discrete system. From this it is possible to define "[…] the finite element process as a method of approximation to continuum problems such that

a) the continuum is divided into a finite number of parts (elements), the behavior of which is specified by a finite number of parameters, and

b) the solution of the complete system as an assembly of its elements follows precisely the same rules as those applicable to *standard discrete problems*" (Zienkiewicz & Taylor, 2000, p. 2).

### 3.2.3 Convergence Criteria

When performing a finite element analysis, some requirements must be satisfied regarding the convergence. This is to make sure convergence to the correct result, and in that case base your assumptions about the analysis on the correct result. These convergence criteria are as follows (Zienkiewicz & Taylor, 2000, p. 31):

- *Criterion* 1. The displacement function chosen should be such that it does not permit straining of an element to occur when the nodal displacements are caused by a rigid body motion.

- *Criterion* 2. The displacement function has to be of such a form that if nodal displacements are compatible with a constant strain condition such constant strain will in fact be obtained.

- *Criterion* 3. The displacement functions should be chosen such that the strains at the interface between elements are finite (even though they may be discontinuous).

## 3.3 Von Mises Yield Criterion

The steel material will yield in a one-dimensional stress state, when the stress $\sigma$ reaches the yield stress $f_y$. This is not adequate information when dealing with a multidimensional stress state. A criterion is therefore required; stating what combination of stresses ($\sigma$, $\tau$) that leads to

yielding. One of these criterions is called the von Mises yield criterion. In a three-dimensional stress state, yielding occurs when the elastic distortion energy is equal to the distortion energy in a one-dimensional stress state. This is the von Mises yield criterion, and experiments supports this way of approaching the yield criterion. The equations for the criterion are as follows:

Two-dimensional state:

$$\sqrt{\sigma_1^2 + \sigma_1^2 - \sigma_1\sigma_2} = f_y \qquad (3.1)$$

$$\sqrt{\sigma_x^2 + \sigma_y^2 - \sigma_x\sigma_y + 3\tau_{xy}^2} = f_y \qquad (3.2)$$

Three-dimensional state:

$$\frac{1}{\sqrt{2}}\sqrt{(\sigma_1 - \sigma_2)^2 + (\sigma_2 - \sigma_3)^2 + (\sigma_3 - \sigma_1)^2} = f_y \qquad (3.3)$$

$$\sqrt{\sigma_x^2 + \sigma_y^2 + \sigma_z^2 - (\sigma_x\sigma_y + \sigma_y\sigma_z + \sigma_z\sigma_x) + 3(\tau_{xy}^2 + \tau_{yz}^2 + \tau_{zx}^2)} = f_y \qquad (3.4)$$

The yield criterion is represented with a circular cylindrical surface with axis that coincides with the line $\sigma_1=\sigma_2=\sigma_3=1$ in a three-dimensional stress state. The criterion represents an ellipse in $\sigma_1$-$\sigma_2$-plane, which is the two-dimensional stress state, and is the cylinders sectional area with the $\sigma_1$-$\sigma_2$-plane. The material is elastic as long as the stresses in a material point are inside the ellipse or cylinder. If the point is situated on the ellipse or the cylinder surface, the material is yielding. The material point cannot be situated outside of the ellipse or the cylinder. An illustration of von Mises yield criterion in two-dimensional and three-dimensional stress states are shown in Figure 3.1 below. Notice that no matter how high the stresses are, the material point will be elastic if $\sigma_1=\sigma_2=\sigma_3$. (Larsen, 2010, pp. 63-65).
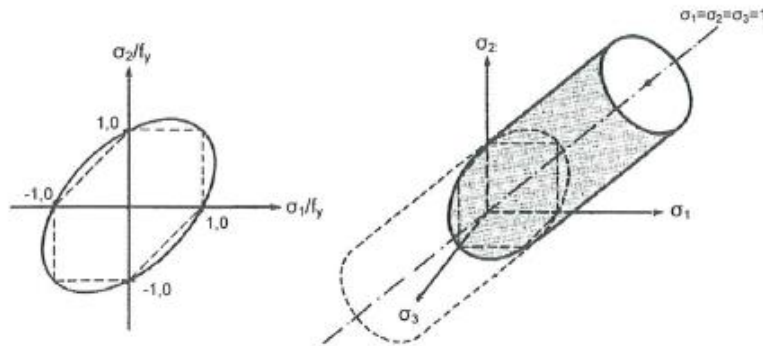


**Figure 3.1: Von Mises yield criterion in two-dimensional and three-dimensional stress states (Larsen, 2010, p. 64).**

## 3.4 Tension Elements

The connecting link is a tension governed, structural element. The cross section of the connecting link has the same shape as an eye-bar. The cross section of the connecting link is shown in Figure 3.2 and the shape of the eye-bar is shown in Figure 3.3.
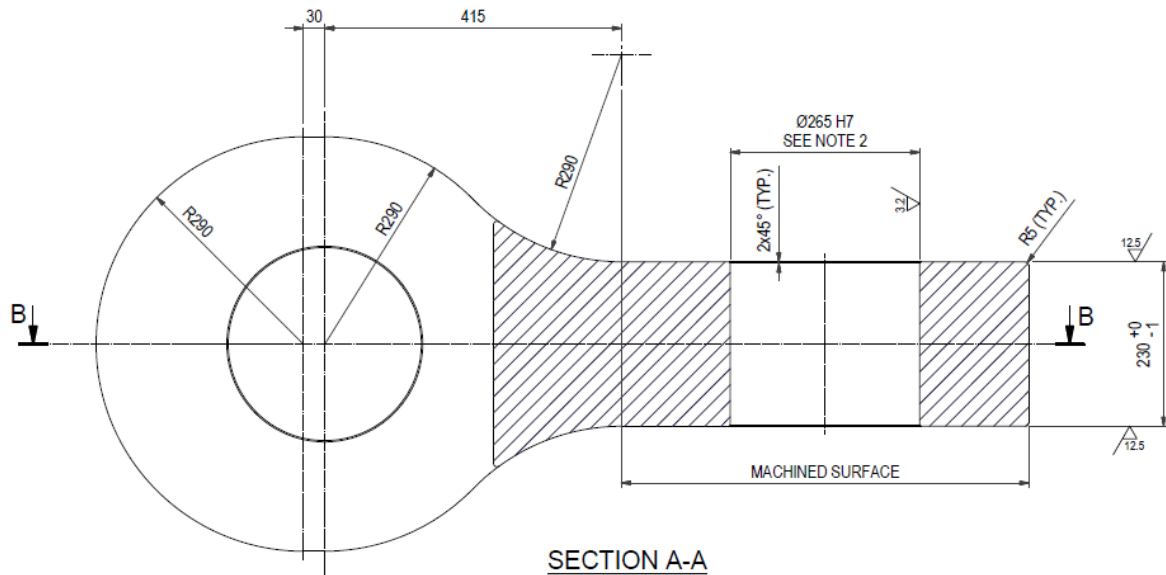


**Figure 3.2: The cross section of the connecting link (National Oilwell Varco, 2014e).**
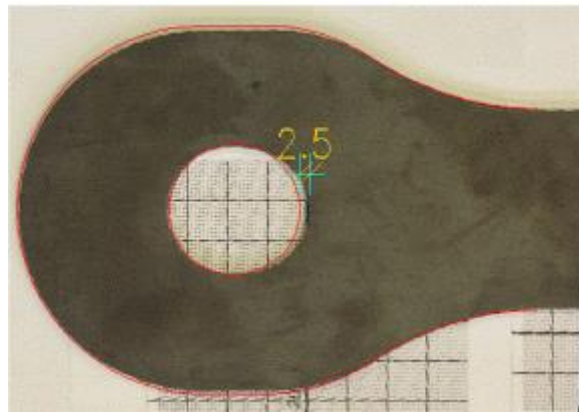


**Figure 3.3: The eye-bar (Vértes, 2006, p. 7).**

Regarding the design of the eye-bar, the failure should occur in the straight part of the bar, and not in the head. The reason for this is because of easy detection of failure among other aspects, like easy calculations. Failure in the straight part of the bar is ensured by the geometry. In this thesis, recommendations will be considered when optimizing the "eye-bar" of the connecting link. Beke's recommendation results in the smallest eye-bar, and is also the most favorable option regarding the development of the deformations (Vértes, 2006, p. 3). Hence, Beke's recommendations are applied in the master's thesis. The eye-bar size

according to old recommendations is listed in Table 3.1 below, and the notation of the eye-bar sizes are shown in Figure 3.4 below.
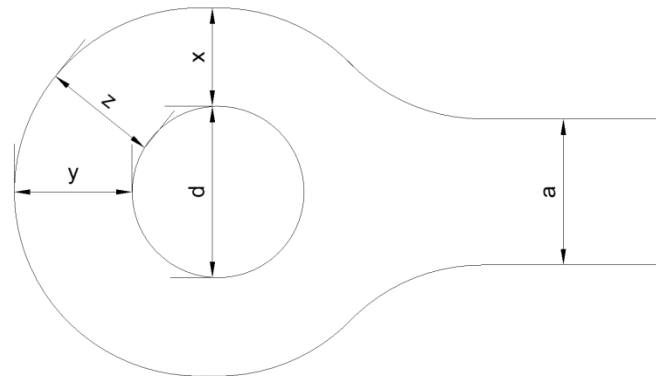


Figure 3.4: Notation of the eye-bar sizes (Vértes, 2006, p. 2).

Table 3.1: Eye-bar sizes according to old recommendations (Vértes, 2006, p. 3).

| Oval head | x | y | d/a | Other restriction, comment |
|---|---|---|---|---|
| Beke | 0,5-0,63a | 0,75-0,6a | - | z ≥ 0,66a |
| Cooper | 0,5a | 0,75a | 1 | - |
| Gerber | 0,55a | 0,75a | - | - |
| Häseler | 0,61a | 0,916a | - | in case of d = 2/3 a |
| Berkley | 0,625a | 1,0a | 0,75 | - |
| Winkler | 0,72a | 0,94a | - | in case of d = 2/3 a |
| **Circular head** | | | | |
| Beke | >0,66a | >0,66a | - | - |
| General formulas (USA) | 0,665a-0,75a | 0,665a-0,75a | - | Rounding radius at the neck is larger than the diameter of the head |

## 3.5   Stress Concentrations

Stress concentrations are relevant for the thesis, since the connecting link consist of holes.

### 3.5.1   Introduction

A stress concentration is known as a high stress gradient which occurs in a small, localized area of a structure. The two most common stress concentrations are a) discontinuities in continuum and b) contact forces. Changes in geometry and material properties are included in discontinuities in continuum. The disruption of the smooth flow of stresses through a structure is due to the rapid change in geometry. Examples of geometry changes can be plates in tension or bending with holes, notches, steps, and so on, shafts in tension, bending and torsion with holes, notches, steps, keyways, and so on, rough surface finishes, and external and

13

internal cracks. Alloy formulation, grain size and orientation, and foreign material can be included in changes regarding the material properties at macroscopic and microscopic level. With the contact forces, the high stress gradients occur near the point of contact, which in turn decreases when moving away from the contact area. (Budynas, 1999, pp. 364-365). In Figure 3.5 a loaded plate (a), a photoelastic model (b) and the stress distribution (c) for a plate with a hole is shown.
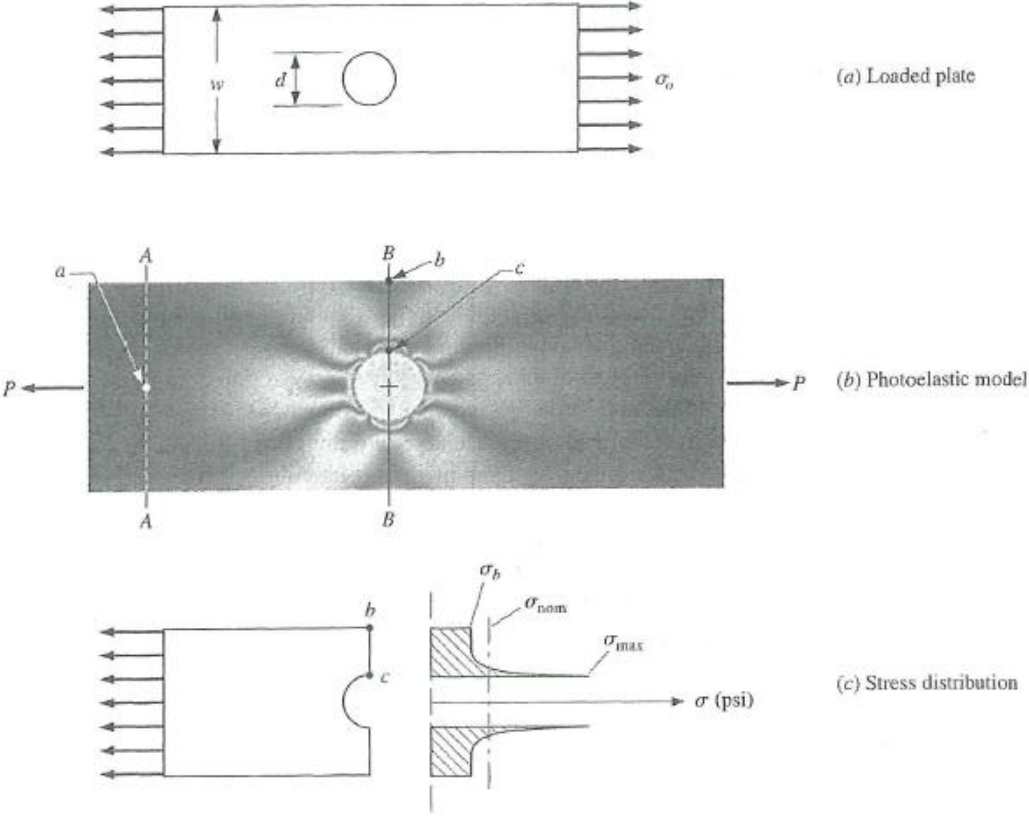


**Figure 3.5: Stress distribution for a plate in tension containing a centrally located hole (Budynas, 1999, p. 366).**

### 3.5.2   Determination of the Stress Concentration Factor and the Flow Analogy

Numerical methods or experimental methods can be used to determine the stress concentration factor. The finite element method is usually used as a numerical method, but problems around the accuracy of the results must be addressed. With stress concentration problems, it is necessary to apply a very fine mesh of elements to the model, which again leads to accurate results. Due to the very fine mesh, the model will contain a lot of elements that will need more computer resources than related problems without a stress concentration. When trying to reduce the stress concentrations, it can be helpful to use an intuitive method called the flow analogy. This means that it is possible to consider a plate, with a circular hole in the center of the plate, as a fluid flow field. If the plate was applied uniformly loads, those would be transformed into a uniform fluid flow field, which is illustrated in Figure 3.6 below.
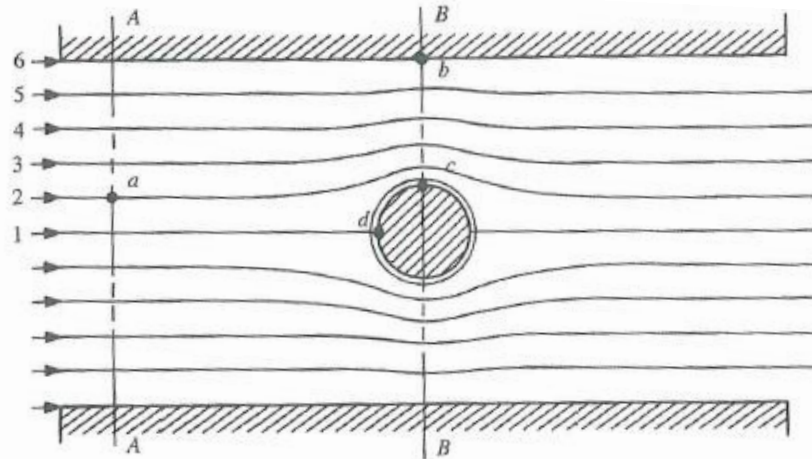
**Figure 3.6: The flow analogy - reducing stress concentrations (Budynas, 1999, p. 368)**

In the beginning of the plate where section A-A is shown, the flow is uniform, and in the end of the plate the flow is uniform, due to symmetry. The streamlines inside the plate needs to adjust when the fluid particles come closer to section B-B and the circular hole. This means, particles close to streamline 1 will have to make the largest adjustment to move around the obstacle they are approaching. The particles accelerate until the approach of section B-B, which is the maximum velocity the particles obtain, and can be found in point c. After section B-B the particles decelerate back to the original uniform velocity, and move towards the end of the plate. At the edge of the hole the maximum stress can be found, and this point correspond to point c in Figure 3.6 above. One can benefit from using this flow analogy to see how the fluid flow change if different suggestions are tried out. Two examples that could be possible to reduce the stress concentration are; making the circular hole into an ellipse or by drilling two smaller relief holes close to the original hole. The suggestion with an elliptic hole is a reduction of material, while the two small relief holes will improve the flow transition and thereby reduce the stress concentration. The stress concentration reduction is often made by removing material from nearby areas that are low-stressed. The stress concentration area will then be relieved from the high stresses and moved toward the low-stressed area. This leads to a smaller stress value in the high-stressed areas. (Budynas, 1999, pp. 367-369).

## 3.6   Contact Stresses

The stresses cannot be determined without considering deflection, when a roller or sphere is in line or point contact with another body. Usually the results of the analysis of stress are not affected by deflection. Often when considering a beam in bending, the deflection of the beam is neglected when the force analysis and stress analysis is conducted on the model. But when

15

a load P is transmitted from the roller to the flat surface, and the deflections are ignored, the transmitted force area is zero and the stresses would be infinite. The conclusion would then be that no force can be transmitted. This is an incorrect assumption, and this indicates that the deflections of the components must be taken into account. In design where forces are transmitted through contact from one machine element to another, e.g., gearing, roller bearings, cams, and pin joints in linkages, contact-stress can be a problem. Line contact and point contact are the two main types of contact problems. (Budynas, 1999, pp. 357-358).

## 3.7 Fatigue

Various design criteria must be checked for the connecting link, and fatigue is one of them.

### 3.7.1 Introduction

When designing a structure, various design criteria must be checked for specific loading conditions and environments. Fatigue is relevant when designing the connecting link due to repetitive loading, stress concentrations and material properties among others. The definition of fatigue is "[…] a damage process in the metal due to fluctuating stresses and strains. Although the stresses and strains may be well below the static resistance level of the metal, the damage is accumulating cycle by cycle and after a certain number of load fluctuations a failure will occur" (Lassen & Récho, 2006, p. 15). It can take several years before the damage accumulation will attain a critical level for structures in service, which is why fatigue must be checked.

### 3.7.2 Fatigue and Finite Element Analysis

Regarding an Finite Element Analysis (FEA) from a fatigue point of view, the scope is to find out the geometrical stress concentrations at critical hot-spots. To achieve adequate reliability in the fatigue life calculations, the accuracy have to be very high when using the geometrical stress method. The stress analysis is based on the fatigue test data and associated S-N curve, but the effect of all stress concentrations must be taken into account when performing a stress analysis. The modeling involves applying the model a fine mesh using thin shell elements or volume elements, and the welds are not included, since small details are excluded in the model. Considerations regarding element type, element size, and extrapolation techniques for stresses are therefore a part of the analysis. When deciding on the element size, a general rule of thumb is that it should not be considerably larger than the plate thickness close to the hot-spots. (Lassen & Récho, 2006, p. 104).

### 3.7.3 S-N Curves

The S-N curves have a significant role when estimating fatigue in a structure, because they describe the fatigue strength of the different critical details of a structure. The S-N curves are connected to the relation between the stress range ΔS that are applied and the number of cycles N to failure. The curves are supposed to be linear for a log-log scale during constant amplitude loading. They maintain linear until the curves reach a fatigue-limit, and under this limit, the fatigue life appears to be infinite. The curves are determined by laboratory tests with different requirements to each curve. These requirements are: type of welded detail, geometry, fabrication quality, environmental condition, and loading condition. Usually uni-axial loading is used with constant amplitude. Considering the fatigue limit, the area above is called the finite life area, and these curves are calculated with the use of linear regression. For the case regarding variable amplitude loading, some type of damage accumulation formula needs to be addressed. (Lassen & Récho, 2006, pp. 75-76).

### 3.7.4 S-N Life Predictions

The S-N life prediction can be determined by dividing the curves into classification groups. A, B, C, D, E, F, G, and W are the classification groups for welded flat plates, and classification group T is used for tubular joints. For curves that represent seawater with cathodic protection, the curves change slope -1/m from m = 3 to m = 5 at $N = 10^6$ cycles. For curves that represent air the fatigue limit is supposed to occur at $N = 10^7$ cycles. (Lassen & Récho, 2006, pp. 120-121). The equation below can carry out each S-N curve for welded plates (Lassen & Récho, 2006, p. 122) (National Oilwell Varco, 2013, p. 13):

$$logN_i = logA_2 - m \cdot log\left[\Delta\sigma_i \left(\frac{T}{T_{ref}}\right)^k\right] \qquad (3.5)$$

Where:

$N_i$ = the predicted number of cycles of failure under stress range $\Delta\sigma_i$
$logA_2$ = intercept of log N axis by S-N curve
m = the inverse slope of the S-N curve
$\Delta\sigma_i$ = stress range
T = thickness through which the potential fatigue crack will grow
$T_{ref}$ = reference thickness equal to 25 mm
k = thickness exponent on fatigue strength

### 3.7.5 Constant Amplitude Loading and Variable Amplitude Loading

Constant amplitude test data are the basis for the S-N curves, but when a welded detail in a structure is applied a load; it will be a variable amplitude load. When making life predictions, this will become a problem. It is possible to show the stress spectrum on a histogram format,

by cycle counting. Each block is like a stress block, which represents a stress range $\Delta\sigma_i$ and a number of cycles $n_i$ with relation to the stress range. This is illustrated in Figure 3.7 below:
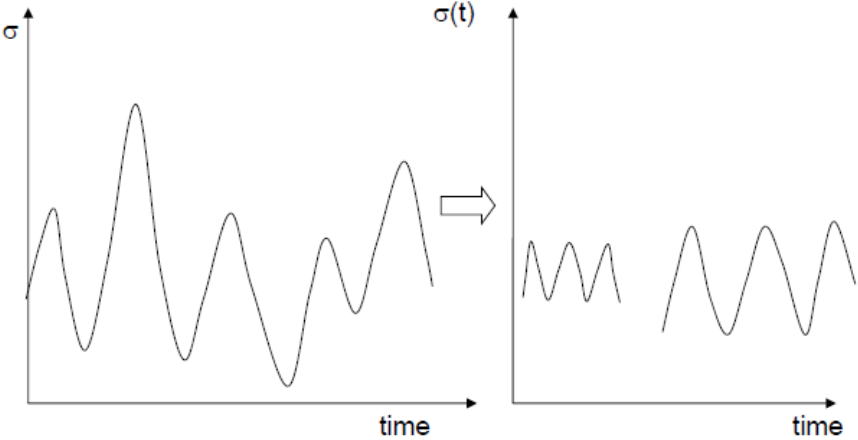


**Figure 3.7: Cycle counting of variable amplitude loading (Lassen & Récho, 2006, p. 85).**
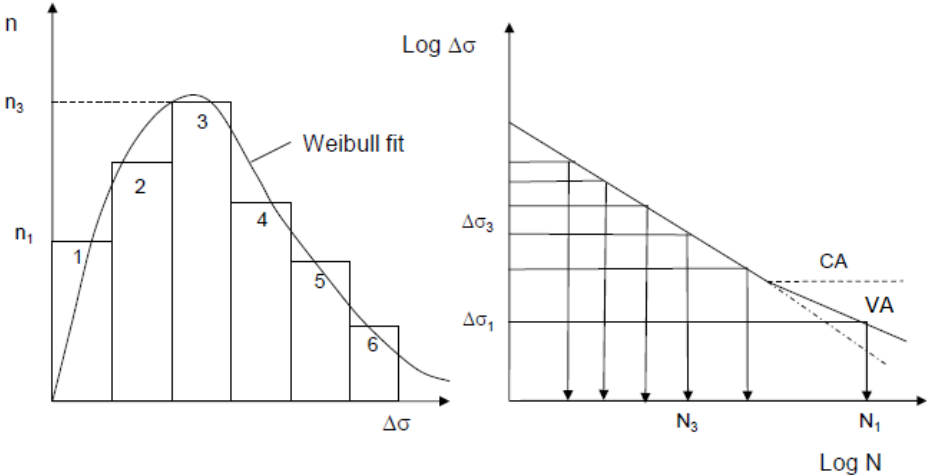


**Figure 3.8: Load spectrum given in six stress blocks and corresponding fatigue lives (Lassen & Récho, 2006, p. 85).**

The histogram shown in Figure 3.8 is connected to Figure 3.7. The validity of the load spectrum can be for a given period of time, also called short-term load spectrum, or the load spectrum can be representative for the entire service life, called long-term load spectrum. When the detail of interest is applied with variable amplitude, and the fatigue strength for the detail is applied with constant amplitude, it will be difficult to make life predictions. One way to solve this is to assume that each stress block contributes to the fatigue damage given by its damage ratio $n_i/N_i$, where; $n_i$ = the number of cycles actually occurring and $N_i$ = the number of cycles to failure according to the S-N curve for the actual stress range. For each stress block, this ratio is less than 1.0. (Lassen & Récho, 2006, pp. 84-85).

### 3.7.6 The Miner's Summation Rule

In this thesis the Miner's summation rule is applied in the fatigue calculations. The Miner summation rule is used to find the damage accumulation with the following equation (Lassen & Récho, 2006, p. 86) (National Oilwell Varco, 2013, p. 10):

$$D = \sum_{i=1}^{i=k} \left( \frac{n_i}{N_i} \right) \hspace{5cm} (3.6)$$

Where:
      D        = damage ratio
      k        = number of stress blocks considered
      $n_i$      = actual number of stress cycles for stress block no. i
      $N_i$     = number of stress cycles before failure if stress block no. i is considered only.
              Calculated from equation (2.1) for the actual stress range $\Delta\sigma_i$

From this it is possible to calculate the predicted fatigue life (PFL) (Lassen & Récho, 2006, p. 86) (National Oilwell Varco, 2013, p. 13):

$$L_p = PFL = \frac{L}{D} \hspace{5cm} (3.7)$$

For a time span $L_p$, one year long-term load spectrum can be suitable.

The design fatigue factor (DFF) can thereafter be found from the following equation (Lassen & Récho, 2006, p. 86) (National Oilwell Varco, 2013, p. 13):

$$DFF = \frac{PFL}{TSL} \hspace{5cm} (3.8)$$

The DFF is an additional safety margin, since the design S-N curves also include safety margins. It is dependent on the importance of the structural component with respect to structural integrity, and whether or not the structural component can be inspected and repaired. The target service life (TSL) is a given factor.

### 3.8 Design Optimization

Optimization is the same as minimization or maximization. Design can be divided into two different types; a functional design and an optimized design. "A functional design is one that meets all of the preestablish design requirements, but allows for improvements to be made in certain areas of the design." (Moaveni, 2008, p. 772). This means requirements that are given or set by the functionality of the part, such as the size of the part, which loads it must hold, which material to be used and how much it should cost. Design improvement begins when all the requirements are collected and decided on. "Design optimization is always based on some

criterion such as cost, strength, size, weight, reliability, noise, or performance." (Moaveni, 2008, p. 772). If the optimization criterion of the part would be the weight, then the problem would be to minimize the weight of the part. It is possible to solve this in different ways, like selecting another type of material or perform stress analysis on the part and see where it is possible to remove material from certain sections without compromising the loading and factor of safety requirements. An engineering system consists of various components. It is important to keep in mind that optimizing individual components within the engineering system is not equivalent to optimizing the system. (Moaveni, 2008, pp. 772-773). Figure 3.9 below illustrates how an optimization procedure is conducted.
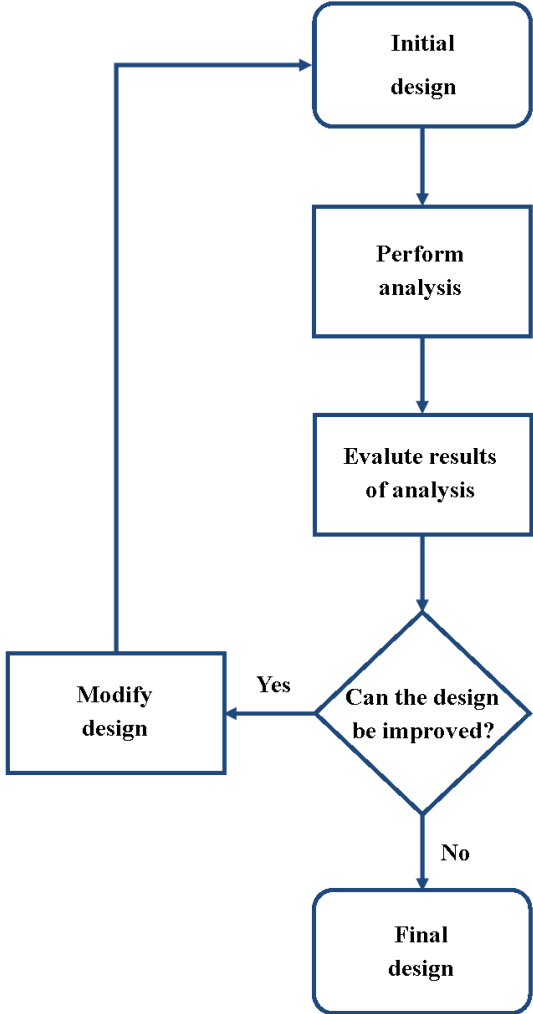


**Figure 3.9: An optimization procedure. Improvements in a design come from the process of starting with an initial design, performing an analysis, looking at results, and deciding whether or not we can improve the initial design. (Moaveni, 2008, p. 773).**

## 3.9 Rules and regulations

This master's thesis uses the Eurocode series and Det Norske Veritas (DNV) when optimizing the connecting link.

### 3.9.1 Eurocode series

From the Eurocode 0: Basis of Structural Design you can find the field of application of Eurocodes: "The Member States of the EU and EFTA recognize that Eurocodes serve as reference documents for the following purposes:

- as a means to prove compliance of building and civil engineering works with the essential requirements of Council Directive 89/106/EEC, particularly Essential Requirement No1 − Mechanical resistance and stability − and Essential Requirement No2 − Safety in case of fire;
- as a basis for specifying contracts for construction works and related engineering services;
- as a framework for drawing up harmonized technical specifications for construction products (ENs and ETAs)" ("Eurocode 0 - Basis of Structural Design," 2008, p. 5).

The Structural Eurocode programme comprises the following standards generally consisting of a number of Parts:

- Eurocode 0: Basis of Structural Design
- Eurocode 1: Actions on structures
- Eurocode 2: Design of concrete structures
- Eurocode 3: Design of steel structures
- Eurocode 4: Design of composite steel and concrete structures
- Eurocode 5: Design of timber structures
- Eurocode 6: Design of masonry structures
- Eurocode 7: Geotechnical design
- Eurocode 8: Design of structures for earthquake resistance
- Eurocode 9: Design of aluminium structures

The relevant Eurocodes for this thesis are Eurocode 0, Eurocode 1 and Eurocode 3.

### 3.9.2 Det Norske Veritas

Det Norske Veritas (DNV) merged with Germanisher Lloyd (GL) in September 2013, and formed DNV GL Group. Their experience and technological competence within the maritime

industry is used to develop and introduce oil and gas verification, inspection and risk management services, among other fields and industries. All rules and regulations are available online on www.dnvgl.com, and their rules and regulations are preferred within the oil and gas industry. (DNV GL, 2015).

When looking at the connecting link as a structural component, the following two offshore standards are the most relevant standards:

- DNV-OS-C101: Design of Offshore Steel Structures, General (LRFD method)
- DNV-OS-E301: Position Mooring

The following requirement must be satisfied when checking the connecting link as a structural component: "Strength may also be documented by non-linear analysis using recognized programmes and procedures. A load factor of 1.1 is to be taken into account in the analysis. Plastic strain shall only occur at stress concentrations in local areas. Max allowable local plastic peak strain is not to exceed 5%" (DNV-OS-E301, 2013, p. 62).

When looking at the connecting link as a mooring component, the following two offshore standards are the most relevant standards:

- DNV-OS-E302: Offshore Mooring Chain
- DNV-OS-E304: Offshore Mooring Steel Wire Ropes

The fatigue analysis of the connecting link is done according to the following standard:

- DNVGL-RP-0005: RP-C203: Fatigue design of offshore steel structures

These rules and regulations will be applied in the master's thesis when dealing with the optimization of the connecting link.

## 3.10 LRFD Method

The applied standard is the DNVs DNV-OS-C101 (2014). The design principles of DNV are based on the load and resistance factor design (LRFD) method. This is a design method where the target safety level is obtained as closely as possible by applying load and resistance factors to characteristic reference values of the basic variables. These variables are defined as:

- Loads acting on the structure
- Resistance of the structure or resistance of materials in the structure

By using deterministic factors representing the variation in load and resistance, and the reduced probabilities that various loads will act simultaneously at their characteristic values, the target safety level is achieved.

The level of safety of a structural element is considered to be satisfactory if the design load effect ($S_d$) does not exceed the design resistance ($R_d$):

$$S_d \leq R_d \tag{3.9}$$

A design load effect is obtained by multiplying the characteristic load by a given load factor:

$$F_d = \gamma_f \cdot F_k \tag{3.10}$$

Where:
$F_d$ = design load
$\gamma_f$ = load factor
$F_k$ = characteristic load

A design load effect is the most unfavorable combined load effect derived from the design loads, and may, if expressed by one single quantity, be expressed by:

$$S_d = q\,(F_{d1},\ldots, F_{dn}) \tag{3.11}$$

Where:
$S_d$ = design load effect
$q$ = load effect function

The design resistance ($R_d$) is determined as follows:

$$R_d = \frac{R_k(f_k)}{\gamma_m} \tag{3.12}$$

Where:
$R_k$ = characteristic resistance
$f_k$ = the characteristic material strength
$\gamma_m$ = material factor

# 4   Method

The master's thesis is performed by using finite element software as well as analytical calculations. The final shape of the connecting link was approached through analyses in ANSYS, to find the stress distribution and deformation, and analytical calculations by performing design checks according to DNVs standards (see Section 3.9.2). The software of interest is ANSYS Mechanical APDL 15.0, with license ANSYS Professional NLS. ANSYS makes it possible to solve non-linear problems by using numerical approximation, and it have been used to determine the utilization for the Minimum Breaking Load condition. To determine the utilization for the Ultimate Limit States, hand calculations are performed using Mathcad spread sheets. Regarding the fatigue analysis, calculations of the predicted fatigue life have been done using Excel spread sheets. The bearing wear assessment has also been performed in an Excel spread sheet.

# 5 Optimization of the Connecting Link

The stress distribution of the original connecting link showed low stress levels in large areas. These should be removed, so that the connecting link will be better utilized. A general stress level can be higher, and therefore give a more "uniform" utilization. This will not be possible at the stress concentration areas. These areas are mainly located around the holes of the connecting link. Figure 5.1 show the stress distribution for the original connecting link (see also ref. Appendix B, Figure B - 14.
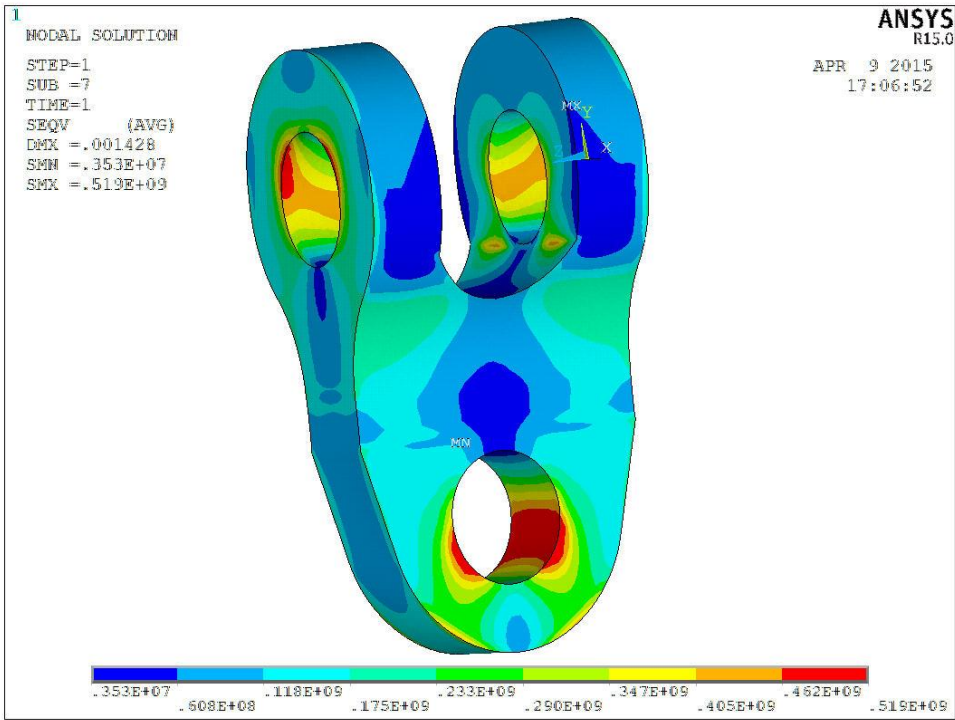


Figure 5.1: The stress distribution for the original connecting link, ref. Appendix B, Figure B - 14.

## 5.1 Drawings of the Original Connecting Link

The geometry of the original connecting link is shown in the following drawings, Figure 5.2 and Figure 5.3. In this thesis, the connecting link that is applied for optimization is called the original connecting link. NOV calls it connecting link type 1. They have different kinds of connecting links with minor changes in the geometry, but the design principles are the same for all of the connecting links. The drawings will be used to model the original connecting link. The modeling regarding the optimization will be based on these drawings as well.
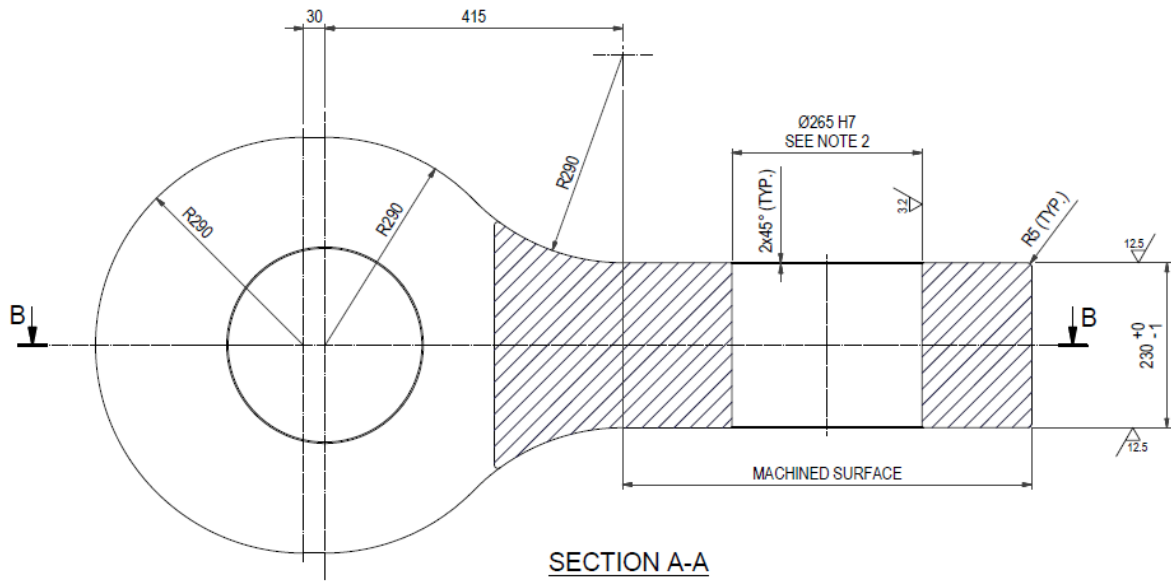
**Figure 5.2: The original connecting link's geometry - eye-bar, ref. Appendix A (National Oilwell Varco, 2014e).**
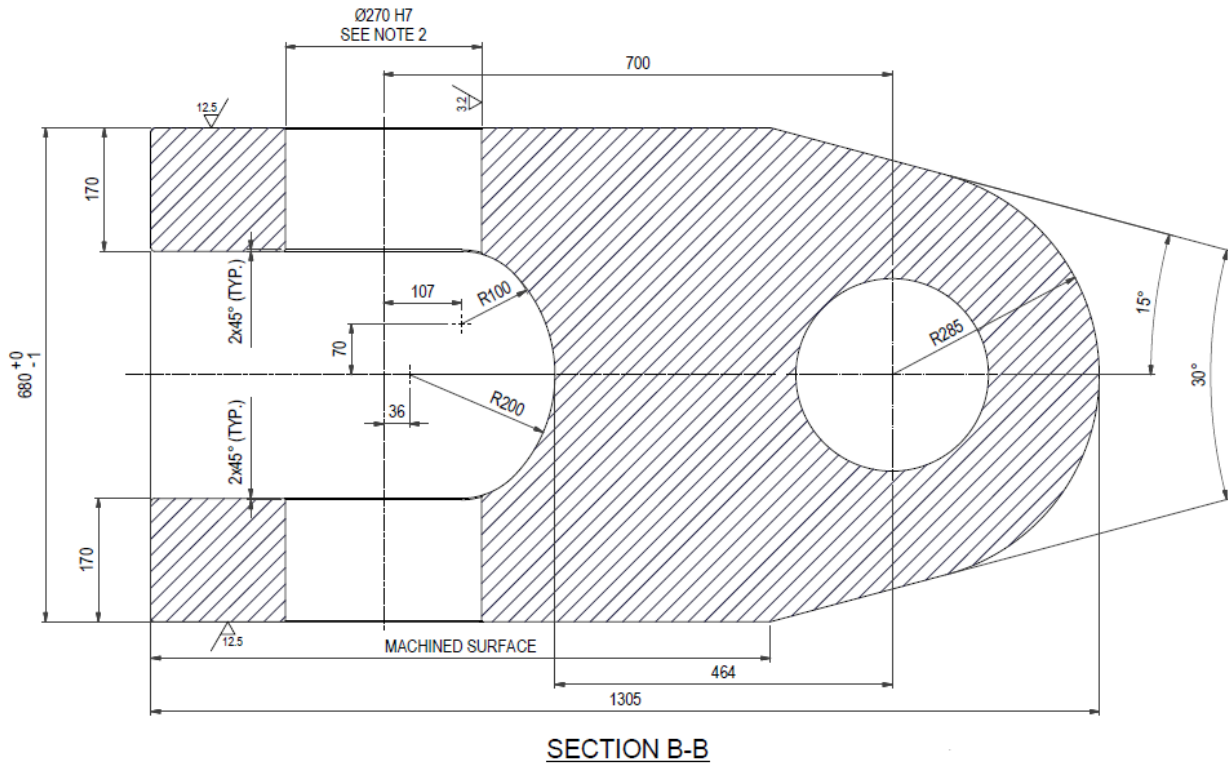


**Figure 5.3: The original connecting link's geometry – top view, ref. Appendix A (National Oilwell Varco, 2014e).**

## 5.2 Suggestions for the Optimization of the Connecting Link

In the following tables five different suggestions, regarding the optimization of the connecting link, will be presented. For some of the suggestions there will be stepwise changes, to illustrate how the changes influence the result. From this it will be possible to determine the final geometry of the connecting link, based on the achieved results.

26

**Table 5.1: Optimizations of the connecting link - suggestion A.1 and A.2**
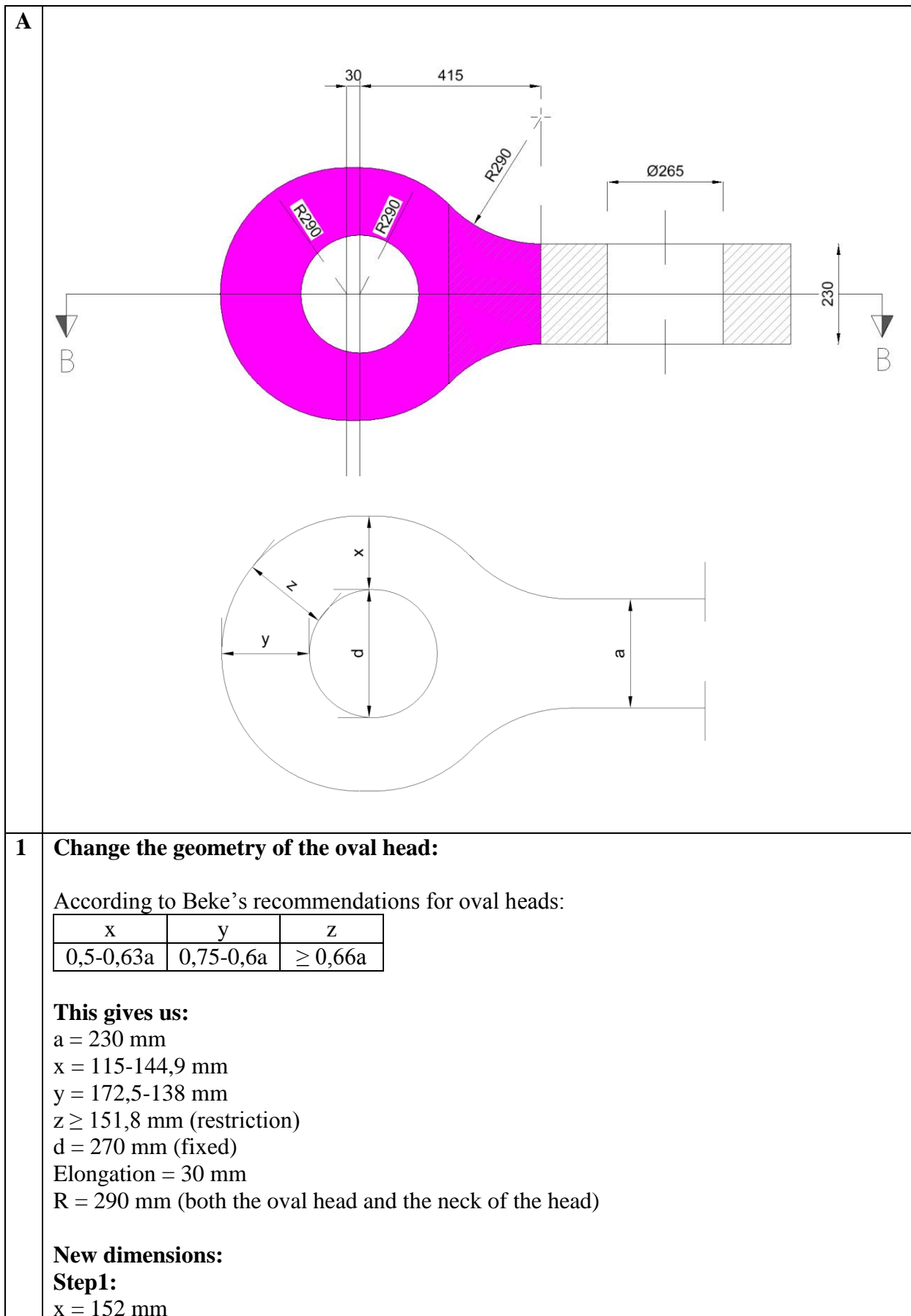
| A |  |
|---|---|
| **1** | **Change the geometry of the oval head:**<br><br>According to Beke's recommendations for oval heads:<br><br>| x | y | z |<br>|---|---|---|<br>| 0,5-0,63a | 0,75-0,6a | ≥ 0,66a |<br><br>**This gives us:**<br>a = 230 mm<br>x = 115-144,9 mm<br>y = 172,5-138 mm<br>z ≥ 151,8 mm (restriction)<br>d = 270 mm (fixed)<br>Elongation = 30 mm<br>R = 290 mm (both the oval head and the neck of the head)<br><br>**New dimensions:**<br>**Step1:**<br>x = 152 mm |

| | |
|---|---|
| | y = 182 mm<br>z = 172 mm<br>d = 270 mm (fixed)<br>Elongation = 30 mm<br>R = 287 mm (the oval head)<br>R = 299,7 mm (the neck of the head)<br><br>**Step 2:**<br>x = 145 mm<br>y = 175 mm<br>z = 165 mm<br>d = 270 mm (fixed)<br>Elongation = 30 mm<br>R = 280 mm (the oval head)<br>R = 324,4 mm (the neck of the head)<br><br>**Step 3:**<br>x = 135 mm<br>y = 165 mm<br>z = 155 mm<br>d = 270 mm (fixed)<br>Elongation = 30 mm<br>R = 270 mm (the oval head)<br>R = 363,1 mm (the neck of the head) |
| 2 | **Make the head circular:**<br><br>According to Beke's recommendations for circular heads:<br><br>| x | y |<br>|---|---|<br>| > 0,66a | > 0,66a |<br><br>**This gives us:**<br>a = 230 mm<br>x > 151,8 mm<br>y > 151,8 mm<br>d = 270 mm (fixed)<br>Elongation = 30 mm<br>R = 290 mm (both the oval head and the neck of the head)<br><br>**New dimensions:**<br>x = 152 mm<br>y = 182 mm<br>z = 172 mm<br>d = 270 mm (fixed)<br>No elongation<br>R = 287 mm (the circular head)<br>R = 299,7 mm (the neck of the head) |

**Table 5.2: Optimization of the connecting link - suggestion B.1**
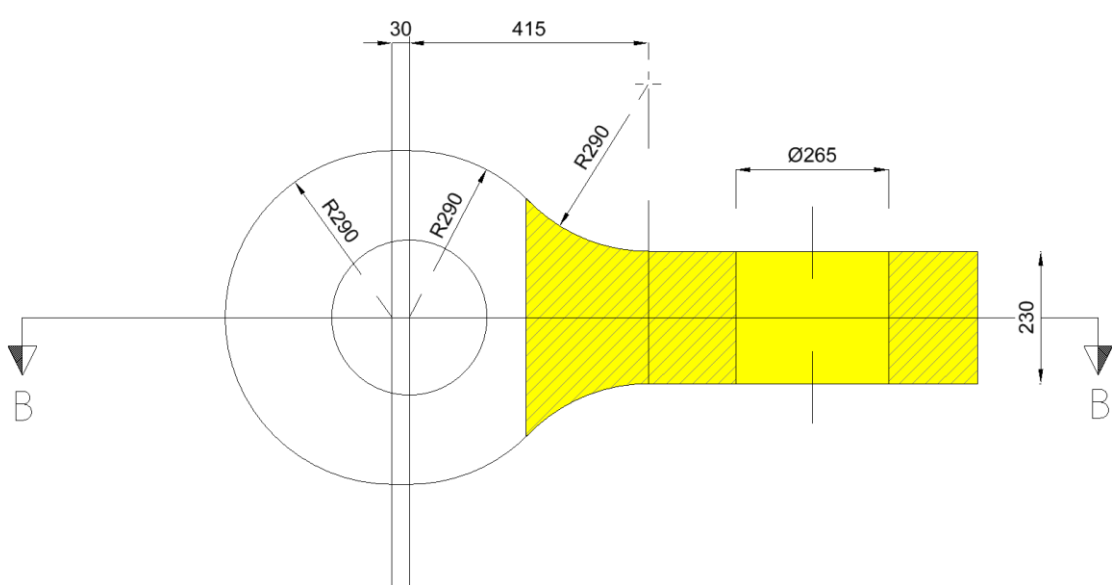
| B | |
|---|---|
| |  |
| **1** | **Change the thickness of the connecting link:**<br><br>According to the bearing load capacity the thickness of 230 mm can be reduced.<br><br>**Through different steps, various dimensions will be tried out:**<br>Step 1: the connecting link thickness = 220 mm and the radius of the neck = 278,4 mm<br>Step 2: the connecting link thickness = 210 mm and the radius of the neck = 268,0 mm<br>Step 3: the connecting link thickness = 200 mm and the radius of the neck = 258,2 mm |
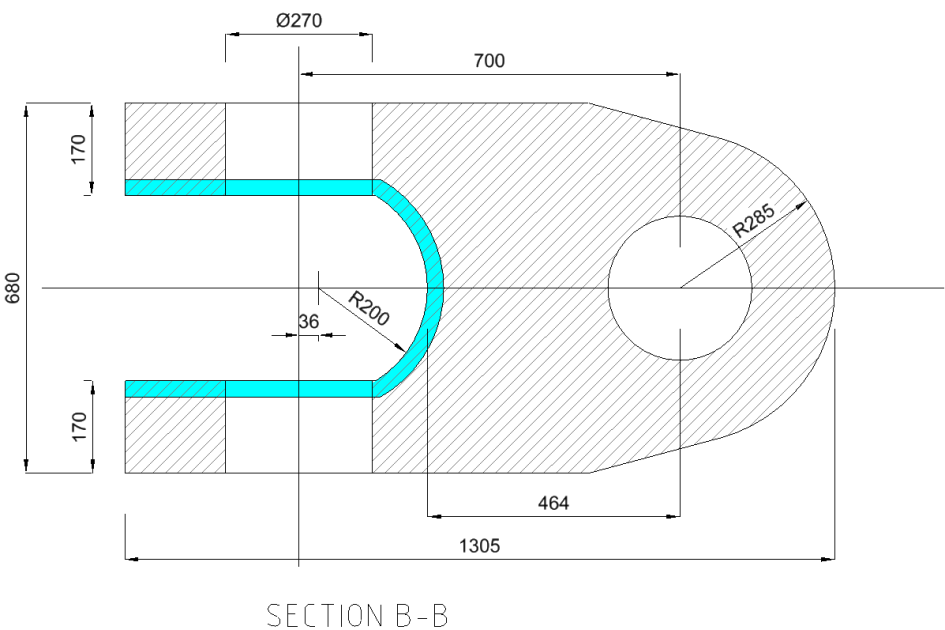
**Table 5.3: Optimization of the connecting link - suggestion C.1**

| C | |
|---|---|
| |  SECTION B-B |
| **1** | **Model the connecting link with a more defined head/neck:**<br><br>Reduce the amount of steel by removing the "red parts". The point is to make a more defined head and neck by making three cylinders with radius of: R285, R285 and R200. These cylinders will then intersect and make a more curvy line, which leads to a more defined head and neck. |

**Table 5.4: Optimization of the connecting link - suggestion D.1**

| D | |
|---|---|
| | SECTION B-B |
| **1** | **Make the gap between the two holes in the connecting link deeper:**<br><br>Reduce the amount of steel by making the gap deeper into the connecting link, removing the "green part". From the center of the two pin holes and to where the gap ends; the distance can be up to 415 mm and with a radius of 200 mm. The distance of 415 mm is connected to the length given on the drawing with the "eye-bar" (second drawing).<br><br>**Through different steps, various distances will be tried out:**<br>Step 1: 300 mm<br>Step 2: 415 mm |

**Table 5.5: Optimization of the connecting link - suggestion E.1**

| E | |
|---|---|
| | <br>SECTION B-B |
| **1** | **Change the thickness of the two oval heads (remove the blue part):**<br><br>According to the bearing load capacity the thickness of 170 mm can be reduced.<br><br>**Through different steps, various dimensions will be tried out:**<br>Step 1: oval head thickness = 160 mm and radius = 210 mm (the radius in the gap)<br>Step 2: oval head thickness = 150 mm and radius = 220 mm (the radius in the gap)<br>Step 3: oval head thickness = 140 mm and radius = 230 mm (the radius in the gap) |

# 6 Initial Data

In Section 6.1, the values are given and determined by the company. In Section 6.2 and 6.3, the information is obtained from the two projects of interest; Heidrun and Gina Krog FSO.

## 6.1 Material Properties

The material properties for the new connecting link are shown in Table 6.1.

**Table 6.1: Material Properties**

| Component | Material grade | Yield strength [MPa] | Ultimate strength [MPa] |
|---|---|---|---|
| New connecting link | R3S | 490 | 770 |

The material properties for link pins were given from the supplier documentation (National Oilwell Varco, 2015b, pp. 58-66).

The following general material properties are used shown in Table 6.2.

**Table 6.2: General Steel Properties**

| Property | Value |
|---|---|
| Density, $\rho$ | 7850 kg/m$^3$ |
| Young's modulus, E | 2.1 x 10$^5$ N/mm$^2$ |
| Shear modulus, G | 0.8 x 10$^5$ N/mm$^2$ |
| Possion's ratio, $\nu$ | 0.3 |

## 6.2 Design Principles

### 6.2.1 Ultimate Limit States (ULS)

For analysis in ULS, two sets of load combinations, a) and b), shall be used when combining the design loads (DNV-OS-C101, 2014).

The load factors for combinations a) and b) are given in Table 6.3.

**Table 6.3: Load Factors, $\gamma_f$, for Ultimate Limit State.**

| Combination of design loads | Load categories | | | |
|:---:|:---:|:---:|:---:|:---:|
| | **G** | **Q** | **E** | **D** |
| a) | 1.3 | 1.3 | 0.7 | 1.0 |
| b) | 1.0 | 1.0 | 1.3 | 1.0 |

Load categories are:

G     = Permanent load
Q     = Variable functional load
E     = Environmental load
D     = Deformation load

In this strength assessment a load factor of 1.3 has been used for both static and dynamic loads (conservative) for the ULS condition.

The material factor $\gamma_m$ in ULS is 1.15.

### 6.2.2 Accidental Limit States (ALS)

For analysis in ALS, the following load and material factors are given in Table 6.4 (DNV-OS-C101, 2014).

**Table 6.4: Load Factor and Material Factor, ALS**

| | Accidental limit state |
|:---|:---:|
| **Load factor, $\gamma_f$** | 1.0 |
| **Material factor, $\gamma_m$** | 1.0 |

### 6.2.3 Minimum Breaking Load (MBL) Condition

The local strength of structures for long-term mooring is to be designed for a load equal to the characteristic breaking strength of the mooring lines. According to (DNV-OS-E301, 2013, p. 62) Section 4; "Strength may also be documented by non-linear analysis using recognized programmes and procedures. A load factor of 1.1 is to be taken into account in the analysis. Plastic strain shall only occur at stress concentrations in local areas. Max allowable local plastic peak strain is not to exceed 5%".

### 6.3 Mooring Loads

The mooring loads are given by the company. Maximum line tension when the buoy is connected to the FSO for the different conditions is shown in Table 6.5.

**Table 6.5: Mooring Line Loads**

| Case | Description | Tension [kN] |
|:---:|:---:|:---:|
| ULS<br>100 years return period | Max. tension | 6700 |
| ALS (one line broken)<br>10000 years return period | Max. tension | 9400 |
| MBL<br>Minimum Breaking Load | Max. tension | 16169 |

In ULS, the design factor is calculated as (ref. Section 6.2.1):

$\gamma_d = 1.3 \times 1.15 = 1.495$

The design factor used in ULS is higher than the ratio of ALS load to ULS load (1.495>9400/6700). This implies that ULS always gives a higher utilization factor than ALS; and the connecting link will therefore only be checked for ULS and MBL loads.

This connecting link is symmetrical which results in a geometric out of plane angle of 0°. The bearing out of plane angle (slip angle) is 5.0° for ULS and ALS load case (ref. Section 2.2). In MBL condition the torque from the MBL load will cause the turret to slip and hence cause the mooring line to become in line with the center of the turret, resulting in zero out of plane angle.

The out of plane angle for the different load cases are summarized in Table 6.6.

**Table 6.6: Out of Plane Angle for the New Connecting Link**

| Case | Out of plane slip angle [°] |
|:---:|:---:|
| New connecting link – ULS Tension | 5.0 |
| New connecting link – MBL Tension | 0 |

# 7  ANSYS Model

NOV has run solutions on the connecting link earlier, but they did not include pins, lugs (which are connected to the turret), washers and rings. Two different models of the new connecting link were modeled, since the thesis is intended to include these parts in the analyses. The first model includes the two pins, and the second model includes the two pins in addition to lugs, washers and rings. The two models are shown in Figure 7.1 and Figure 7.2.
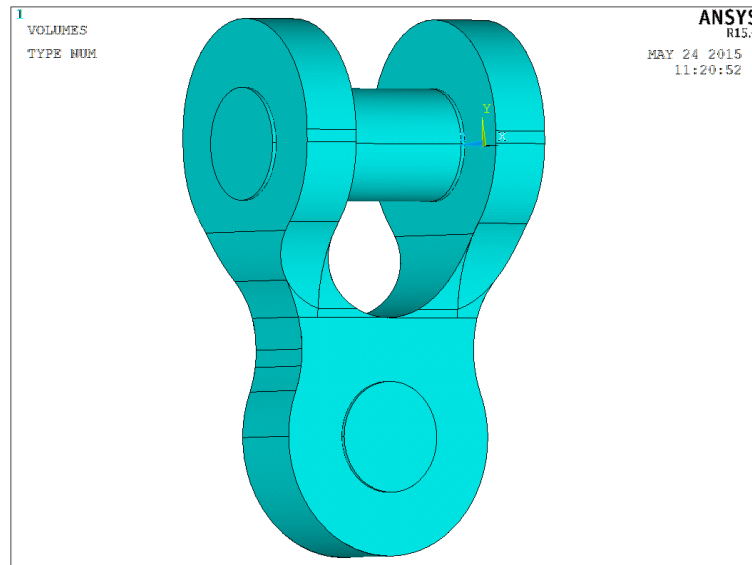


**Figure 7.1: The new connecting link with pins.**
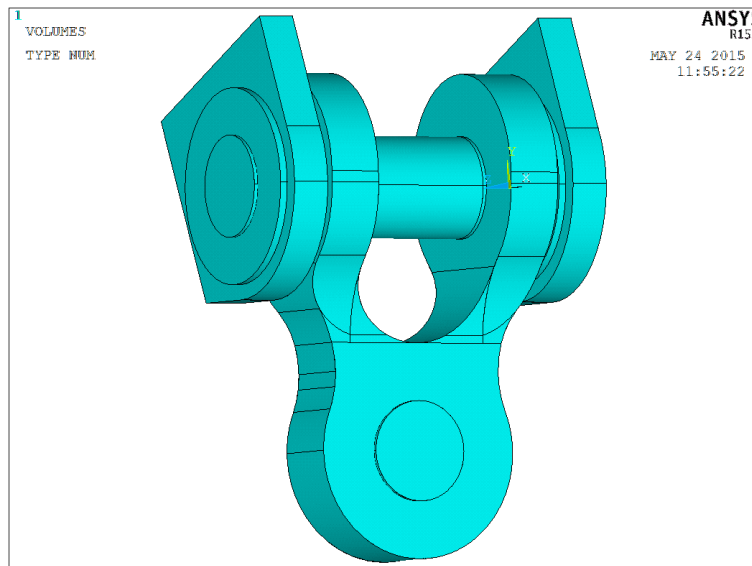


**Figure 7.2: The new connecting link with pins, lugs, washers and rings.**

In the following sections, the different steps in how the modeling of the connecting link was carried out will be presented.

## 7.1 Geometry

The geometry of the connecting link was obtained from the drawings shown in Figure 5.2 and Figure 5.3. Some of the modeling was done in 2D and other parts were made in 3D. The different volumes were in the end added, and then divided into separate volumes. The volumes need one shared area, instead of having two separate areas. In this way the volumes will not affect the result when running the solution. When modeling the different suggestions, the model was made from scratch or an existing model was modified into the suggestion of interest. The final geometry of the connecting link was made from scratch.

## 7.2 Material Models

One material model was defined for the connecting link. It was defined as a linear isotropic material with modulus of elasticity equal to $2.1 \cdot 10^5$ N/mm$^2$ and Possion's ratio equal to 0.3, and a bilinear isotropic hardening material with yield stresses equal to 490 MPa and tangent modulus equal to $1.87 \cdot 10^3$ N/mm$^2$. Different material models were applied for the two pins as well.

## 7.3 Element Type

The element type was set to be a solid brick element type with 20 nodes. This is a higher order 3D structural solid element with quadratic displacement behavior, which is well suited for modeling of irregular meshes. The element type has three degrees of freedom per node: translations in the nodal x, y, and z directions.

## 7.4 Mesh

Swept mesh has been used as much as possible when meshing the model. The areas inside of the two oval heads were refined to achieve a more accurate result, since the stress concentrations are located near the holes. The element size for the connecting link and the two pins have been set to 15 mm, but the size has been set to 100 mm for the mid part of the pin located towards the turret. The lugs, washers and rings have also been set to a size equal to 100 mm, but the areas connected with the pin are also refined. This was done for the final connecting link. Regarding the different suggestions for the optimization of the connecting link, the settings were almost the same as the aforementioned. The only differences were that the element size was set to 20 mm, without refinement at the areas inside of the two oval heads, and the lugs, washers and rings were not included in the analysis. The reason for this was to save time, since it took about 30 minutes running each of the solutions before getting a

result, and it was in total thirteen suggestions that needed to be solved (more than one time). In Figure 7.3 the mesh of the new connecting link is shown.
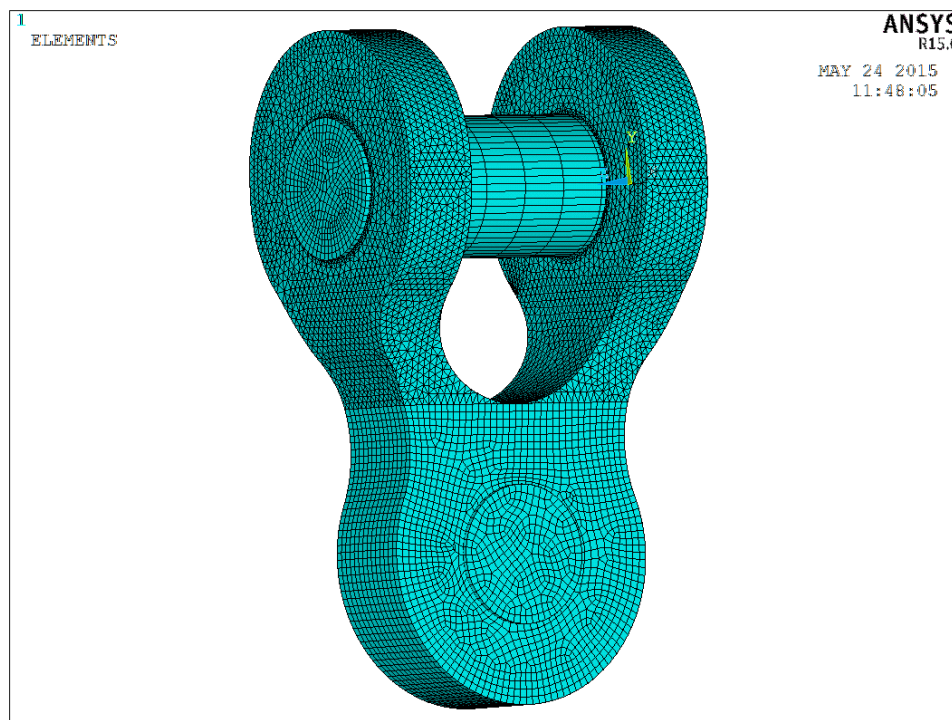


**Figure 7.3: The mesh of the new connecting link.**

The modeling involves applying the model a fine mesh, and the element size should not be considerably larger than the plate thickness. The mesh must be verified, so that considerations regarding the results from ANSYS are based on the right assumptions. To verify that the mesh is good enough, the element size is set to one size and a coarser and finer mesh are applied in two separate models. These results are then compared to validate that the determined element size is adequate to achieve correct results from the analyses performed in ANSYS. The element size was determined to be 15 mm, and the coarser and finer element sizes were therefore set to be 20 mm and 10 mm. For the three models with different element sizes, both von Mises stresses and equivalent plastic strain results were compared. For the model with element size equal to 15 mm, the highest von Mises stress was 539 MPa. With element size equal to 20 mm, the highest von Mises stress was decreased to 534 MPa. The finer mesh model with element size equal to 10 mm, the highest von Mises stress was increased to 579 MPa. The stress distribution for the three models was almost exactly the same. The equivalent plastic strain for the model with element size equal to 15 mm was 0.80%, for the model with element size equal to 20 mm, the equivalent plastic strain was 0.70%, and for the finer mesh model with element size equal to 10 mm, the equivalent plastic strain was 0.94%. In Figure

7.4 and Figure 7.5 the above-mentioned results are shown. The results can also be found in Appendix J.
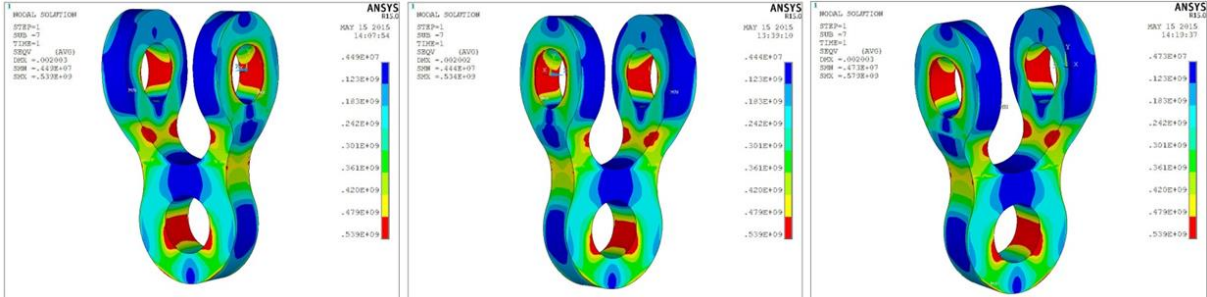


**Figure 7.4: The von Mises result for the three models with element size of respectively 15 mm, 20 mm and 10 mm.**
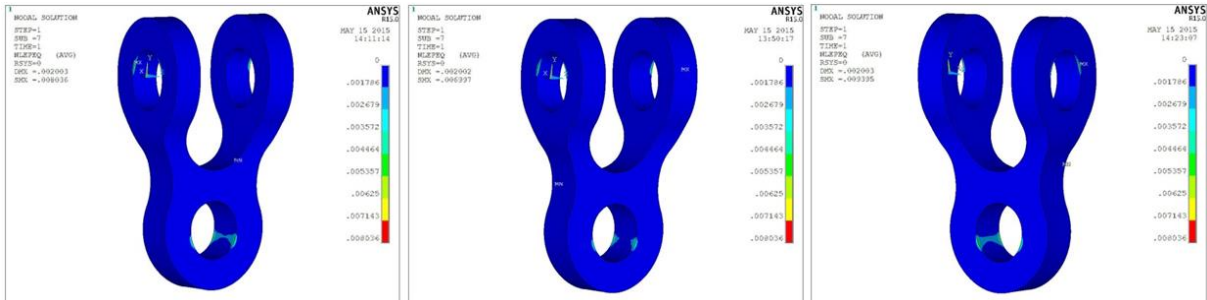


**Figure 7.5: The equivalent plastic strain result for the three models with element size of respectively 15 mm, 20 mm and 10 mm.**

Based on the results it can be concluded that the determined element size is appropriate and acceptable to achieve adequate results. To achieve adequate reliability and validity in the results from analyses performed in ANSYS, the element size is therefore set to 15 mm.

## 7.5   Contact Pair

After the model is meshed, contact pairs are applied. The areas of the pin towards the socket are set as the target, and the areas inside of the hole of the connecting link are set as the contact. The same are done with the pin towards the turret; the areas of the pin are set as the target and the areas inside of the two oval heads are set as the contact, but a contact pair is made separately for each of the two holes. These three contact pairs are shown in Figure 7.6 below. The contact behavior and other settings are set as default, except for the penetration tolerance, the pinball region, friction coefficient, initial penetration, and automatic contact adjustment. Penetration tolerance are set to 0.001, pinball region are set to 0.05 and "constant" are ticked off, friction coefficient are set to 0.2, initial penetration are set to "include offset only" and automatic contact adjustment are set to "close gap/reduce

40

penetration". When the lugs, washers and rings were included in the model, contact pair between the area of the ring and the connected area of the connecting link was also applied.
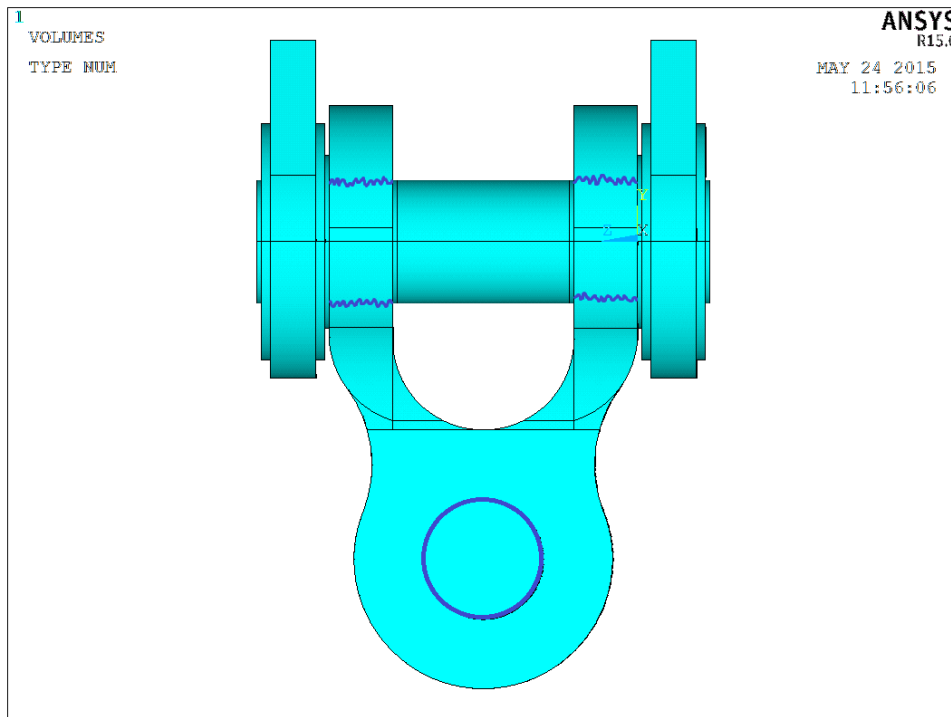


Figure 7.6: Contact pairs between the connecting link and the two pins marked in blue.

## Loads and Constraints

For the Minimum Breaking Load (MBL) condition, a pressure load was applied on top of the pin towards the socket (half of the area of the pin). The load represent a MBL equal to 16 500 kN. For the Ultimate Limit State (ULS) condition, a pressure load was applied on top of the pin towards the socket, in addition to a pressure load applied on the side of the pin towards the socket. This load represents a ULS load equal to 6700 kN, and a bearing out of plane angle (slip angle) equal to 5.0° (National Oilwell Varco, 2014c, p. 13). When running the solution for the different suggestions, only the MBL condition was considered to achieve results. The decisions for the final geometry of the connecting link are therefore based on what the MBL results shows for each of the suggestions for the optimization of the connecting link.

Constraints were also applied to the model, which will imitate how the connecting link and the connected parts are acting in real-life. The end area, on both sides of the pin towards the socket, was applied constraints in x and z direction. The area of the connecting link around the hole towards the socket, was also applied similar constraints in x and z direction. The pin towards the turret was applied constraints in all degrees of freedom (translations in x, y, and z

41

direction and rotations in x, y, and z direction) at the end area on both sides. The area of the connecting link around the holes towards the turret, was applied constraints in x and z direction. When the lugs, washers and rings were included in the model, the area of the lug that was connected to the turret was also applied with a constraint in all degrees of freedom. The applied load and the constraints for the new connecting link are illustrated in Figure 7.7.
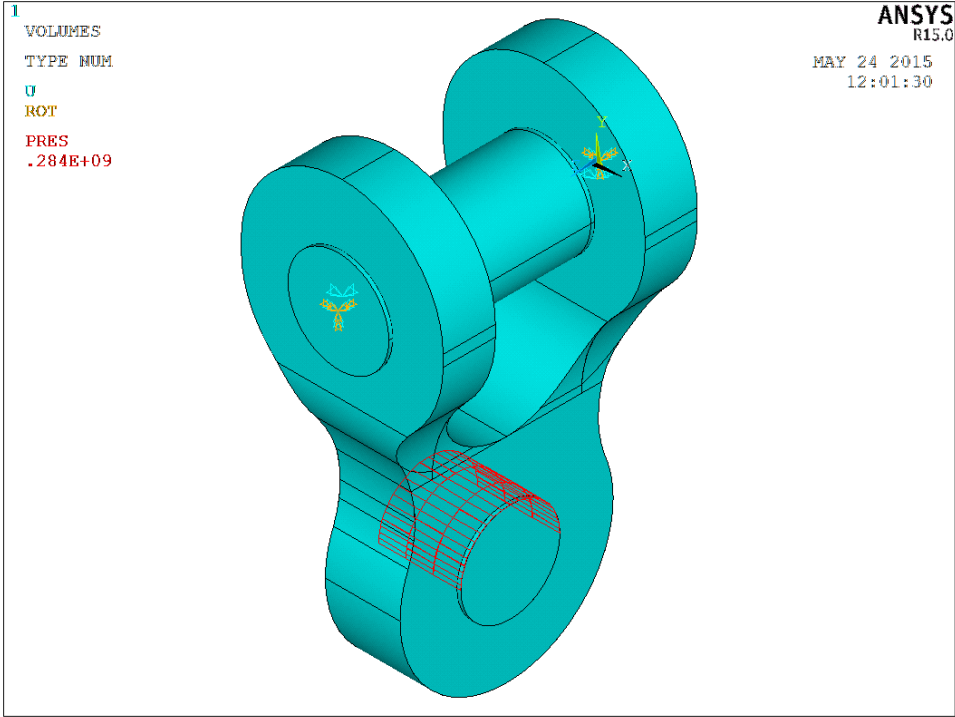


**Figure 7.7: The applied load and the constraints for the new connecting link.**

## 7.6 Analyses

A static non-linear $2^{nd}$ order analysis is chosen for the new connecting link.

## 7.7 Postprocessing

When the solution is done, the results can be plotted. The nodal solution for the von Mises stresses, $1^{st}$ principal stresses, and equivalent plastic strains are the most important results. The reaction solutions and nodal loads are also checked, so that the applied load is equal to the resulting load. The same scale is used on each of the results, which makes it possible to compare the different results and decide on the conclusions. The results are presented and analyzed in Chapter 8, and the results can also be found in the Appendices.

# 8 Results and Analysis
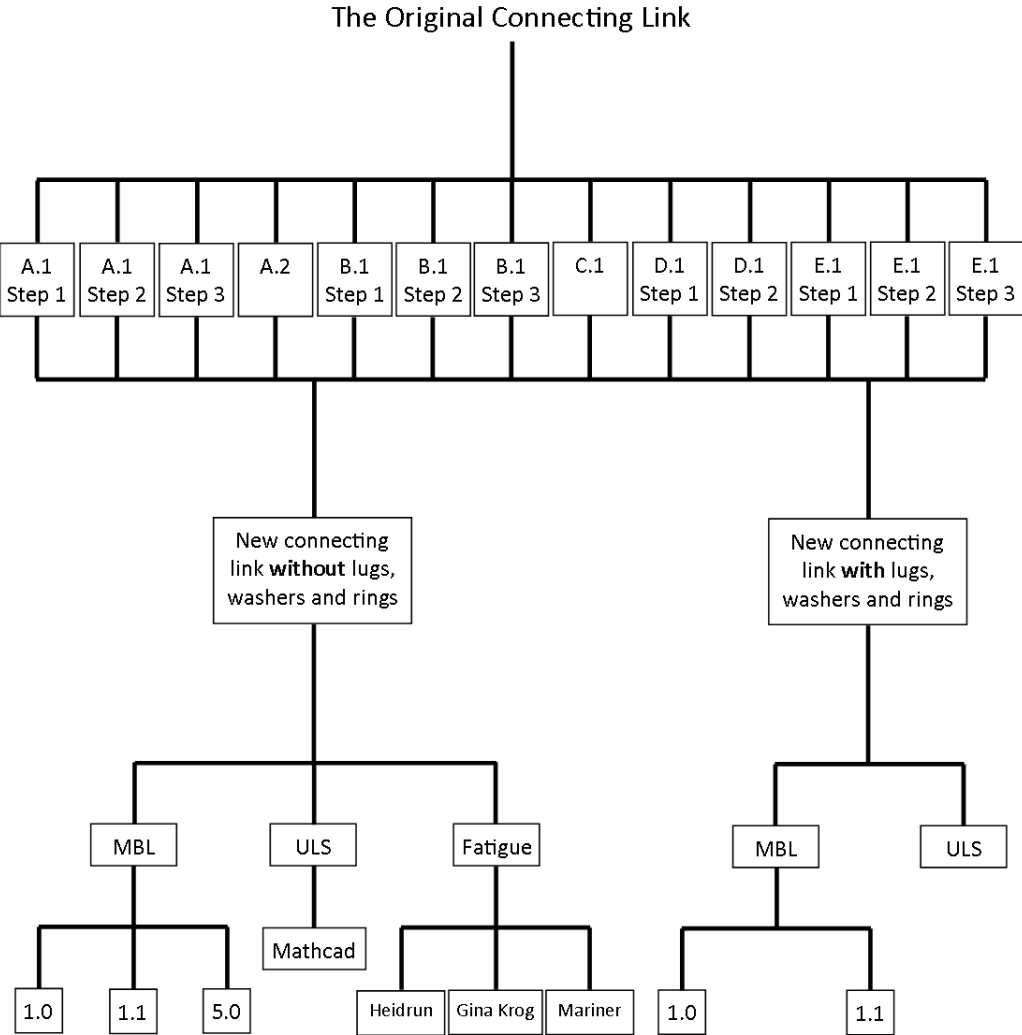


**Figure 8.1: An overview of all the models and calculations carried out in the master's thesis.**

An overview of all the models and calculations carried out in the master's thesis are shown in Figure 8.1 above. The starting point is the original connecting link, which leads to five suggestions with steps, resulting in thirteen models in total. The combination of the five suggestions leads to two new models: a connecting link without lugs, washers and rings, and a connecting link with lugs, washers and rings. The connecting link without lugs leads to models and calculations within Minimum Breaking Load (MBL), Ultimate Limit State (ULS) and fatigue. The MBL analyses are carried out in ANSYS for MBL, MBLx1.1 and MBLx5. Mathcad spread sheets are used in the ULS calculations and the maximum principal stress are found through the analysis in ANSYS. For the fatigue calculations, a spread sheet in Excel is used to find the Predicted Fatigue Life (PFL) for the connecting link. The PFL depends on the load spectra for the project of interest, and in this thesis three different load spectra's are used.

For the connecting link with lugs, analyses in ANSYS are carried out for MBL and MBLx1.1. For the ULS condition, only analysis in ANSYS is carried out. Figure 8.1 summarizes the information given above on how the results and analyses are conducted in the master's thesis.

## 8.1 The Results from the Suggestions for the Optimization of the Connecting Link

Figure 8.2 below show how the model looked like when the solution for the different suggestions for the optimization was performed in ANSYS.
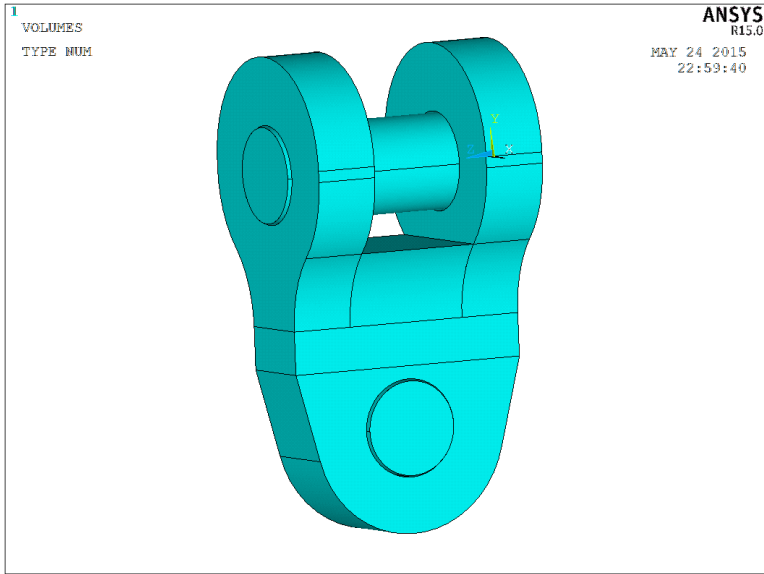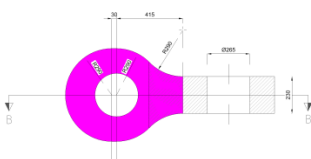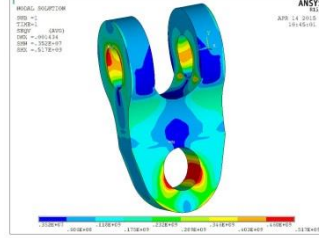


**Figure 8.2: The model of the original connecting link with pins.**

Further on, only the connecting link is selected when the results are presented.

### 8.1.1 Detailed Tables of the Results from the Suggestions
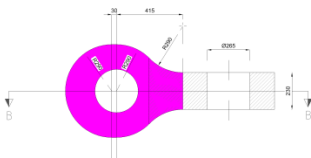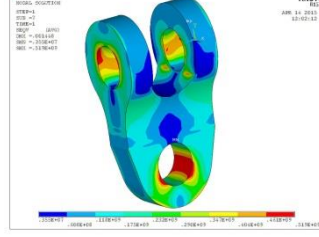
In the following tables the results from the suggestions for the optimization of the connecting link will be presented. The tables are connected to each of the suggestions and the following steps, if the suggestion is divided into stepwise changes. These results are based on the Minimum Breaking Load of 16 500 kN, which is applied as a pressure load at the top of the pin towards the socket. The original connecting link is applied the same load and steel grade as the connecting links modeled for each of the suggestions. This makes it possible to compare the original connecting link with the suggestions for the optimization. See also Appendix B, Figure B - 14 for the result for the original connecting link. The results obtained from the optimization analyses are shown as the von Mises stresses, see also Appendix B, Figure B - 1 to B - 13.

**Table 8.1: The result for suggestion A.1 Step 1, ref. Appendix B, Figure B - 1.**

| Suggestion number | Peak value | Location of peak value | Average value | Figure | Weight | Comments |
|---|---|---|---|---|---|---|
| A.1 Step 1 | 517 MPa | Pinhole towards turret | 118 MPa | Suggestion:<br><br>Result:<br> | 1307 kg | The radius of the two oval heads is decreased with 3 mm. According to Beke's recommendations. |

Suggestion A.1 Step 1 did not deviate that much from the original connecting link. The peak stress changed from 519 MPa to 517 MPa, and the peak values are concentrated only on small areas. The average value did not change, but the weight was reduced by 14 kg. The only change in the geometry was the radius of the two oval heads. The radius decreased 3 mm, from 290 mm to 287 mm.

**Table 8.2: The result for suggestion A.1 Step 2, ref. Appendix B, Figure B - 2.**

| Suggestion number | Peak value | Location of peak value | Average value | Figure | Weight | Comments |
|---|---|---|---|---|---|---|
| A.1 Step 2 | 519 MPa | Pinhole towards turret | 118 MPa | Suggestion:<br><br>Result:<br> | 1276 kg | The radius of the two oval heads is decreased with 10 mm. According to Beke's recommendations. |

The result for suggestion A.1 Step 2 was exactly the same as the original connecting link, except for the weight. The weight decreased 45 kg. The peak values are concentrated only on small areas. The change in the geometry was that the radius of the two oval heads was decreased from 290 mm to 280 mm.

**Table 8.3: The result for suggestion A.1 Step 3, ref. Appendix B, Figure B - 3.**

| Suggestion number | Peak value | Location of peak value | Average value | Figure | Weight | Comments |
|---|---|---|---|---|---|---|
| A.1 Step 3 | 523 MPa | Pinhole towards turret | 119 MPa | Suggestion: <br><br> Result: <br>  | 1232 kg | The radius of the two oval heads is decreased with 20 mm. According to Beke's recommend-ations. |
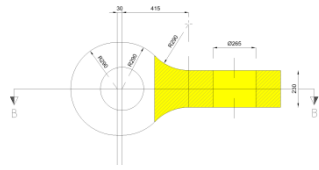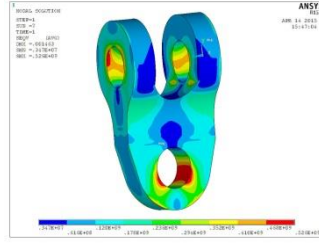
The peak stress in the case of suggestion A.1 Step 3 increased, but only 4 MPa, which is almost nothing in this comparison. Peak values are concentrated only on small areas. The average value was 119 MPa, 1 MPa higher than the original connecting link. The weight was reduced by 89 kg, which is notable. The radius of the two oval heads changed from 290 mm to 270 mm.

**Table 8.4: The result for suggestion A.2, ref. Appendix B, Figure B - 4.**

| Suggestion number | Peak value | Location of peak value | Average value | Figure | Weight | Comments |
|---|---|---|---|---|---|---|
| A.2 | 521 MPa | Pinhole towards turret | 116 MPa | Suggestion: <br><br> Result: <br>  | 1262 kg | Make the head circular → no elongation. Decrease the radius of the head with 3 mm. According to Beke's recommend-ations. |
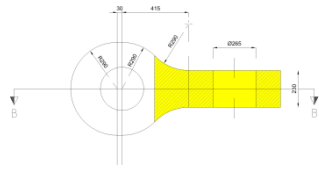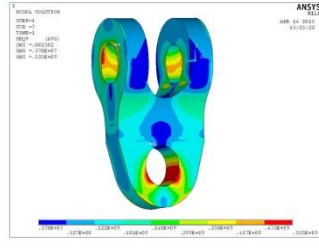
Suggestions A.2 was to make the two heads circular instead of oval. This resulted in an increased peak stress from 519 MPa to 521 MPa, again – almost negligible. Peak values are concentrated only on small areas. The average value changed from 118 MPa to 116 MPa. The weight was reduced by 59 kg, from 1321 kg to 1262 kg. The radius of the circular head was set to be 287 mm, according to Beke's recommendations.

**Table 8.5: The result for suggestion B.1 Step 1, ref. Appendix B, Figure B - 5.**

| Suggestion number | Peak value | Location of peak value | Average value | Figure | Weight | Comments |
|---|---|---|---|---|---|---|
| B.1 Step 1 | 526 MPa | Pinhole towards turret | 120 MPa | Suggestion: <br><br> Result:  | 1293 kg | Change the thickness of the connecting link. The thickness is decreased with 10 mm. |

The peak stress in the case of suggestion B.1 Step 1 increased 7 MPa. Peak values are concentrated only on small areas. The average value increased 2 MPa. The weight was reduced by 28 kg, due to the change in the thickness of the connecting link, from 230 mm to 220 mm.

**Table 8.6: The result for suggestion B.1 Step 2, ref. Appendix B, Figure B - 6.**

| Suggestion number | Peak value | Location of peak value | Average value | Figure | Weight | Comments |
|---|---|---|---|---|---|---|
| B.1 Step 2 | 535 MPa | Pinhole towards turret | 122 MPa | Suggestion: <br><br> Result:  | 1265 kg | Change the thickness of the connecting link. The thickness is decreased with 20 mm. |

The peak stress in the case of suggestion B.1 Step 2 increased 16 MPa, from 519 MPa to 535 MPa. Peak values are concentrated only on small areas. The average value increased 4 MPa and the weight was reduced by 56 kg. The thickness of the connecting link changed from 230 mm to 210 mm.

**Table 8.7: The result for suggestion B.1 Step 3, ref. Appendix B, Figure B - 7.**

| Suggestion number | Peak value | Location of peak value | Average value | Figure | Weight | Comments |
|---|---|---|---|---|---|---|
| B.1 Step 3 | 518 MPa | Pinhole towards turret | 118 MPa | Suggestion:<br>Result:<br> | 1237 kg | Change the thickness of the connecting link. The thickness is decreased with 30 mm. |
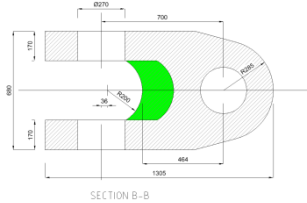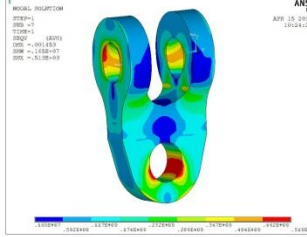
Suggestion B.1 Step 3 did not deviate that much from the original connecting link. The peak stress decreased 1 MPa and the average value was the same. Peak values are concentrated only on small areas. The weight was reduced quite a lot, 84 kg, due to the change of the thickness of the connecting link, from 230 mm to 200 mm.

**Table 8.8: The result for suggestion C.1, ref. Appendix B, Figure B - 8.**

| Suggestion number | Peak value | Location of peak value | Average value | Figure | Weight | Comments |
|---|---|---|---|---|---|---|
| C.1 | 540 MPa | Pinhole towards turret | 122 MPa | Suggestion:<br>Result:<br> | 1245 kg | Model the connecting link with a more defined head/neck. |
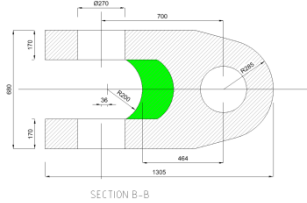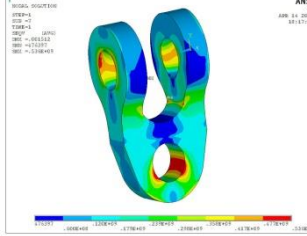
The peak stress in the case of suggestion C.1 increased 21 MPa, which is notable. Peak values are concentrated only on small areas. The average value increased 4 MPa, and the weight was reduced by 76 kg. The geometry change was to model the connecting link with a more defined head/neck for the part of the connecting link located towards the socket, see also figure above.

**Table 8.9: The result for suggestion D.1 Step 1, ref. Appendix B, Figure B - 9.**

| Suggestion number | Peak value | Location of peak value | Average value | Figure | Weight | Comments |
|---|---|---|---|---|---|---|
| D.1 Step 1 | 519 MPa | Pinhole towards turret | 117 MPa | Suggestion:<br><br>Result:<br> | 1261 kg | Make the gap deeper (reduce the amount of steel by removing the "green part"). Change the distance to 300 mm. |

Suggestion D.1 Step 1 did not deviate that much from the original connecting link, except for the weight. It was reduced by 60 kg, and this was due to making the gap between the two oval heads deeper into the connecting link. From the center of the two oval heads and to where the gap ends, the distance is set to 300 mm. This distance was 236 mm for the original connecting link. Peak values are concentrated only on small areas.
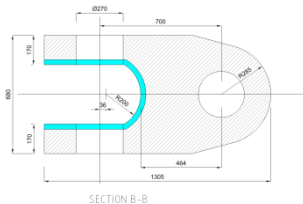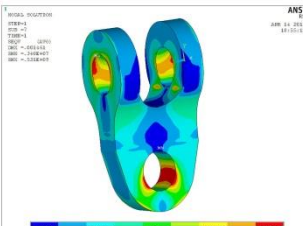
**Table 8.10: The result for suggestion D.1 Step 2, ref. Appendix B, Figure B - 10.**

| Suggestion number | Peak value | Location of peak value | Average value | Figure | Weight | Comments |
|---|---|---|---|---|---|---|
| D.1 Step 2 | 536 MPa | In the gap between the two oval heads | 120 MPa | Suggestion:<br><br>Result:<br> | 1180 kg | Make the gap deeper (reduce the amount of steel by removing the "green part"). Change the distance to 415 mm. |

The peak stress in the case of suggestion D.1 Step 2 increased 17 MPa, and the average value increased 2 MPa. Peak values are concentrated only on small areas. This suggestion was the
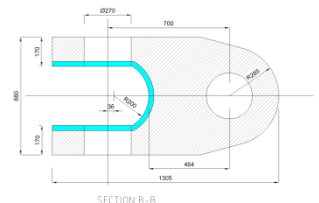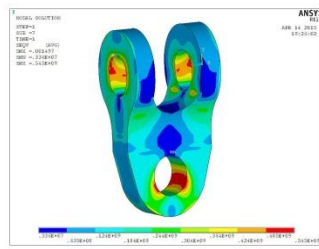
only one that had a different location of the peak value. The rest of the suggestions had peak stresses in the pinhole towards turret, but for this suggestion the location of the peak stress was in the gap between the two oval heads. The weight was reduced a lot, from 1321 kg to 1180 kg, resulting in a weight reduction of 141 kg. This was therefore the suggestions with the highest weight reduction. The distance from the center of the two oval heads to where the gap ends was set to be 415 mm, which makes the gap 179 mm deeper into the connecting link than the original connecting link.

**Table 8.11: The result for suggestion E.1 Step 1, ref. Appendix B, Figure B - 11.**

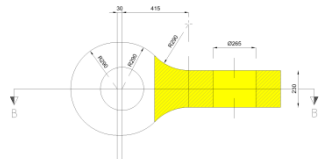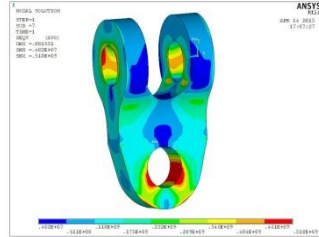| Suggestion number | Peak value | Location of peak value | Average value | Figure | Weight | Comments |
|---|---|---|---|---|---|---|
| E.1 Step 1 | 531 MPa | Pinhole towards turret | 121 MPa | Suggestion:<br><br>Result:<br> | 1281 kg | Change the thickness of the two oval heads. The thickness is decreased with 10 mm. |
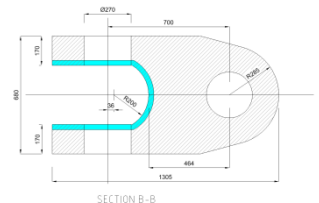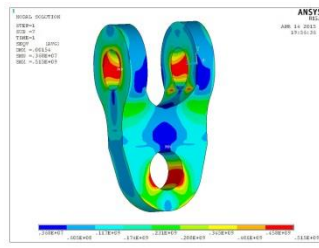
The result for suggestion E.1 Step 1 did not deviate that much from the other suggestions. The peak stress increased 12 MPa and the average value increased 3 MPa. Peak values are concentrated only on small areas. The weight was reduced by 40 kg. The thickness of the two oval heads was changed from 170 mm to 160 mm.

**Table 8.12: The result for suggestion E.1 Step 2, ref. Appendix B, Figure B - 12.**

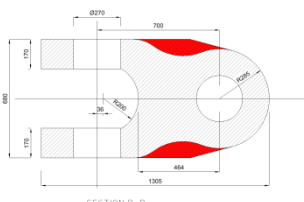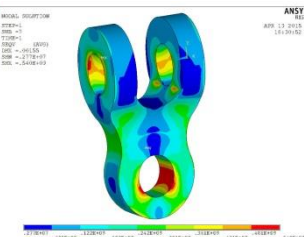| Suggestion number | Peak value | Location of peak value | Average value | Figure | Weight | Comments |
|---|---|---|---|---|---|---|
| E.1 Step 2 | 545 MPa | Pinhole towards turret | 124 MPa | Suggestion:<br><br>Result: | 1240 kg | Change the thickness of the two oval heads. The thickness is decreased with 20 mm. |

Suggestion E.1 Step 2 had the highest stress values of all the suggestions. The peak stress was 545 MPa and the average value was 124 MPa. Peak values are concentrated only on small areas. The weight was reduced by 81 kg, and this was due to the change in the thickness of the two oval heads, from 170 mm to 150 mm.

**Table 8.13: The result for suggestion E.1 Step 3, ref. Appendix B, Figure B - 13.**

| Suggestion number | Peak value | Location of peak value | Average value | Figure | Weight | Comments |
|---|---|---|---|---|---|---|
| E.1 Step 3 | 515 MPa | Pinhole towards turret | 117 MPa | Suggestion:<br><br>Result: | 1199 kg | Change the thickness of the two oval heads. The thickness is decreased with 30 mm. |

Suggestion E.1 Step 3 had the lowest peak value of all the suggestions. The peak stress decreased 4 MPa from the original connecting link. The average value also decreased 1 MPa. Peak values are concentrated only on small areas. The weight reduction was the second highest reduction, with a reduction of 122 kg. The thickness of the two oval heads changed from 170 mm to 140 mm.

### 8.1.2 Summary of the Results from all Suggestions

Summarized results from the different suggestions with steps, regarding the Minimum Breaking Load condition are shown in Table 8.14.

**Table 8.14: Summarized table with the results from all suggestions.**

| Suggestion number | Highest value [MPa] | Location of the highest value | Average value [MPa] | Weight [kg] | Note |
|---|---|---|---|---|---|
| Original connecting link | 519 | Pinhole towards turret | 118 | 1321 | Original dimensions:<br>Radius of the oval head = 290 mm<br>Thickness of the oval head = 170 mm<br>Thickness of the connecting link = 230 mm<br>From the center of the two pin holes and to where the gap ends; distance = 236 mm |
| A.1 Step 1 | 517 | Pinhole towards turret | 118 | 1307 | Changes in the dimensions:<br>Radius of the oval head = 287 mm |
| A.1 Step 2 | 519 | Pinhole towards turret | 118 | 1276 | Changes in the dimensions:<br>Radius of the oval head = 280 mm |
| A.1 Step 3 | 523 | Pinhole towards turret | 119 | 1232 | Changes in the dimensions:<br>Radius of the oval head = 270 mm |
| A.2 | 521 | Pinhole towards turret | 116 | 1262 | Changes in the dimensions:<br>The oval head is made circular → no elongation. Radius of the circular head = 287 mm |
| B.1 Step 1 | 526 | Pinhole towards turret | 120 | 1293 | Changes in the dimensions:<br>Thickness of the connecting link = 220 mm |
| B.1 Step 2 | 535 | Pinhole towards turret | 122 | 1265 | Changes in the dimensions:<br>Thickness of the connecting link = 210 mm |
| B.1 Step 3 | 518 | Pinhole towards turret | 118 | 1237 | Changes in the dimensions:<br>Thickness of the connecting link = 200 mm |
| C.1 | 540 | Pinhole towards turret | 122 | 1245 | Model the connecting link with a more defined head and neck by making three cylinders with radius of: R285, R285 and R200. |
| D.1 Step 1 | 519 | Pinhole towards turret | 117 | 1261 | Changes in the dimensions:<br>From the center of the two pin holes and to where the gap ends; distance = 300 mm |
| D.1 Step 2 | 536 | In the gap between the two oval heads | 120 | 1180 | Changes in the dimensions:<br>From the center of the two pin holes and to where the gap ends; distance = 415 mm |
| E.1 Step 1 | 531 | Pinhole towards turret | 121 | 1281 | Changes in the dimensions:<br>Thickness of the oval head = 160 mm |
| E.1 Step 2 | 545 | Pinhole towards turret | 124 | 1240 | Changes in the dimensions:<br>Thickness of the oval head = 150 mm |
| E.1 Step 3 | 515 | Pinhole towards turret | 117 | 1199 | Changes in the dimensions:<br>Thickness of the oval head = 140 mm |

All of the suggestions have acceptable results, and in next section a combination of each of the suggestions will be presented.

## 8.2 Combining the Different Suggestions into One Final Model

Since there was no excessive yield detectable from the results, an abrupt change could be carried out. Each of the suggestions was in the end combined into one final model. All of the "extreme" steps for each of the suggestions resulted in acceptable values, and it was decided to combine the different suggestions into a new connecting link. The following suggestions were combined: A.1 Step 3, B.1 Step 3, C.1, D.1 Step 2 and E.1 Step 3. The model was made from scratch, since the geometry was totally different. The new connecting link and the original connecting link are shown in 3D in Figure 8.3; in this way it is possible to see the volume change. The weight reduction of the new connecting link is 477 kg, from 1321 kg to 844 kg.
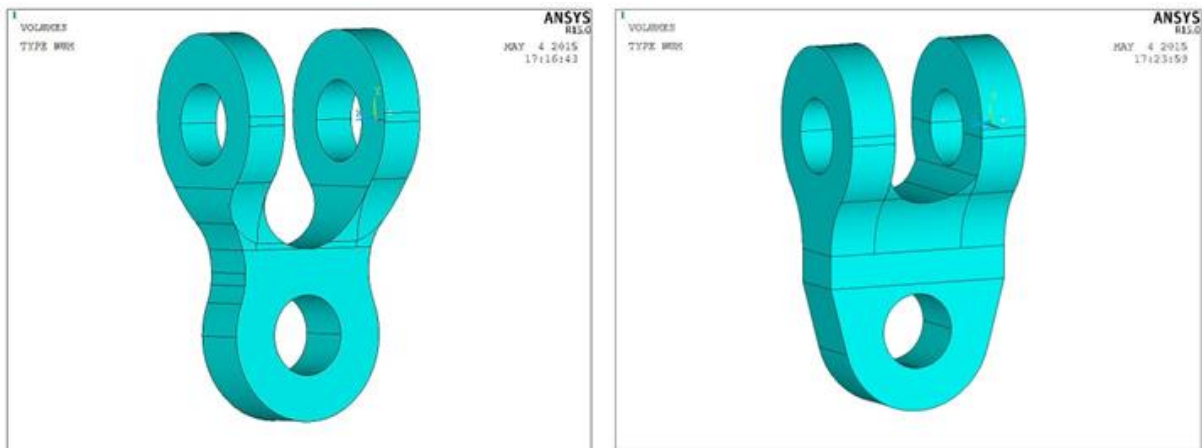


**Figure 8.3: Left: The new connecting link – Weight = 844 kg. Right: The original connecting link – Weight = 1321 kg.**

## 8.3 The New Connecting Link without Lugs, Washers and Rings

Figure 8.4 below show how the model looked like when the solution for the new connecting link without lugs, washers and rings was performed in ANSYS (see also Chapter 0).
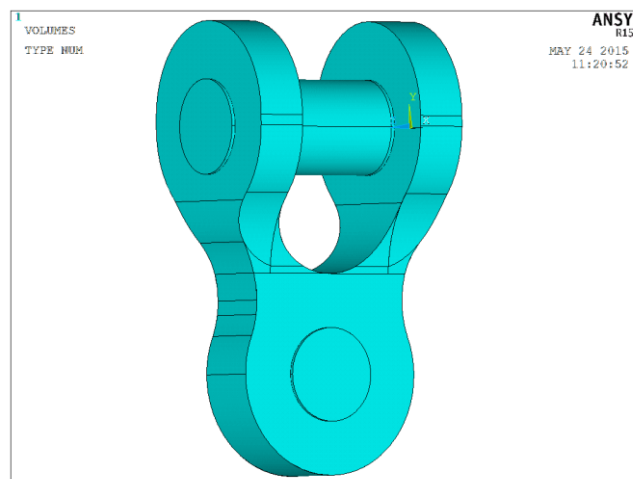


**Figure 8.4: The model of the new connecting link without lugs, washers and rings.**

Further on, only the connecting link is selected when the results are presented. The new connecting link without lugs, washers and rings will be introduced in the following subsections.

### 8.3.1 Analysis Method for the New Connecting Link

In Table 8.15 the analysis methods for the connecting link in different conditions are shown.

Table 8.15: Analysis Method for the New Connecting Link

| Component | Analysis method | |
| --- | --- | --- |
| | ULS | MBL |
| New connecting link | Hand calculations | FEA |

Hand calculations are performed using Mathcad spread sheets (Matchcad 15). The FE analyses are performed using the computer program ANSYS Mechanical APDL 15.0, with license ANSYS Professional NLS (ANSYS Mechancial APDL 15.0). First, the MBL results will be presented, then the ULS results, and in the end the fatigue results. The bearing wear assessment will also be shortly presented.

### 8.3.2 The Minimum Breaking Load Results

For the MBL condition a non-linear FE-analysis was performed to document the equivalent plastic strains in the new connecting link. According to DNV-OS-E301 (2013, p. 62), the maximum allowable plastic strain is 5%. The achieved result for the MBL condition showed that the equivalent plastic strain was 0.80%. This is a small value compared to the allowed value of 5%. For the MBLx1.1 the equivalent plastic strain was 0.98%, which is also quite small compared to the allowed value of 5%. In Figure 8.5 and Figure 8.6 the results for MBL and MBLx1.1 are shown.
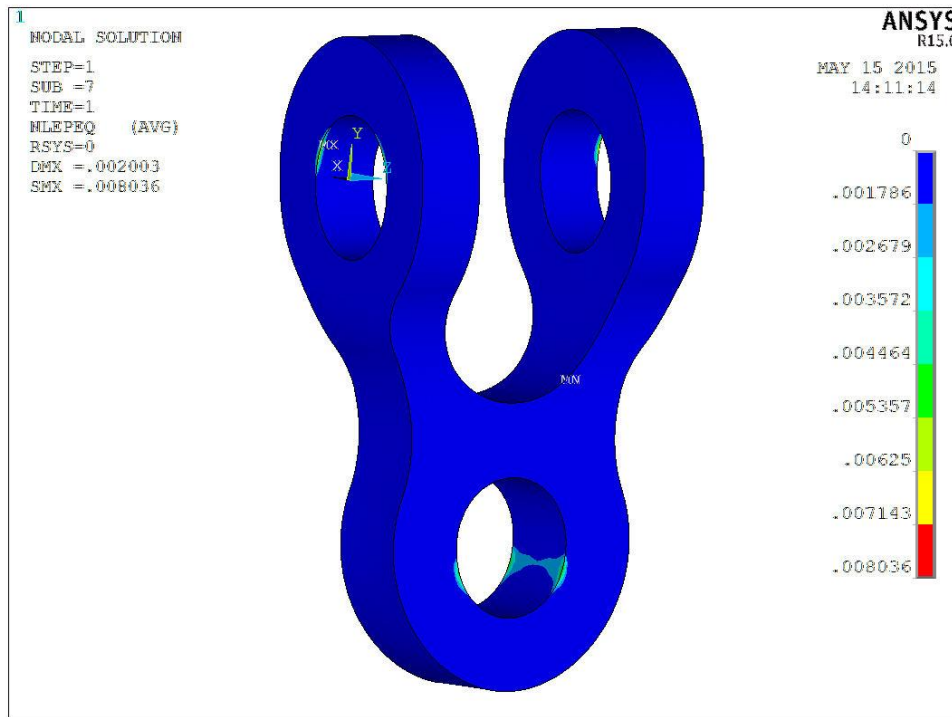
**Figure 8.5: The equivalent plastic strain result for the new connecting link - MBL condition, ref. Appendix C, Figure C - 1.**
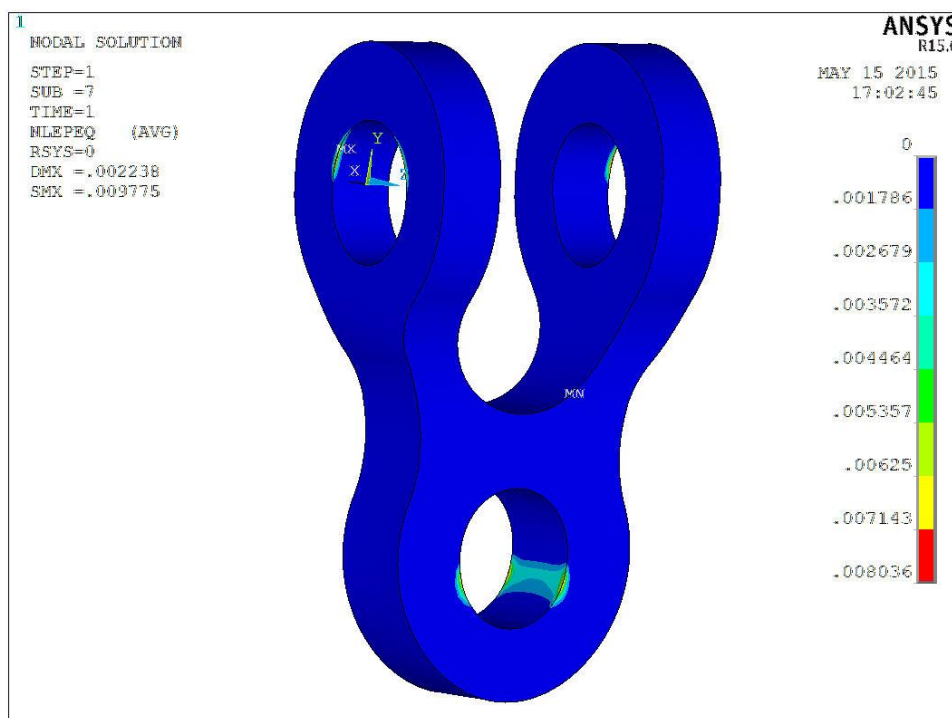


**Figure 8.6: The equivalent plastic strain result for the new connecting link - MBLx1.1 condition, ref. Appendix C, Figure C - 3.**

The new connecting link was also tested for collapse. A load of MBLx5 was applied to the new connecting link, and the analysis kept running until the connecting link collapsed. The collapse occurred between substep 6 and substep 7, which showed a time equal to 0.3 and 0.35 respectively. The collapse load is therefore the applied load between the time of 0.3 and 0.35. Substep 6 showed an equivalent plastic strain equal to 0.36%, and substep 7 showed an equivalent plastic strain equal to 23%. The collapse load was therefore closer to substep 6 than substep 7, since the equivalent plastic strain of collapse is 5%. To determine the collapse load, the MBL should be multiplied with the applied load, which was MBLx5, and the time used in substep 6. Since the collapse was occurring right after substep 6, the MBLx5 should be multiplied with approximately 0.31, which gives a collapse load of 25575 kN and a MBL condition equal to MBLx1.55. The results for substep 6 and substep 7 are shown in Figure 8.7 and Figure 8.8.
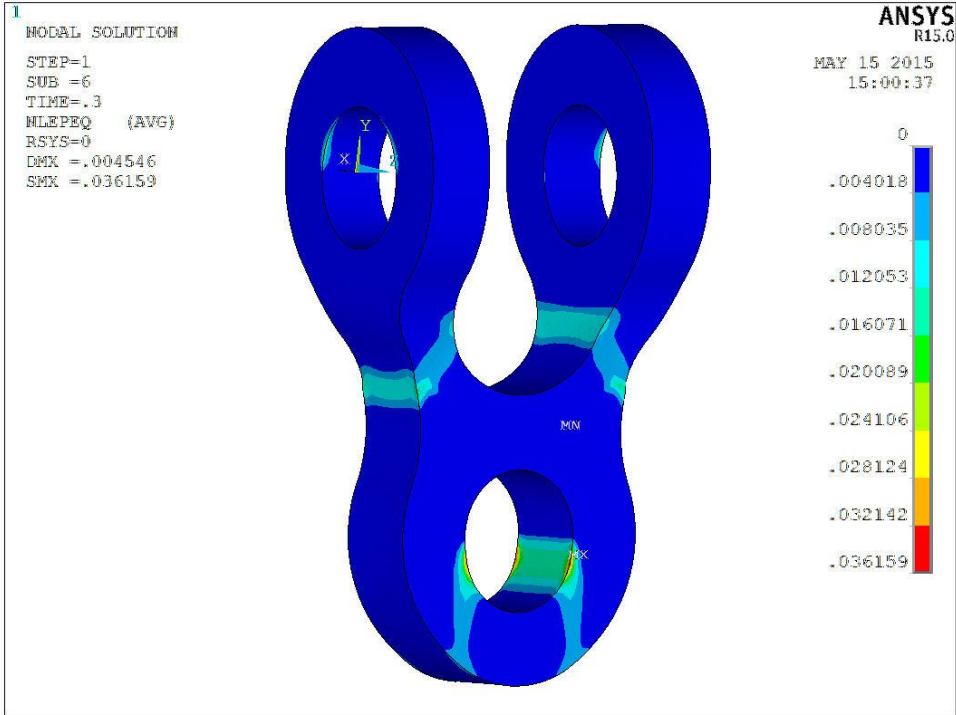


**Figure 8.7: The equivalent plastic strain for the new connecting link – MBLx1.55 condition - substep 6, ref. Appendix C, Figure C - 5.**
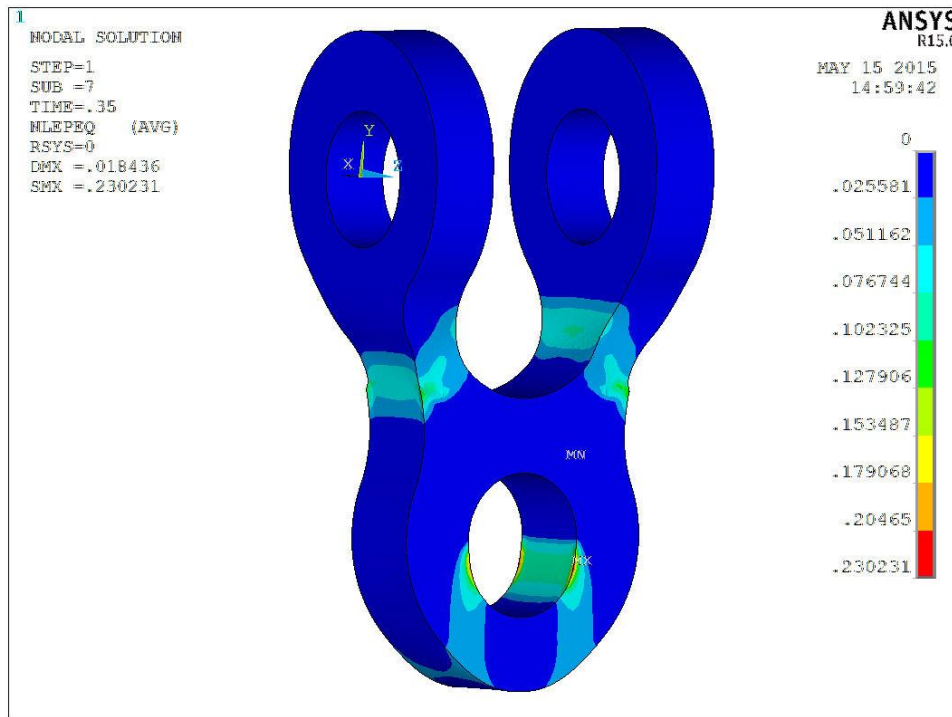
**Figure 8.8: The equivalent plastic strain for the new connecting link – MBLx1.55 condition - substep 7, ref. Appendix C, Figure C - 6.**

From the above-mentioned results it can be concluded that the plastic strain capacity of the new connecting link is within the specified requirements, which is summarized in Table 8.16 below.

**Table 8.16: The results from non-linear FE-analysis of the new connecting link**

| Position | Load Condition | Equivalent Plastic Strain, $\varepsilon_{eqv}$ | Permissible Plastic Strain, $\varepsilon_p$ | Usage factor, $\eta = \varepsilon_{eqv} / \varepsilon_p$ |
|---|---|---|---|---|
| See Appendix C, Figure C - 1 | MBL | 0.80% | 5% | 0.16 |
| See Appendix C, Figure C - 3 | MBLx1.1 | 0.98% | 5% | 0.20 |
| See Appendix C, Figure C - 5 | MBLx1.55 | 5% | 5% | 1 |

The usage factor for the MBL condition is 0.16 and for the MBLx1.1 it is 0.20. The collapse load for the new connecting link is MBLx1.55, which is equal to a load of 25575 kN.

### 8.3.3 The Ultimate Limit States Results

Hand calculations of the new connecting link for the ULS condition can be found in Appendix D. The geometry of the new connecting link is shown in Figure 8.9 and Figure 8.10, and in Appendix F. For location of position and sections, see Figure D - 1 in Appendix D.

The ULS condition is calculated according to the given theory in Chapter 3. Table 8.17 shows the results for the new connecting link towards turret and Table 8.18 show the results for the new connecting link towards socket.

Table 8.17: The result for the new connecting link towards turret.

| Component | Design Condition | Equivalent Stress, $\sigma_{eqv}$ [MPa] | Permissible Stress, $\sigma_p$ [MPa] | Usage factor, $\eta = \sigma_{eqv} / \sigma_p$ |
|---|---|---|---|---|
| Section OP | ULS | 108.31 | 327.76 | 0.33 |
| Point N | ULS | 150.81 | 327.76 | 0.46 |
| Pin hole pressure | ULS | 137.91 | 327.76 | 0.42 |
| Pin hole pressure (bearing) | ULS | 143.21 | 320 | 0.45 |

Table 8.18: The results for the new connecting link towards socket.

| Component | Design Condition | Equivalent Stress, $\sigma_{eqv}$ [MPa] | Permissible Stress, $\sigma_p$ [MPa] | Usage factor, $\eta = \sigma_{eqv} / \sigma_p$ |
|---|---|---|---|---|
| Section CD | ULS | 109.48 | 327.76 | 0.33 |
| Point B | ULS | 175.73 | 327.76 | 0.54 |
| Pin hole pressure | ULS | 160.96 | 327.76 | 0.49 |
| Pin hole pressure (bearing) | ULS | 174.10 | 280 | 0.62 |

From the above-mentioned results it can be concluded that the strength of the new connecting link with respect to excessive yielding are within specified requirements. The maximum usage factor for the connecting link is 0.62.

**Output to Fatigue Calculations**

The Mechanical Transfer Function (MTF) is defined as the relation between the occurring stresses divided by the applied load. Maximum Principal Stress is used. The local hot spot stresses are taken from hand calculations of the connecting link. In Table 8.19 below the MTF is given for the most loaded hot spot as a reference to the fatigue analysis.

To account for the geometric stress concentration in the new connecting link the maximum principal stress is multiplied by a geometrical stress concentration factor (SCF) of 3.27. This is found by taking the maximum principal stress at the relevant hot spot location from a FE-analysis of the new connecting link, see Figure D - 2, Appendix D, divided by the nominal principal stress found from hand calculations, ref. Appendix D. The SCF is therefore:

SCF = 489 MPa / 149.74 MPa = 3.27 (HS, New connecting link)

The Mechanical Transfer Function for the new connecting link is shown in Table 8.19 below.

**Table 8.19: Mechanical Transfer Function, MTF.**

| Hot Spot (HS) | Analysis Method | SCF | Applied Load [kN] | Max. Prinicpal Stress [MPa] | MTF [MPa/kN] | Ref. |
|---|---|---|---|---|---|---|
| HS, New connecting link | Hand calc. | 3.27 | 6700 | 149.74 | 0.0730 | Appendix D |

### 8.3.4 The Fatigue Analysis

The fatigue life predictions are based on the S-N approach and a linear damage accumulation according to the Miner summation rule and failure criterion. The number of cycles to failure is estimated according to a design S-N curve. These design curves are derived from Constant Amplitude (CA) laboratory tests with similar joints. The number of cycles to failure is plotted against the CA stress range. The scatter in fatigue life is modeled by a lognormal distribution at each stress level. The coefficient of variation is assumed constant at different levels. The design curve is drawn through the left tail of the distribution, normally at mean value minus two standard deviations. This corresponds to a probability of failure of 2.3%. (National Oilwell Varco, 2015c, p. 19).

The damage calculations for the new connecting link will be performed using the methods based on the linear damage hypotheses (Miner's rule). The fatigue life predictions are therefore carried out using the S-N curve format as presented in Section 3.7. The calculations of the predicted fatigue life have been done using Excel spread sheets. The calculations are shown in Appendix E.

The S-N curves are based on effective cathodic protection. From the document "STL Buoy Design Brief" it can be read: "Corrosion protection of the STL Buoy is in general based on a heavy duty spray coating in combination with cathodic protection" (National Oilwell Varco, 2014b). The DNV standard "Fatigue Design of Offshore Steel Structures" is used in the classification of the new connecting link, and the classification is shown in Table 8.20 below. According to the standard, S-N curve C should be selected for non-welded details (DNVGL-RP-0005: RP-C203, 2014).

**Table 8.20: Classification of HS.**

| Hot Spot | S-N curve | Log a N<$10^6$ cycles m = 3.0 | Log a N>$10^6$ cycles m = 5.0 | Thickness exponent, k | SCF in the S-N detail as derived by the hot spot method |
|---|---|---|---|---|---|
| **HS** | C | 12.192 | 16.320 | 0.15 | 1.00 |

A Design Fatigue Factor (DFF) of 10 and a Target Service Life (TSL) of 30 is given by the company.

The predicted fatigue life is found for three different projects (and theirs corresponding fatigue load spectra). The results are shown in Appendix E, and in the following subsections, the predicted fatigue life for Gina Krog FSO, Heidrun and Mariner will be presented.

**Gina Krog FSO**

Predicted fatigue life is found to be 8065 years. A fatigue design factor, DFF, of more than 10 is therefore achieved. Equation (3.8) gives the following: DFF = 8065 / 30 = 269. The conclusion for Gina Krog FSO is that the new connecting link for this specified load spectra, have a PFL > TSL · DFF, and are therefore within the specified requirements.

**Heidrun**

Predicted fatigue life is found to be 396 years. A fatigue design factor, DFF, of more than 10 is therefore achieved. Equation (3.8) gives the following: DFF = 396 / 30 = 13. The conclusion for Gina Krog FSO is that the new connecting link for this specified load spectra, have a PFL > TSL · DFF, and are therefore within the specified requirements.

**Mariner**

Predicted fatigue life is found to be 10252 years. A fatigue design factor, DFF, of more than 10 is therefore achieved. Equation (3.8) gives the following: DFF = 10252 / 30 = 342. The conclusion for Gina Krog FSO is that the new connecting link for this specified load spectra, have a PFL > TSL · DFF, and are therefore within the specified requirements.

Table 8.21 shows the summarized results for all of the three projects of interest.

**Table 8.21: Summary of the fatigue results for the three projects of interest.**

| Hot Spot/Project | Appendix | S-N curve | MTF [MPa/kN] | PFL [Years] | Resulting DFF [-] |
|---|---|---|---|---|---|
| HS, New connecting link, Gina Krog FSO | E | C | 0.0730 | 8065 | 269 |
| HS, New connecting link, Heidrun | E | C | 0.0730 | 396 | 13 |
| HS, New connecting link, Mariner | E | C | 0.0730 | 10252 | 342 |

### 8.3.5 Bearing Wear Assessment

The following information is obtained from the documentation for Gina Krog FSO (National Oilwell Varco, 2015b).

**Calculation Model**

The bearing will be subjected to wear. Wear rate can; within certain constraints be considered proportional to normal force and to sliding length. There is no exact approach to estimate the wear of sliding bearings. Nevertheless, a simple linear model based on experimentally found wear rates, bearing pressure and slide path can be used to predict a probable wear level throughout the design life of the structure. The following calculation model is assumed to estimate the wear of the mooring line bearing connections for a given load level and sliding length of the bearing:

$$W = K \cdot p \cdot s \cdot 10^{12} \tag{8.1}$$

Where:

| | |
|---|---|
| w | = wear in [mm] |
| K | = wear factor in [$m^3$/Nm] |
| p | = nominal bearing pressure in [MPa] |
| s | = sliding length in [km] |
| $10^{12}$ | = correction factor to get proper unit [$mm^3$ / ($m^2 \cdot$ km)] |

**Wear Factor**

The wear factor must be determined experimentally. Depending on test conditions, the established wear factors from different tests tend to vary somewhat.

- DEVA BM 362/9P

  $K = 0.16 \cdot 10^{-15}$ $m^3$/Nm

- Orkot TXM

  $K = 3.051 \cdot 10^{-15}$ $m^3$/Nm

**Allowable Wear**

The main purpose of the dynamic mooring line bearing connections is to provide free rotation of the socket relative to the steel structure to which it is connected (connecting link, turret lugs). The following criteria will limit the allowable wear for the mooring line bearing connections:

- Thickness of Orkot TXM sliding layer    10 mm
- Thickness of DEVA BM sliding layer    1.55 mm

**Wear Calculations and Results**

Applying the linear wear model to the wear factors and the slide paths and bearing loads that are given (National Oilwell Varco, 2015b, p. 33), the maximum wear for the dynamic bearings is calculated in Appendix G and summarized in Table 8.22.

Table 8.22: Predicted wear of the mooring line bearing connections.

| Bearing connection no. | Mean bearing pressure (max), [MPa] | Dynamic bearing capacity [MPa] | Max utilization (of bearing capacity) | Annual wear [mm] | Total wear [mm] | Limit sliding layer [mm] |
|---|---|---|---|---|---|---|
| 1. DEVA BM 362/9P | 17.55 | 150 | 0.117 | 0.03 | 0.3 | 1.55 |
| 2. ORKOT TXM | 20.86 | 65 | 0.32 | 0.05 | 0.5 | 10 |

The total wear is based on a design life of 10 years. The dynamic bearing capacity is found in the documentation for Gina Krog FSO (National Oilwell Varco, 2015b, p. 33). The max bearing utilization is far below the maximum allowable flexural bearing pressure of the bearing material. Hence, the capacity of the mooring bearings regarding dynamic bearing pressure is above the requirements.

### 8.3.6  Drawings of the New Connecting Link

The geometry of the new connecting link is shown in the following drawings, Figure 8.9 and Figure 8.10.
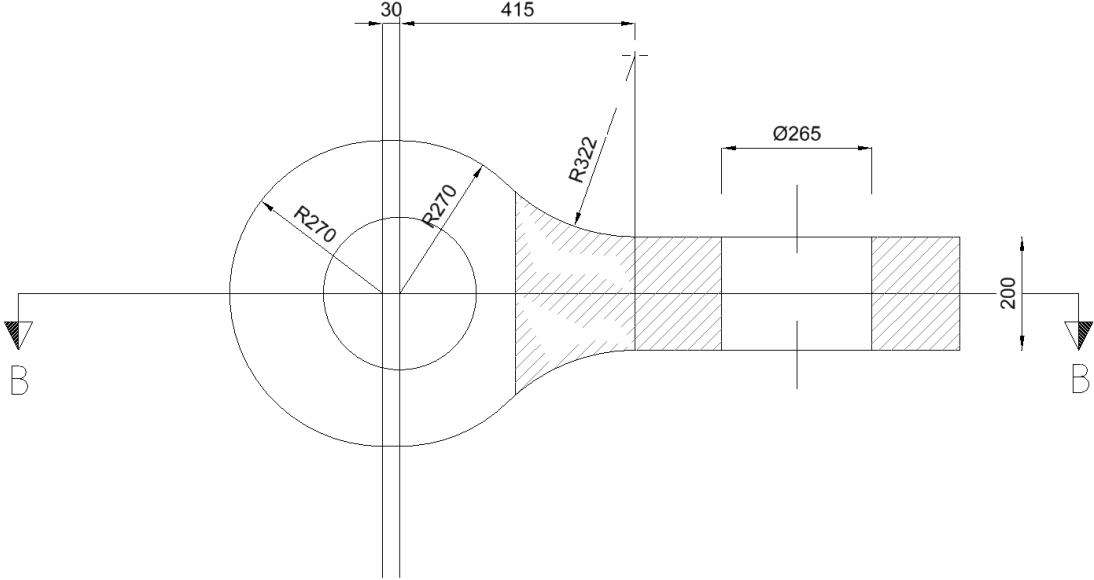


**Figure 8.9: The new connecting link's geometry - eye-bar, ref. Appendix F.**
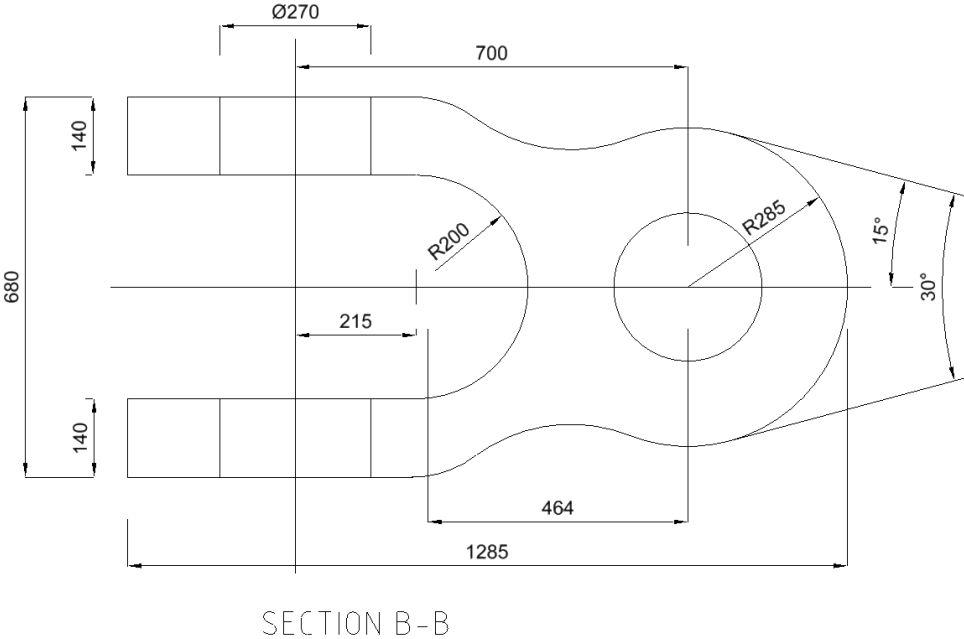


**Figure 8.10: The new connecting link's geometry - top view, ref. Appendix F.**

## 8.4 The New Connecting Link with Lugs, Washers and Rings

Figure 8.11 below show how the model looked like when the solution for the new connecting link with pins, lugs, washers and rings was performed in ANSYS (see also Chapter 0).
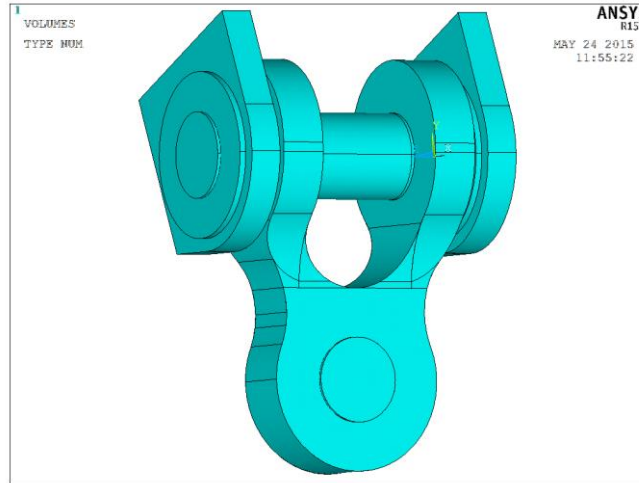


**Figure 8.11: The model of the new connecting link with pins, lugs, washers and rings.**

Further on, only the connecting link is selected when the results are presented. The results for the new connecting link with lugs, washers and rings are in this section only compared to the results for the new connecting link without lugs, washers and rings. The new connecting link with lugs, washers and rings are not analyzed with respect to the different conditions the connecting link is subjected to. The comparison is performed to verify that the model with lugs, washers and rings are appropriate regarding reliable and valid results. First, the minimum breaking load result is presented and compared, and then the ultimate limit states are presented and compared.

### 8.4.1 The Minimum Breaking Load Results
**MBL Condition**

For the MBL condition, the results vary a bit. The connecting link without lugs and so on, had an equivalent plastic strain equal to 0.80%. The connecting link with lugs and so on, has an equivalent plastic strain equal to 0.35%. The difference is therefore 0.45%, which is quite a considerable percentage. The von Mises stress results is also a bit different from the connecting link with lugs from the one without lugs. The highest von Mises stress for the connecting link without lugs is 539 MPa, and for the connecting link with lugs it is 513 MPa. The stress distribution looks almost the same, but the connecting link with lugs has areas with

higher stress concentrations than the one without lugs. The results are shown in Appendix C and Appendix H. Figure 8.12 and Figure 8.13 show the above-mentioned results.
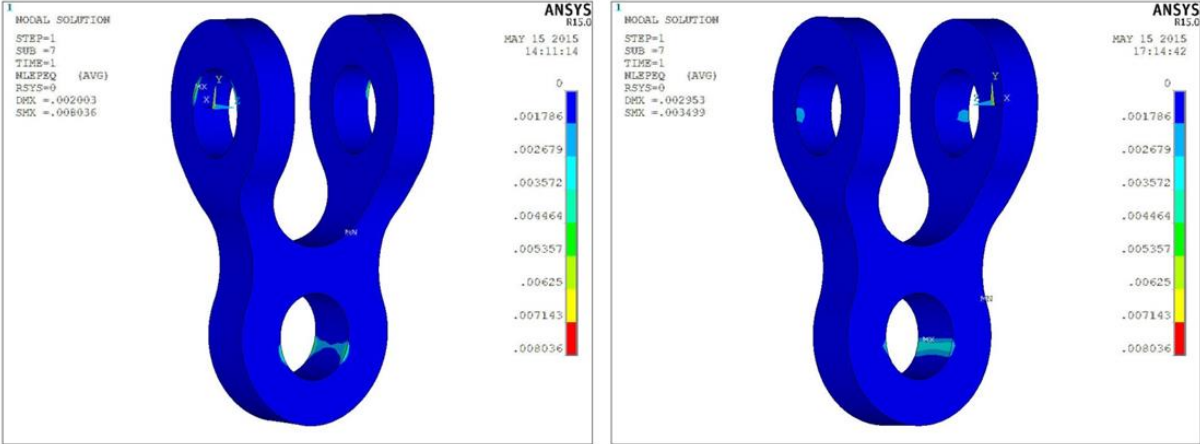


**Figure 8.12: The equivalent plastic strain results for the new connecting link without and with lugs, washers and rings, respectively – MBL condition, ref. Appendix C, Figure C - 1 and Appendix H, Figure H - 1.**
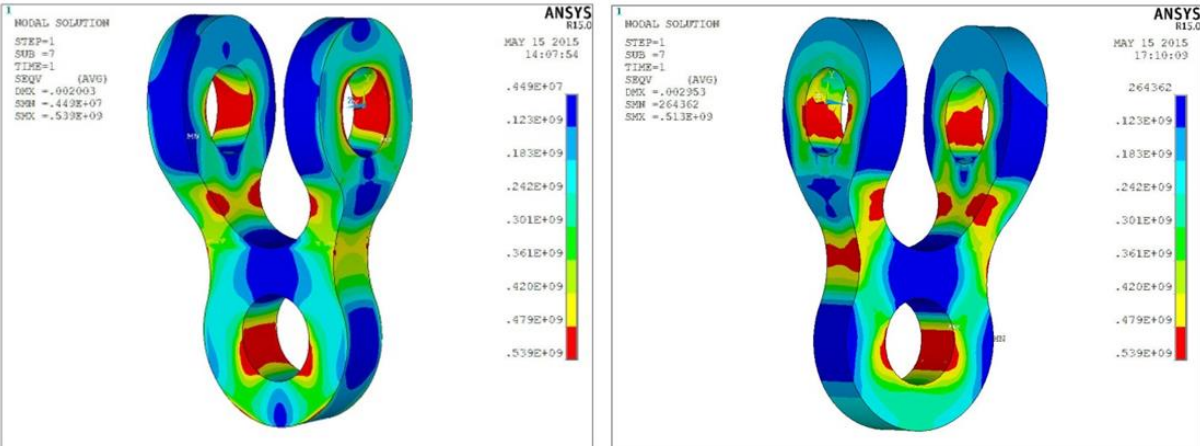


**Figure 8.13: The von Mises stress results for the new connecting link without and with lugs, washers and rings, respectively – MBL condition, ref. Appendix C, Figure C - 2 and Appendix H, Figure H - 2.**

## MBLx1.1 Condition

The results for the MBLx1.1 did not deviate that much from the MBL condition. The equivalent plastic strain result for the connecting link without lugs is 0.98%, and for the connecting link with lugs it is 0.50%. The difference is 0.48%, which is quite a lot. It seems like there are areas with higher equivalent plastic strains for the connecting link with lugs, than for the connecting link without lugs. The highest von Mises stress for the connecting link without lugs are 618 MPa, and for the connecting link with lugs it is 535 MPa. The difference is 83 MPa, which is then showing a quite reduced highest von Mises stress than it really is. The connecting link with lugs has areas with higher stress concentrations than the one without

lugs. The results are shown in Appendix C and Appendix H. Figure 8.14 and Figure 8.15 show the above-mentioned results.
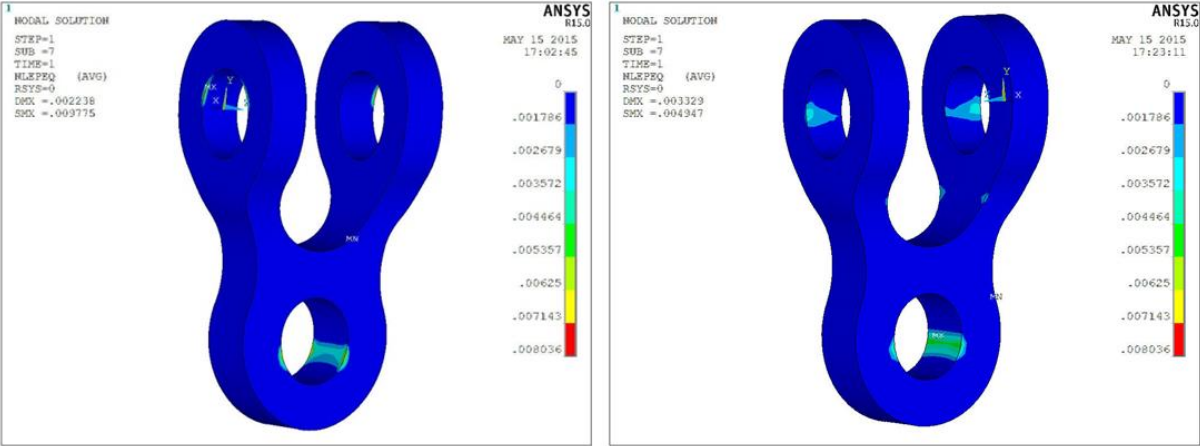


**Figure 8.14: The equivalent plastic strain results for the new connecting link without and with lugs, washers and rings, respectively – MBLx1.1 condition, ref. Appendix C, Figure C - 3 and Appendix H, Figure H - 3.**
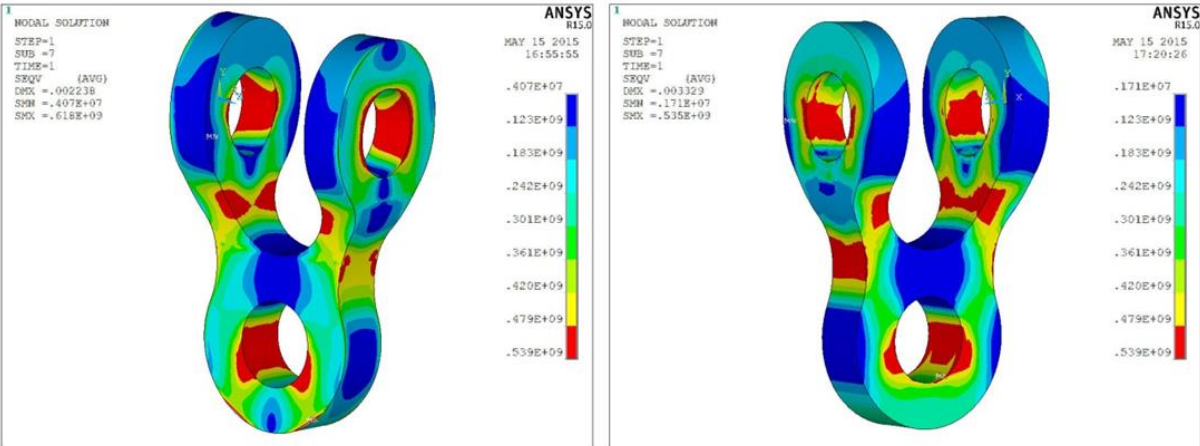


**Figure 8.15: The von Mises results for the new connecting link without and with lugs, washers and rings, respectively – MBLx1.1 condition, ref. Appendix C, Figure C - 4 and Appendix H, Figure H - 4.**

The results for MBL condition and MBLx1.1 condition show some deviations in the equivalent plastic strain, the highest von Mises stress and the stress distribution for the new connecting link with lugs, washers and rings. The new connecting link with lugs, washers and rings are modeled correctly, but it seems like the settings for the connecting link with lugs are not corresponding to the reality of the components working together with the connecting link. Some work with the settings must be done, in such a way that the results from the new connecting link with lugs, washers and rings can be reliable and valid.

### 8.4.2 The Ultimate Limit States Result

For the Ultimate Limit State the maximum principal stress distribution is compared. The maximum principal stress for the new connecting link without lugs, washers and rings is 489 MPa. For the connecting link with lugs, washers and rings, it is 398 MPa. The stress distribution for the two models look quite the same, but the maximum principal stress deviate a lot. The difference is 91 MPa, which is quite a considerable percentage. It seems like there should be some adjustments with the settings here as well. The results are shown in Appendix D Figure D - 2 and Appendix I. Figure 8.16 shows the above-mentioned results.
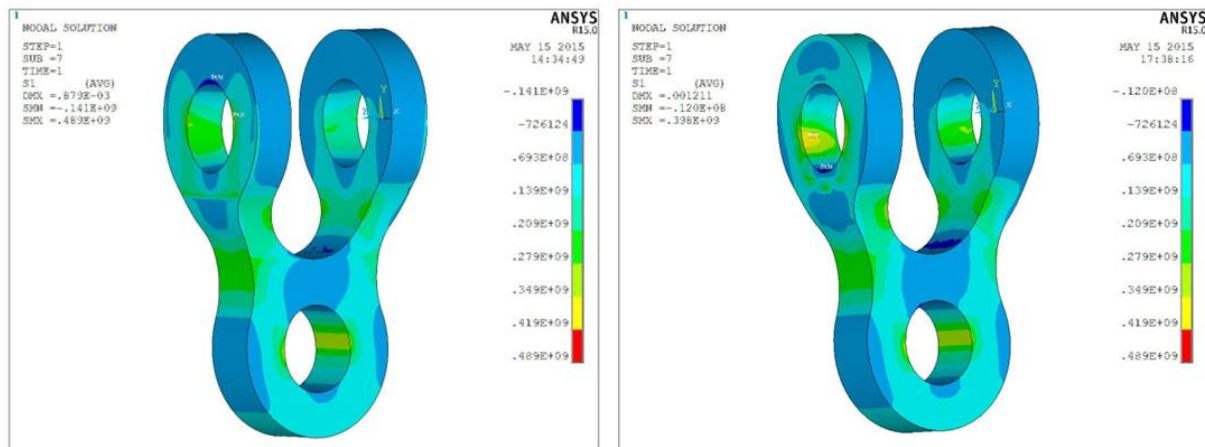


**Figure 8.16: The maximum principal stress for the new connecting link respectively without and with lugs, washers and rings - ULS condition, ref. Appendix D, Figure D - 2 and Appendix I, Figure I - 1.**

## 8.5   Structural Component vs. Mooring Component

The applied DNV standards were presented in Section 3.9.2.

When looking at the connecting link as a structural component, the following two offshore standards are the most relevant standards:

- DNV-OS-C101: Design of Offshore Steel Structures, General (LRFD method)
- DNV-OS-E301: Position Mooring

In this master's thesis, a non-linear solution has been chosen to solve the approach to the problem. The calculations and decisions are done according to both of these standards, but the main principle is based on the following statement: "Strength may also be documented by non-linear analysis using recognized programmes and procedures. A load factor of 1.1 is to be taken into account in the analysis. Plastic strain shall only occur at stress concentrations in local areas. Max allowable local plastic peak strain is not to exceed 5%" (DNV-OS-E301,

2013, p. 62). The plastic strains occurred only at stress concentrations in local areas and did not exceed 5%, which then satisfied the requirements from the offshore standard.

When looking at the connecting link as a mooring component, the following two offshore standards are the most relevant standards:

- DNV-OS-E302: Offshore Mooring Chain
- DNV-OS-E304: Offshore Mooring Steel Wire Ropes

The connecting link can be classified as a mooring chain accessory. From DNV-OS-E302 (2013, p. 23) the following are obtained:

"Mooring chain and accessories will be certified or classified based on the following main activities:

- Design verification
- Approval of manufacturers
- Survey during manufacture"

The thesis will focus on the design verification, since it is about optimization of the connecting link regarding the design. The following design verification statement shall be applied in conjunction with the technical requirements given in Ch. 2 of DNV-OS-E302: "Mooring chain cables and accessories shall be designed according to requirements given in Ch.2 Sec.2 [2.2] and [3.2], respectively. Where designs differ from this, the drawings and calculations shall be submitted to DNV for approval" (DNV-OS-E302, 2013, p. 23). For a chain accessory, e.g. the connecting link, the design requirement is the following: "Accessories shall be manufactured in accordance with ISO 1704 or approved drawings showing the finished dimensions and the surfaces that will be subjected to significant loading. Accessories of unconventional design shall have their drawings accompanied by calculations or design reports" (DNV-OS-E302, 2013, p. 20). The standard also has requirements regarding proof load testing, breaking load testing, mechanical testing, dimensions and tolerances, inspection, repair and identification. Regarding the certification and classification requirements, the design verification section has a reference to DNV-OS-E301, which states the following about the design requirements: "Chain links, shackles and accessories, except anchor shackles for mobile mooring, to be installed on DNV classed units shall be designed, manufactured and tested according to DNV-OS-E302. Tailor made connection elements shall

69

be approved by DNV with respect to structural strength and fatigue" (DNV-OS-E301, 2013, p. 94).

The standards are referring back and forth to each other, and it seems like the requirement of 5% max allowable plastic strain is inevitable. The connecting link can be classified as a mooring component, as long as it fulfills the requirements regarding proof load testing, breaking load testing, mechanical testing, dimensions and tolerances, inspection, repair and identification. The material grade that is chosen for the new connecting link, R3S, is a material grade used for mooring components. This means that the new connecting link is checked for the specified requirements given for the mooring component, ref. Section 8.3. The next step is to carry out an approval from DNV to change the connecting link from a structural component to a mooring component.

# 9   Conclusions

In this chapter the answers are summarized for the questions given in the problem statement section, see Section 1.2. The first research question is as follows:

*1. How does an optimization affect the connecting link, regarding strength and fatigue analysis?*

The strength analysis can be divided into three. The first part is about the MBL condition, the second about the ULS condition, and the last part is about the bearing wear assessment. The results for MBL condition and ULS condition are presented first, and the bearing wear assessment results are presented in the following subsection.

Several design conditions were examined, and the governing design conditions for the connecting link are given below:

- Operating condition, buoy connected, ULS
- Minimum Breaking Load of the mooring line, buoy connected, MBL

By considering the magnitude of the loads and associated design factors, ULS is considered to be the governing case for the design of the connecting link. The utilization factor, $\eta$, is defined as the actual equivalent stress divided by the design resistance. The strength capacity of the new connecting link without lugs, washers and rings was found adequate for all relevant loads. The maximum usage factors for the new connecting link without lugs, washers and rings are given in Table 9.1.

**Table 9.1: Usage factor for the new connecting link without lugs, washers and rings.**

| Component | Design condition | Usage factor, $\eta = \sigma_{eqv} / \sigma_p$ |
|---|---|---|
| Connecting link | ULS | 0.62 |
| | MBL | 0.16 |
| | MBLx1.1 | 0.20 |

Comparing usage factors for the new connecting link without lugs, washers and rings, with the usage factors for Heidrun and Gina Krog, the results are a bit different. The usage factor for ULS condition has decreased when comparing the connecting link used in Heidrun versus the new connecting link. For Heidrun the usage factor in ULS condition was 0.77. For the MBL condition, the usage factor has increased. The usage factor for MBL condition for Heidrun was 0.14. When comparing with Gina Krog FSO the usage factor for ULS condition

71

has increased. The usage factor was 0.51. For the MBL condition, the highest usage factor was 0.098, which means that the usage factor regarding MBL condition for the new connecting link has increased. So, when comparing the new connecting link with the one used in Gina Krog FSO, the usage factor has increased for both MBL condition and ULS condition. Regarding Heidrun, only the usage factor for MBL condition has increased, while the usage factor for ULS condition has decreased.

The total wear is based on a design life of 10 years. The max bearing utilization is far below the maximum allowable flexural bearing pressure of the bearing material. DEVA BM 362/9P has a utilization of 0.117 and Orkot TXM has a utilization of 0.32. Hence, the capacity of the mooring bearings regarding dynamic bearing pressure is above the requirements. Compared with the results from Gina Krog FSO, the usage factors have increased, but that does not matter since the usage factor is still far below the maximum allowable flexural bearing pressure.

Adding up all the results to a total result, the new connecting link has achieved a higher utilization than the connecting links used in Heidrun and Gina Krog FSO.

The Mechanical Transfer Function (MTF) is defined as the relation between the occurring stresses divided by the applied load. Maximum Principal Stress is used. The local hot spot stresses are taken from hand calculations of the connecting link. In Table 9.2 below the MTF is given for the most loaded hot spot as a reference to the fatigue analysis.

**Table 9.2: Mechanical Transfer Function - output to the fatigue calculations.**

| Hot Spot (HS) | Applied load | MTF [MPa / kN] |
|---|---|---|
| HS, New connecting link | Mooring tension T = 6700 kN | 0.0730 |

A Design Fatigue Factor (DFF) of 10 and a Target Service Life (TSL) of 30 is given by the company. The shortest allowable Predicted Fatigue Life (PFL) is therefore 300 years. The predicted fatigue life is found for three different projects and theirs corresponding fatigue load spectra. The fatigue life is predicted by the use of S-N data and the Miner linear summation rule for the damage contribution. For all of the projects of interest; Heidrun, Gina Krog FSO and Mariner, the predicted fatigue lives (PFL) are longer than 300 years (DFF > 10). It can be concluded that the new connecting link without lugs, washers and rings has sufficient strength

with respect to fatigue. A summary of the new connecting link's results for the three projects of interest is shown in Table 9.3.

**Table 9.3: Summary of the fatigue analysis for the new connecting link without lugs, washers and rings.**

| Hot Spot/Project | Appendix | S-N curve | MTF [MPa/kN] | PFL [Years] | Resulting DFF [-] |
|---|---|---|---|---|---|
| HS, New connecting link, Gina Krog FSO | E | C | 0.0730 | 8065 | 269 |
| HS, New connecting link, Heidrun | E | C | 0.0730 | 396 | 13 |
| HS, New connecting link, Mariner | E | C | 0.0730 | 10252 | 342 |

The next research question was the following:

2. *What benefits leads an optimization of the connecting link to?*

The main advantage of the optimization is the weight reduction. The original connecting link weighs 1321 kg, and when the optimization was finished, the new connecting link's weight is 844 kg. The weight reduction is therefore 477 kg, approximately 36%, which is quite a lot. This will affect not only the connecting link, but all the surroundings like the buoy, the locking mechanism located at the Floating Storage Unit (FSU) and many other things related to the connecting link. The STL mooring system configuration for Heidrun and Gina Krog FSO consist of nine and twelve mooring lines, respectively. The connecting link is the connecting point for the mooring lines to the turret. This means that for one single project, the weight reduction will be approximately 4300-5700 kg, just for the connecting link. The buoy might also have a weight reduction, since the connecting links are attached to the buoy, and the weight needed to lift the buoy into the FSU, will also be reduced. The following figure shows the difference in volume between the original connecting link and the new connecting link, Figure 9.1.
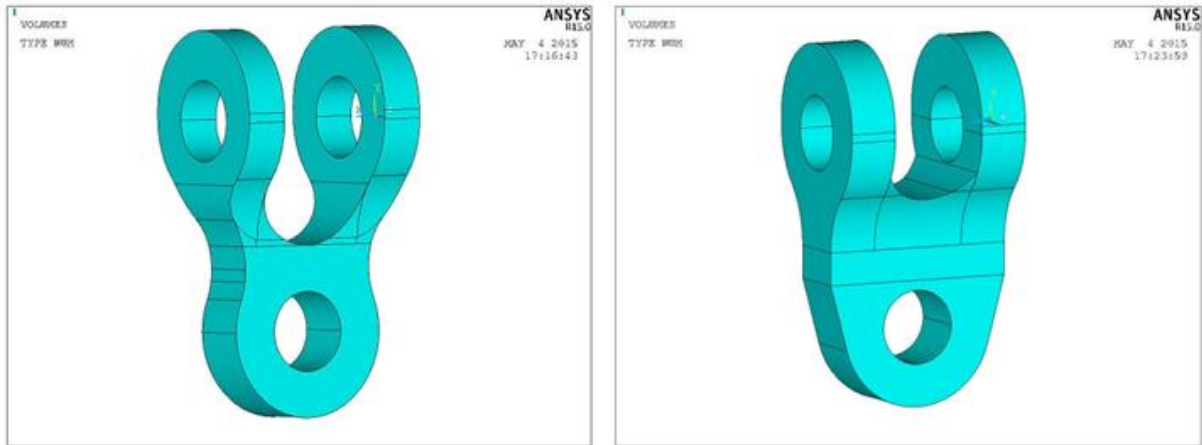
**Figure 9.1: Left: New connecting link - Weight = 844 kg. Right: Original connecting link - Weight = 1321 kg.**

Another aspect of the optimization is the costs. It will be possible to save costs, since the steel amount needed have been reduced quite drastically. One kilo of steel costs about 3 USD, which indicates a cost saving of approximately 12900-17100 USD for each project regarding the material cost of the connecting link. If the fabrication cost is taken into account as well, the cost saving will be even higher, since the fabrication cost is based on the amount of steel produced. An overview of the drawings of the new connecting link is shown in Figure 9.2.
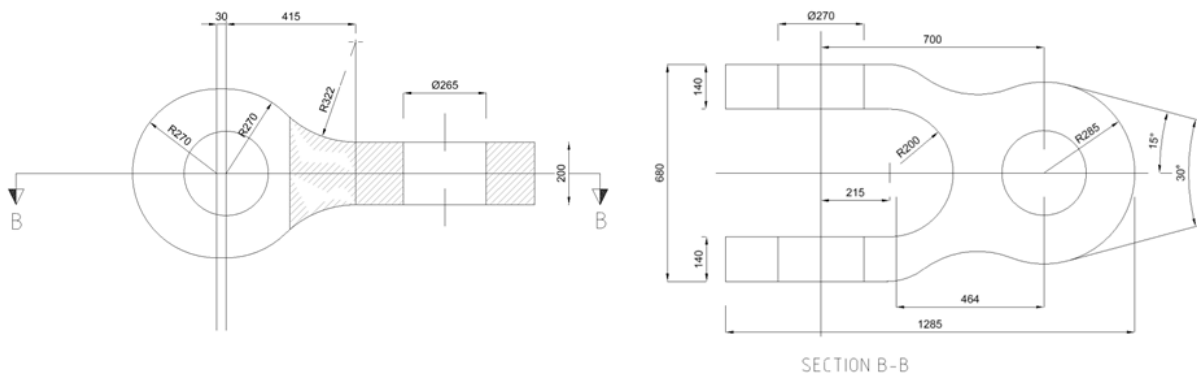


**Figure 9.2: The geometry of the new connecting link. Left: Eye-bar. Right: Top-view. Ref. Appendix F.**

The last research question is as follows:

3. *Which rules and regulations should be taken into account when changing the connecting link from a structural component to a mooring component, and what are the differences in the requirements?*

When looking at the connecting link as a mooring component, the following two offshore standards are the most relevant standards:

- DNV-OS-E302: Offshore Mooring Chain
- DNV-OS-E304: Offshore Mooring Steel Wire Ropes

The connecting link can be classified as a mooring chain accessory. From DNV-OS-E302 (2013, p. 23) the following are obtained:

"Mooring chain and accessories will be certified or classified based on the following main activities:

- Design verification
- Approval of manufacturers
- Survey during manufacture"

The standards are referring back and forth to each other, and it seems like the requirement of 5% max allowable plastic strain is inevitable. The connecting link can be classified as a mooring component, as long as it fulfills the requirements regarding proof load testing, breaking load testing, mechanical testing, dimensions and tolerances, inspection, repair and identification. The material grade that is chosen for the new connecting link, R3S, is a material grade used for mooring components. This means that the new connecting link is checked for the specified requirements given for the mooring component, ref. Section 8.3. The next step is to carry out an approval from DNV to change the connecting link from a structural component to a mooring component.

Weak points with the master's thesis is that the results are based on the same model and settings, which means that if there are something wrong with the model or the settings, the results and conclusions can be wrong. Strong points with the thesis are that the mesh applied on the model in ANSYS is verified. The mesh must be verified, so that considerations regarding the results from ANSYS are based on the right assumptions. To verify that the mesh is good enough, the element size is set to one size and a coarser and finer mesh are applied in two separate models. These results are then compared to validate that the determined element size is adequate to achieve correct results from the analyses performed in ANSYS.

Further work with the optimization could be to include another type of connecting link, different values for the MBL and other material grades. These aspects could be further investigated, to see if there are some differences compared to the results obtained from this master's thesis. Another interesting topic is the possibilities of avoiding real-life testing of the

connecting link. A method description on how to avoid real experiments, so-called virtual experiment, could be interesting to look further into.

# References

ANSYS Mechancial APDL 15.0.

Budynas, R. G. (1999). *Advanced strength and applied stress analysis* (2nd ed.). Boston: McGraw-Hill.

DNV-OS-C101: Design of Offshore Steel Structures, General (LRFD Method) (2014).

DNV-OS-E301: Position Mooring (2013).

DNV-OS-E302: Offshore Mooring Chain (2013).

DNV GL. (2015). Our history - The common history of DNV GL goes back to 1864. from https://www.dnvgl.com/about/in-brief/our-history.html

DNVGL-RP-0005: RP-C203: Fatigue design of offshore steel structures (2014).

Eurocode 0 - Basis of Structural Design, NS-EN 1990:2002+NA:2008 C.F.R. (2008).

Fish, J., & Belytschko, T. (2007). *A first course in finite elements*. Chichester: Wiley.

Larsen, P. K. (2010). *Dimensjonering av stålkonstruksjoner* (2nd ed.). Trondheim: Tapir akademisk forlag.

Lassen, T., & Récho, N. (2006). *Fatigue Life Analyses of Welded Structures*. London: ISTE.

Matchcad 15.

Moaveni, S. (2008). *Finite Element Analysis. Theory and Application with ANSYS. Third Edition.* Minnesota State University, Mankato: Pearson Education, Inc.

National Oilwell Varco. (2013). STL Buoy Turret Connections - Fatigue Analysis. *Heidrun Turret, Mooring and Swivel System*, 1-28.

National Oilwell Varco. (2014a). APL™ Smarter Turret Mooring. from http://fps.nov.com/media/1115/apl-brochure.pdf

National Oilwell Varco. (2014b). STL Bouy Design Brief. *Heidrun Turret, Mooring and Swivel System*, 1-32.

National Oilwell Varco. (2014c). STL Buoy Turret Connections - Strength Analysis. *Heidrun Turret, Mooring and Swivel System*, 1-54.

National Oilwell Varco. (2014d). STL™ Submerged Turret Loading.

National Oilwell Varco. (2014e). Turret Connecting Link Fabrication. *Heidrun Turret, Mooring and Swivel System*.

National Oilwell Varco. (2015a). About NOV - Our Company Structure. from http://nov.com/About_NOV.aspx

National Oilwell Varco. (2015b). Design Report - Strength - Turret Connections. *Gina Krog FSO*, 1-71.

National Oilwell Varco. (2015c). STL Buoy Turret Connections - Fatigue Analysis. *Gina Krog FSO*, 1-31.

Vértes, K. (2006). *Numerical and Experimental Parametric Study of the Ultimate Behaviour of Eye-bars.* (PhD, Budapest University of Techonology and Economics PhD), Katalin Vértes, Budapest.

Zienkiewicz, O. C., & Taylor, R. L. (2000). *The finite element method* (5th ed.). Oxford: Butterworth-Heinemann.

**Appendices**

# Table of Content for the Appendices

**Appendix A**

**Drawings of the original connecting link**

SECTION A-A

SECTION B-B

Figure A – 1: The geometry of the original connecting link – eye-bar and top view

82

**Appendix B**

**Results from the suggestions for the optimization of the connecting link**

**Figure B - 1: Result for suggestion A.1 Step 1.**
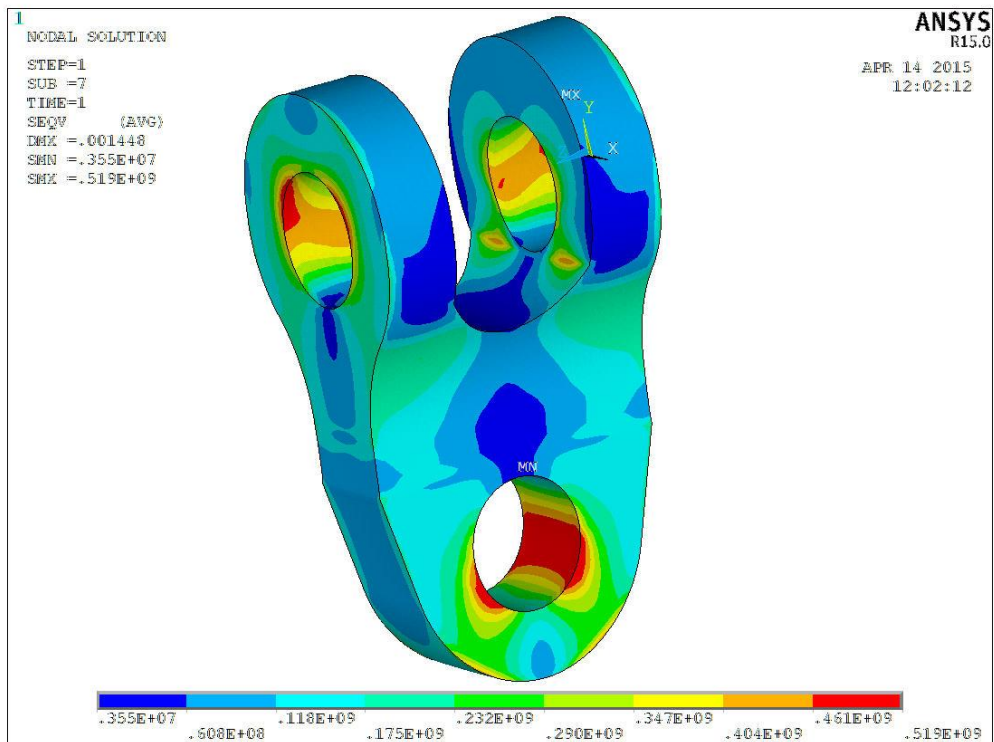


**Figure B - 2: Result for suggestion A.1 Step 2.**
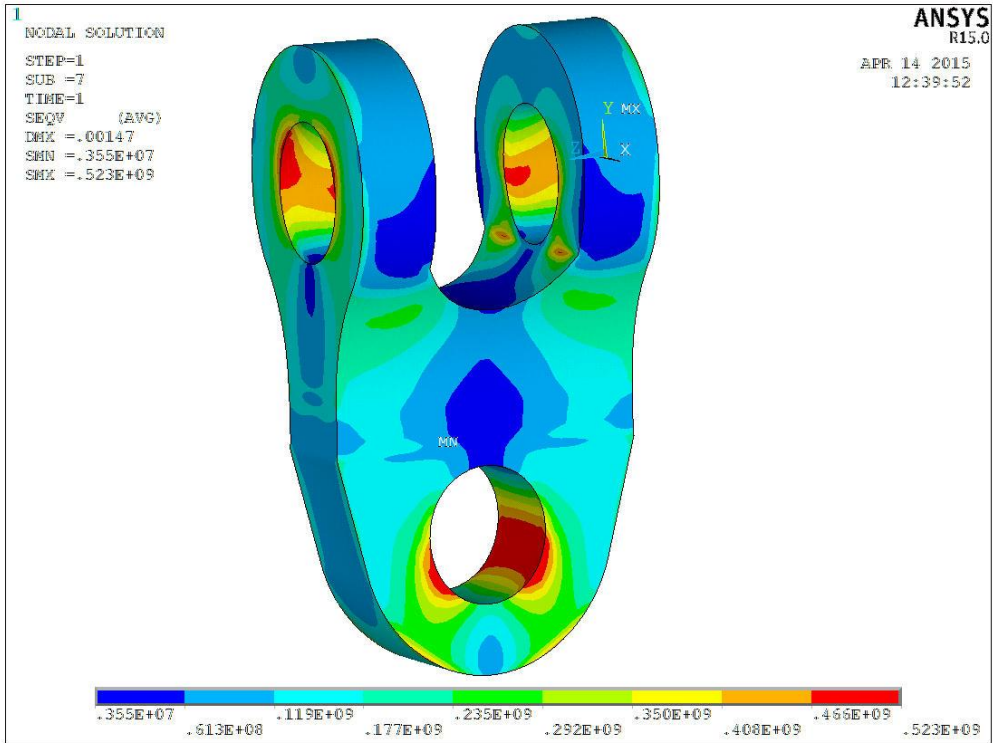
**Figure B - 3: Result for suggestion A.1 Step 3.**
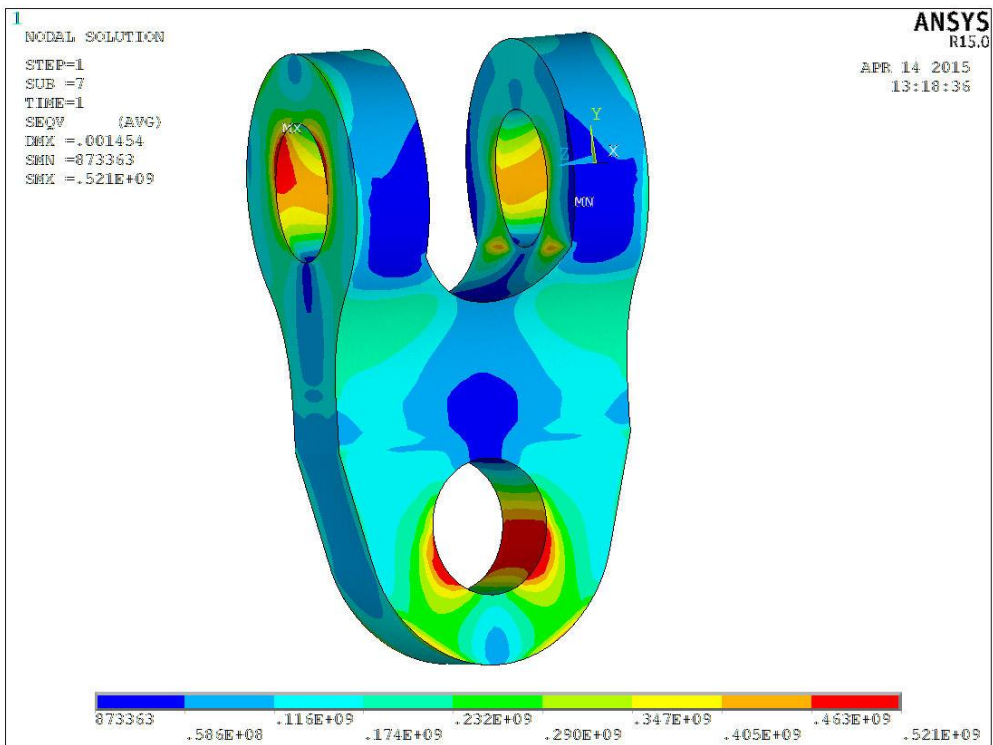


**Figure B - 4: Result for suggestion A.2.**

85
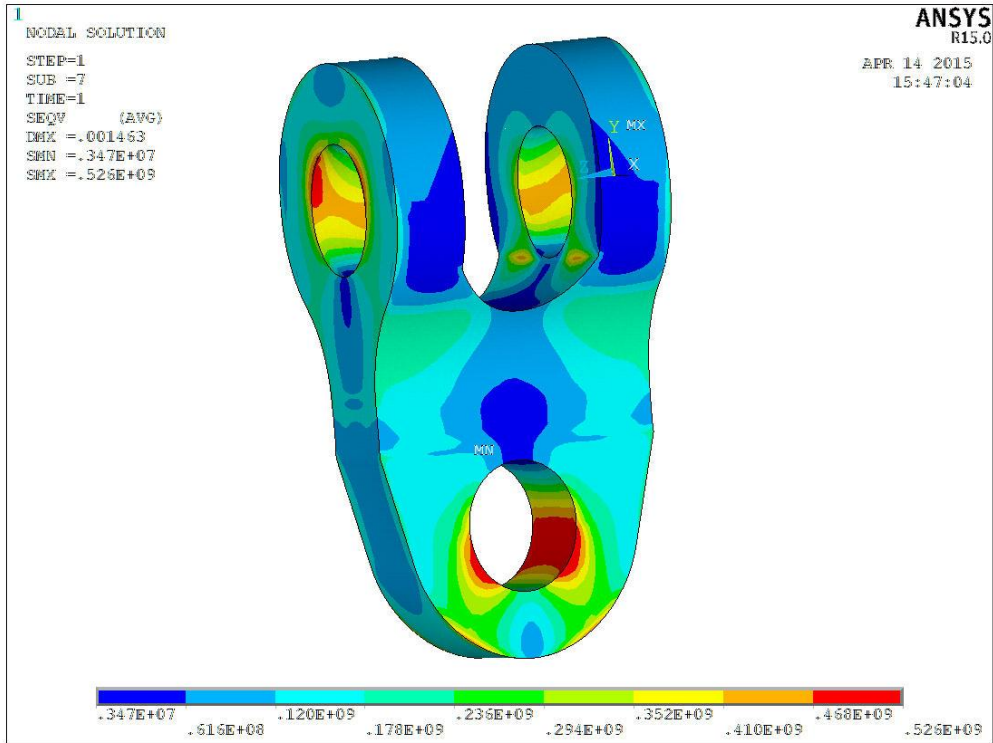
**Figure B - 5: Result for suggestion B.1 Step 1.**
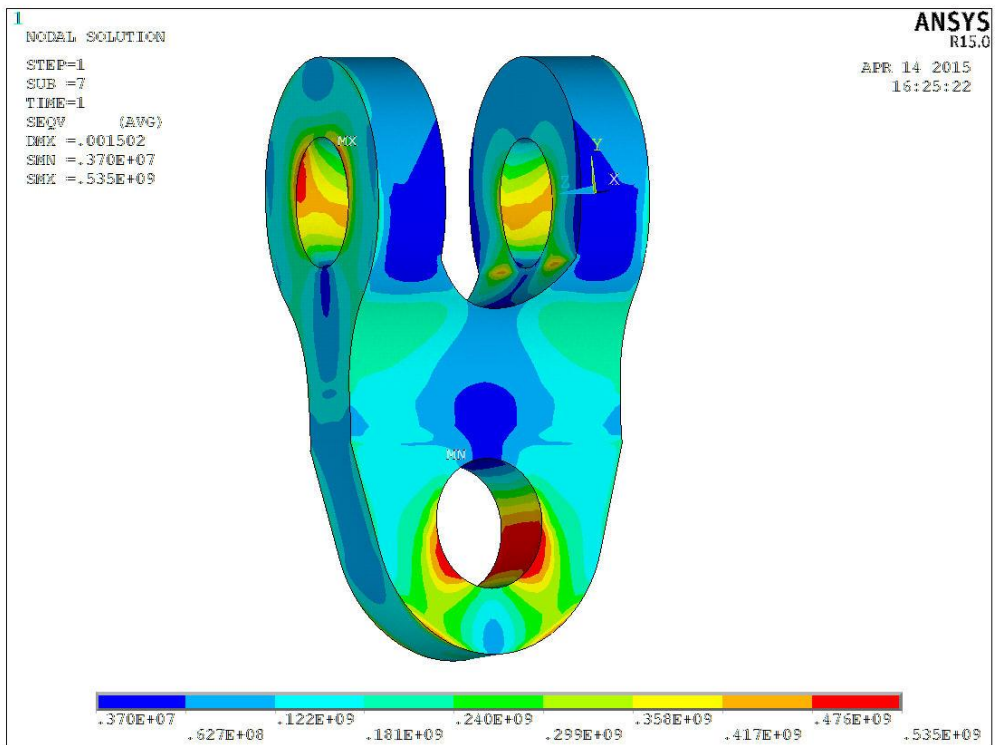


**Figure B - 6: Result for suggestion B.1 Step 2.**
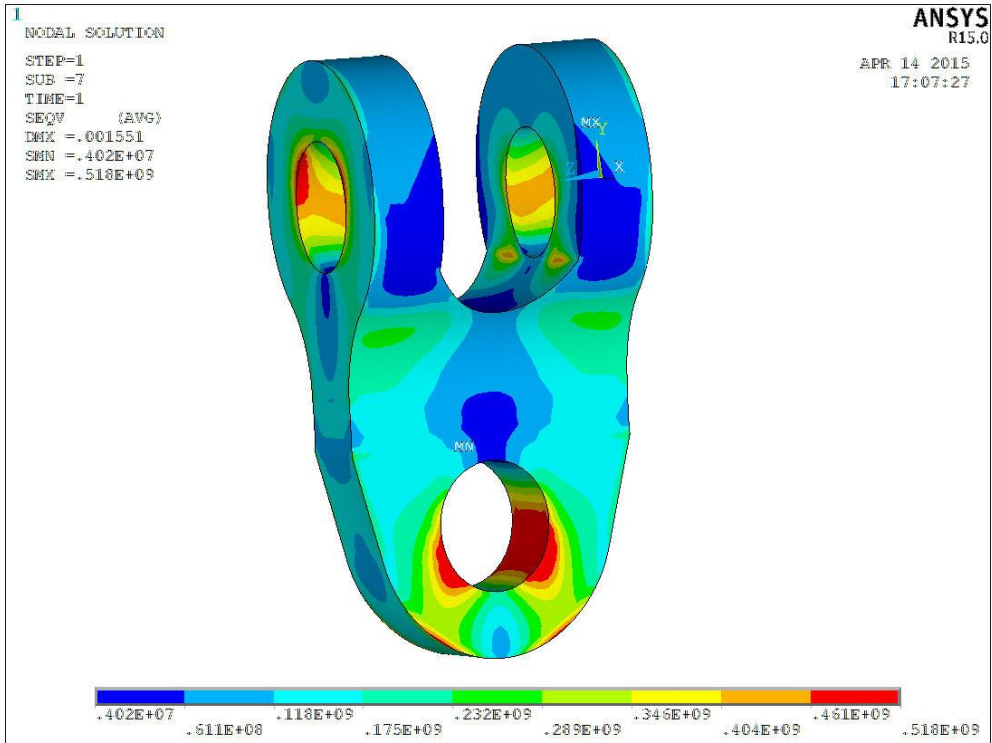
**Figure B - 7: Result for suggestion B.1 Step 3.**
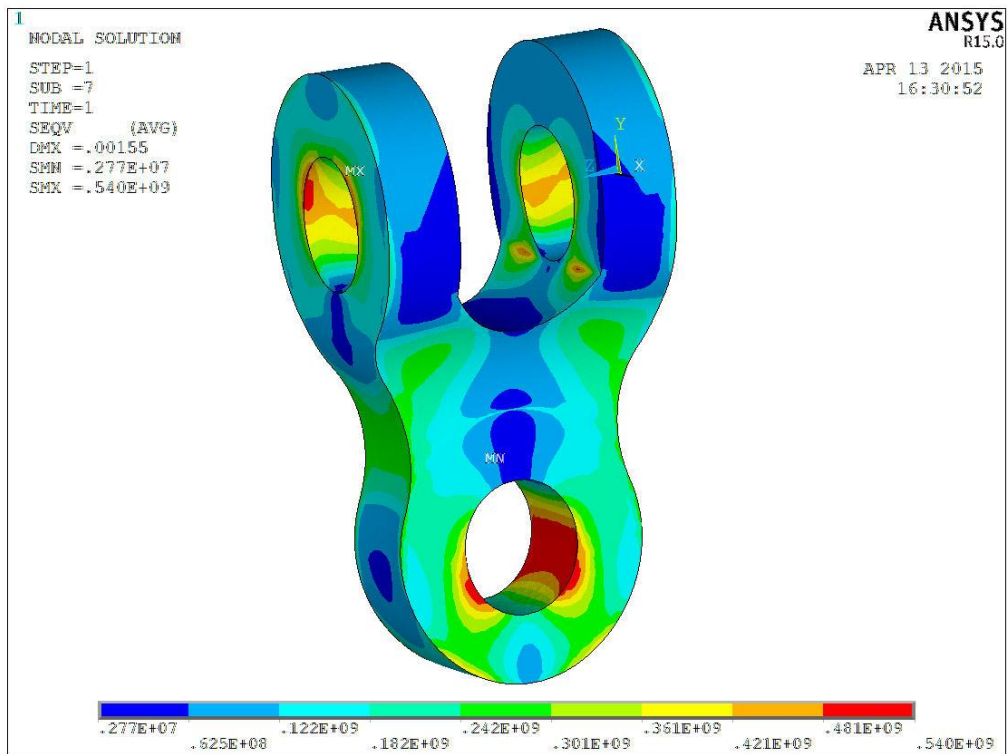


**Figure B - 8: Result for suggestion C.1.**
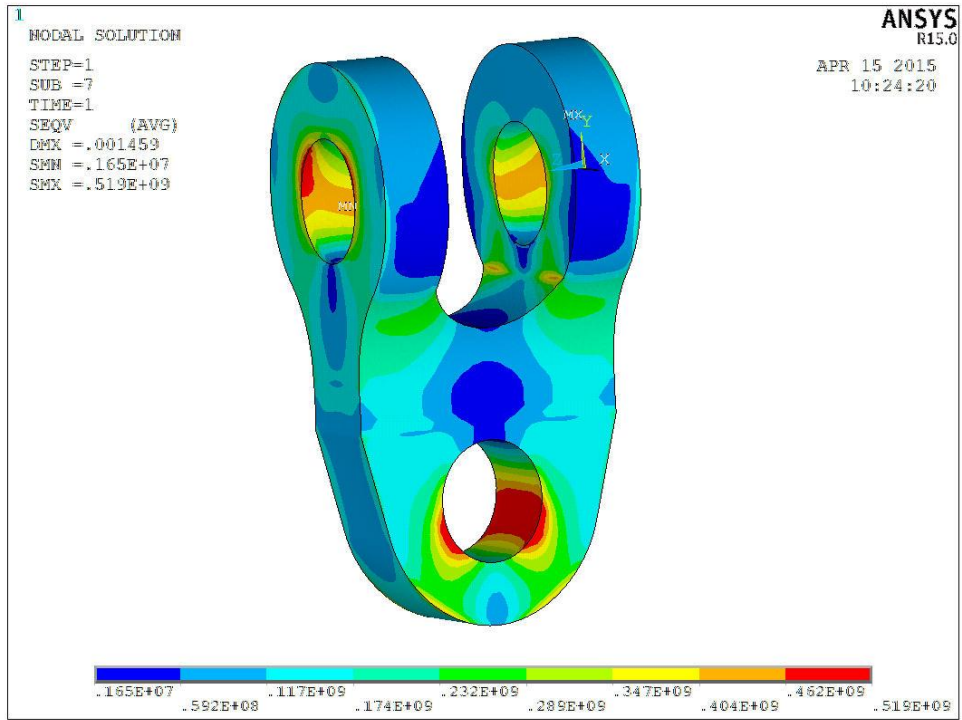
**Figure B - 9: Result for suggestion D.1 Step 1.**
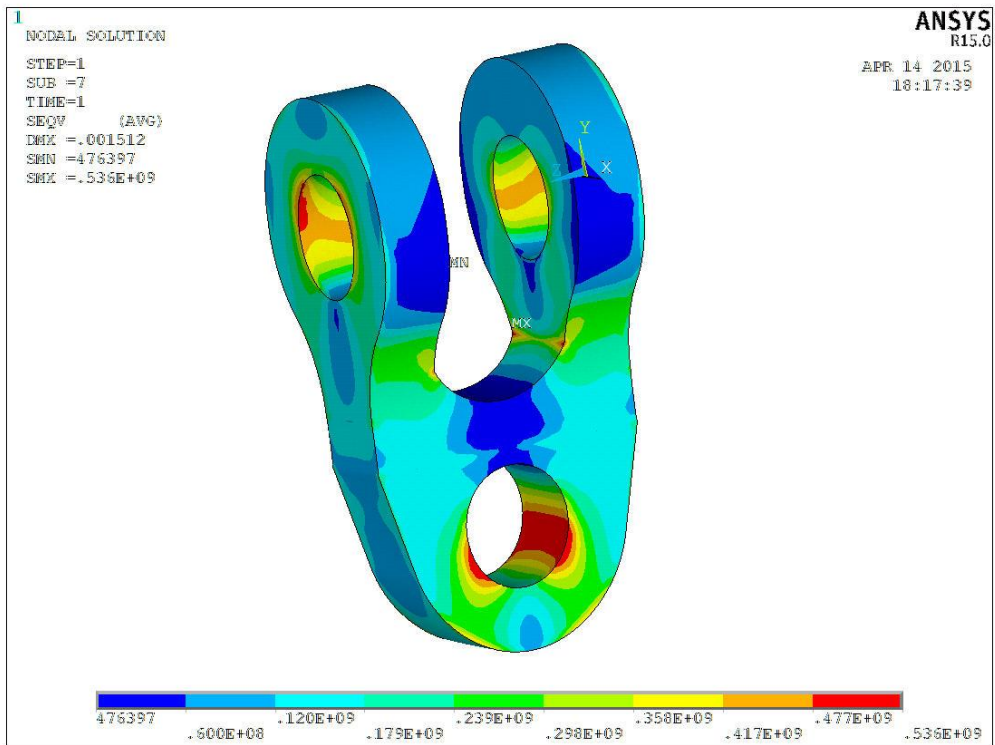


**Figure B - 10: Result for suggestion D.1 Step 2.**
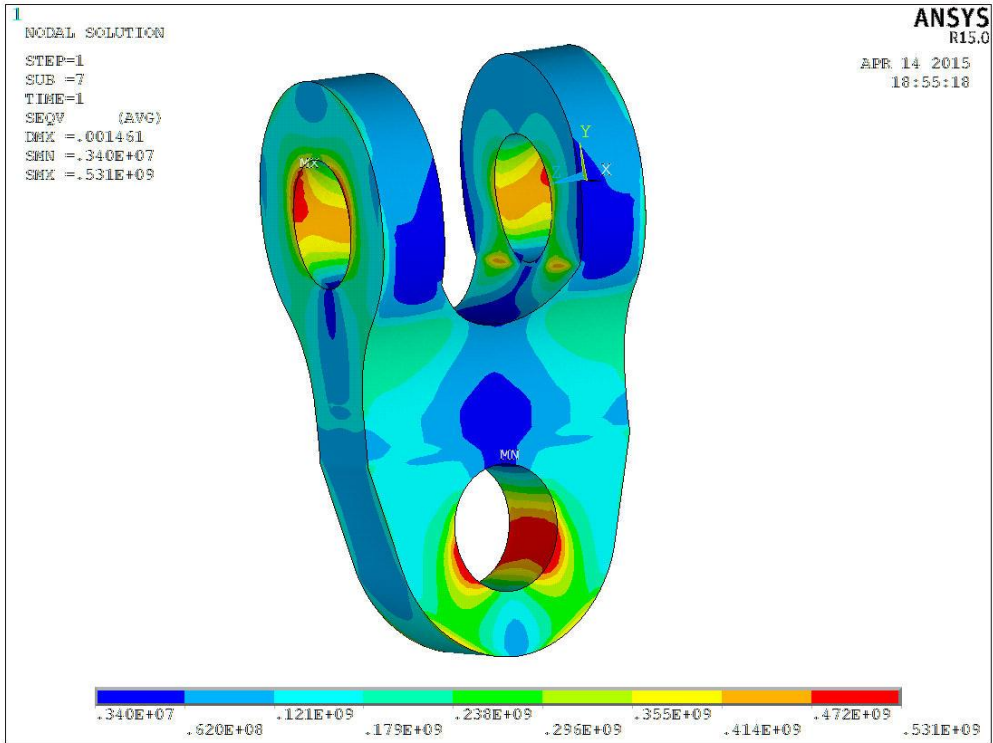
**Figure B - 11: Result for suggestion E.1 Step 1.**
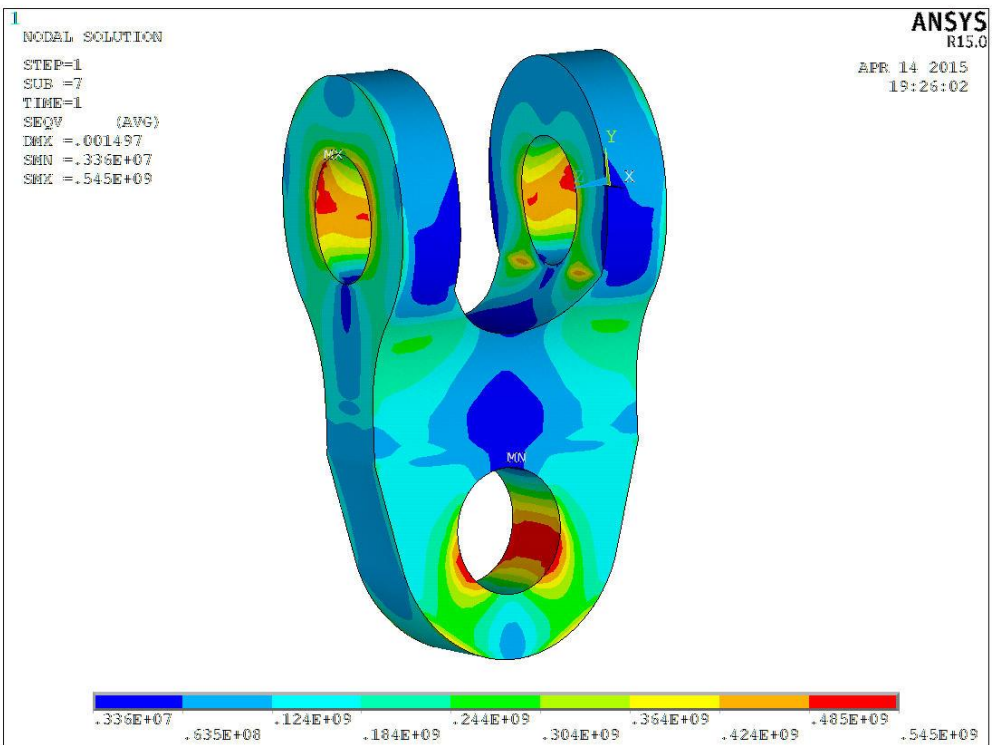


**Figure B - 12: Result for suggestion E.1 Step 2.**
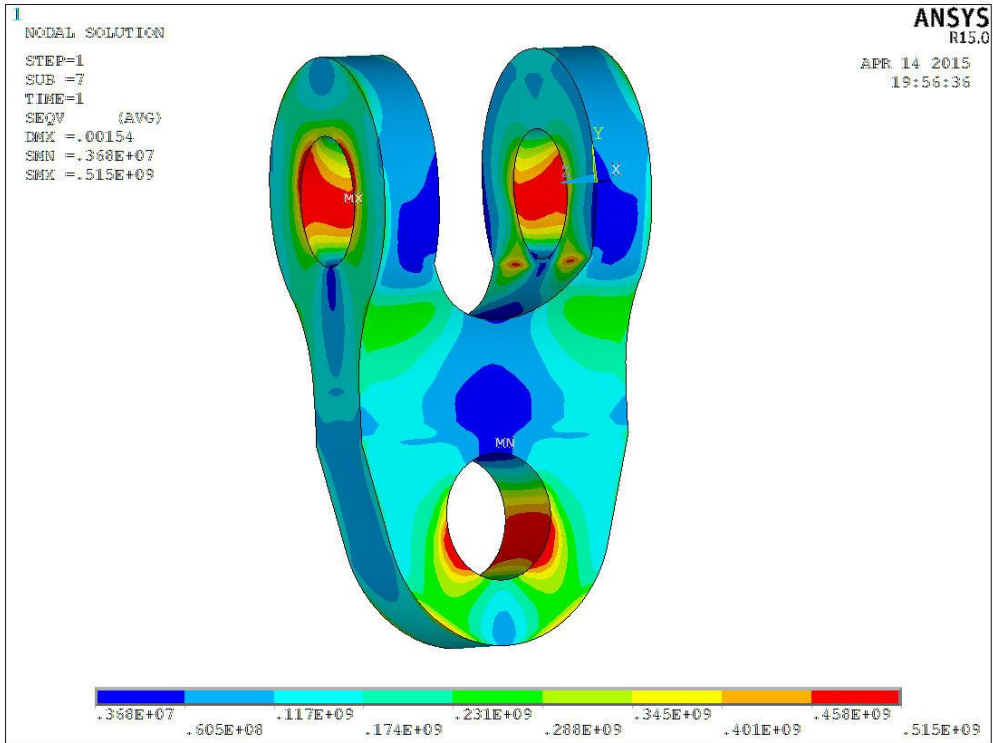
**Figure B - 13: Result for suggestion E.1 Step 3.**
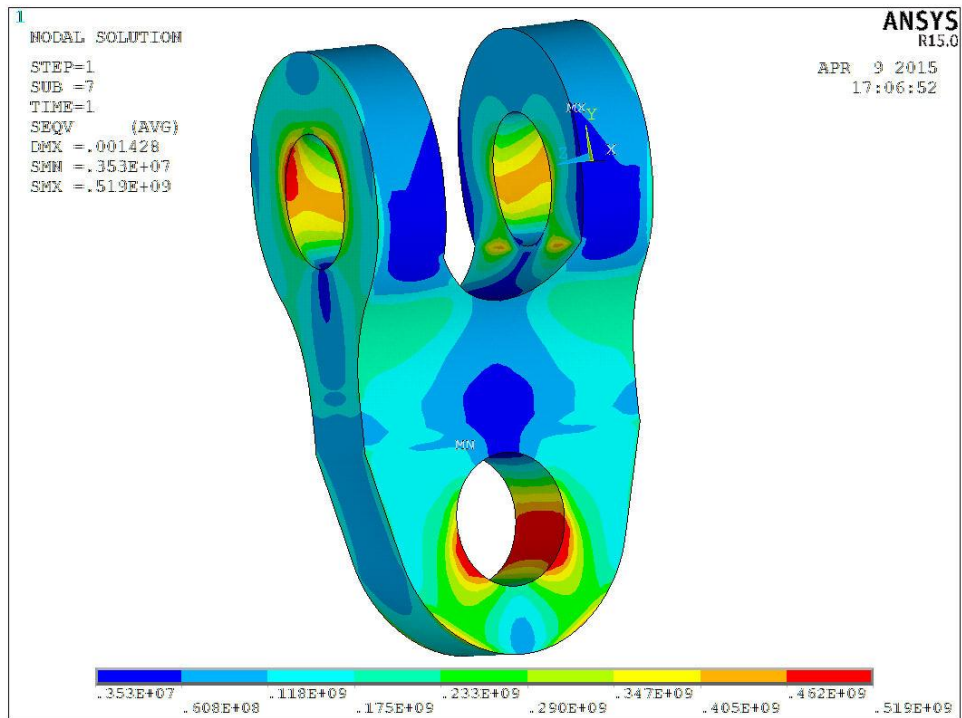


**Figure B - 14: Result for the original connecting link.**

**Appendix C**

**New connecting link without lugs, washers and rings**
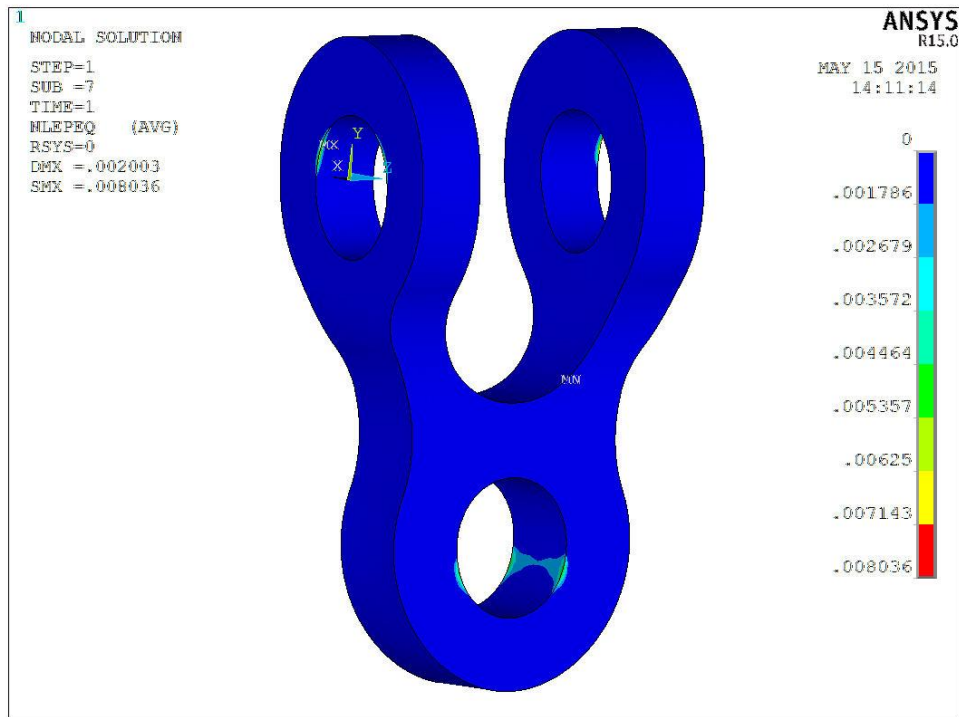
**MBL condition**

**Figure C - 1: The equivalent plastic strain result for the new connecting link – MBL condition**
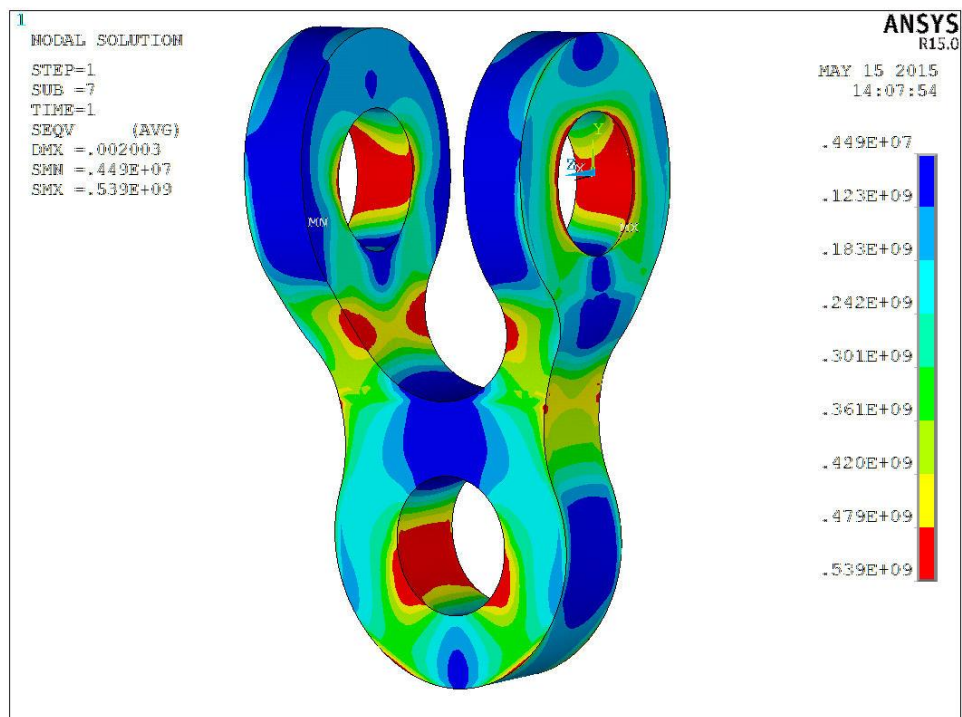


**Figure C - 2: The von Mises stress result for the new connecting link – MBL condition**
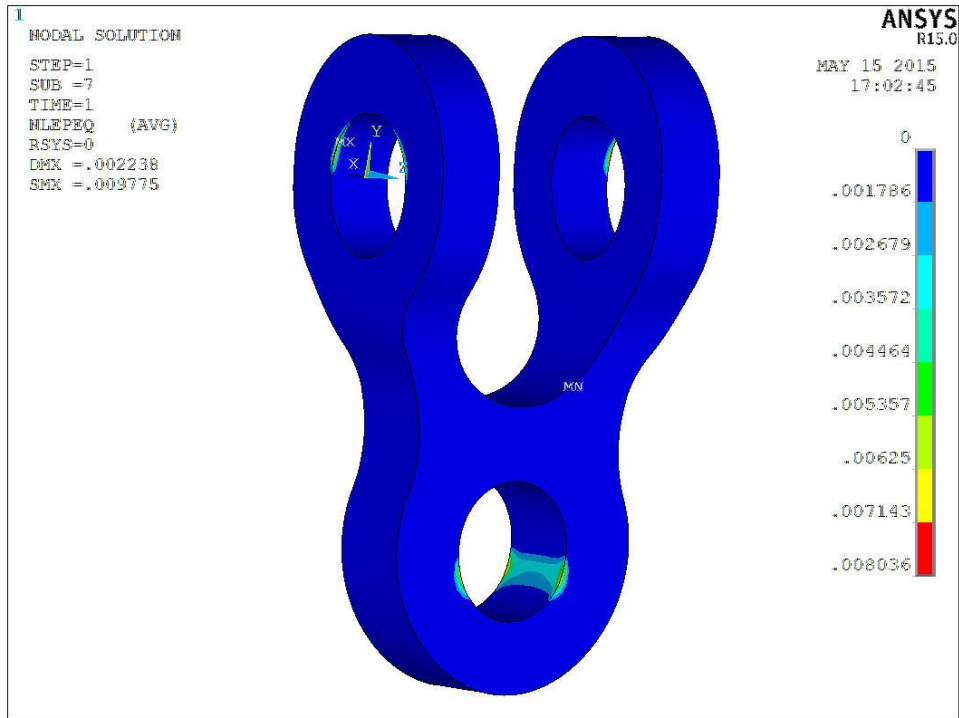
**Figure C - 3: The equivalent plastic strain result for the new connecting link – MBLx1.1 condition**
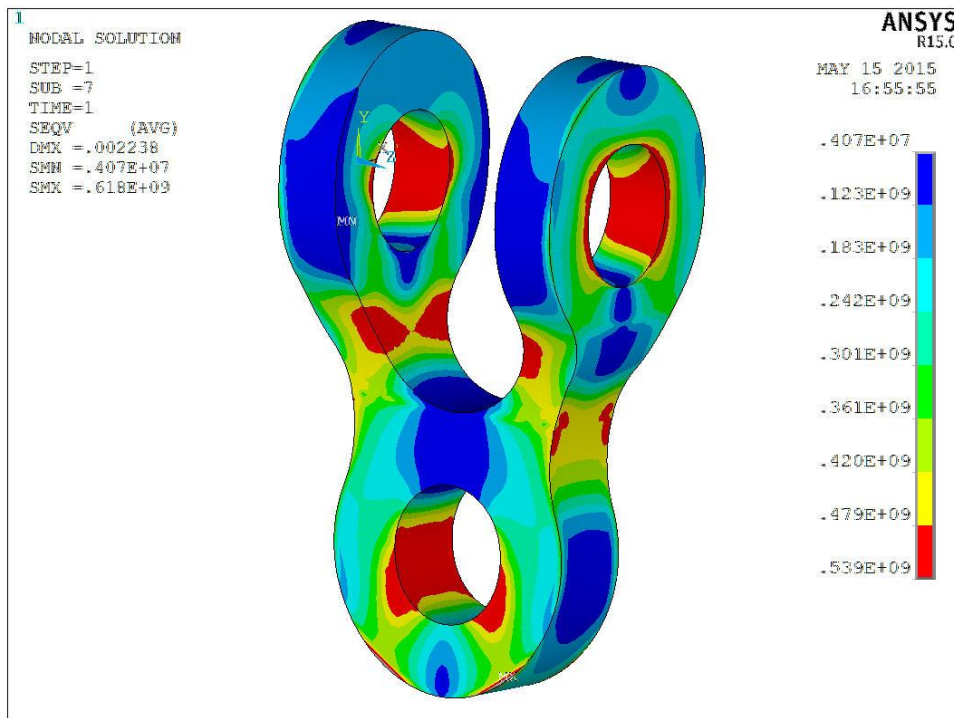


**Figure C - 4: The von Mises stress result for the new connecting link – MBLx1.1 condition**
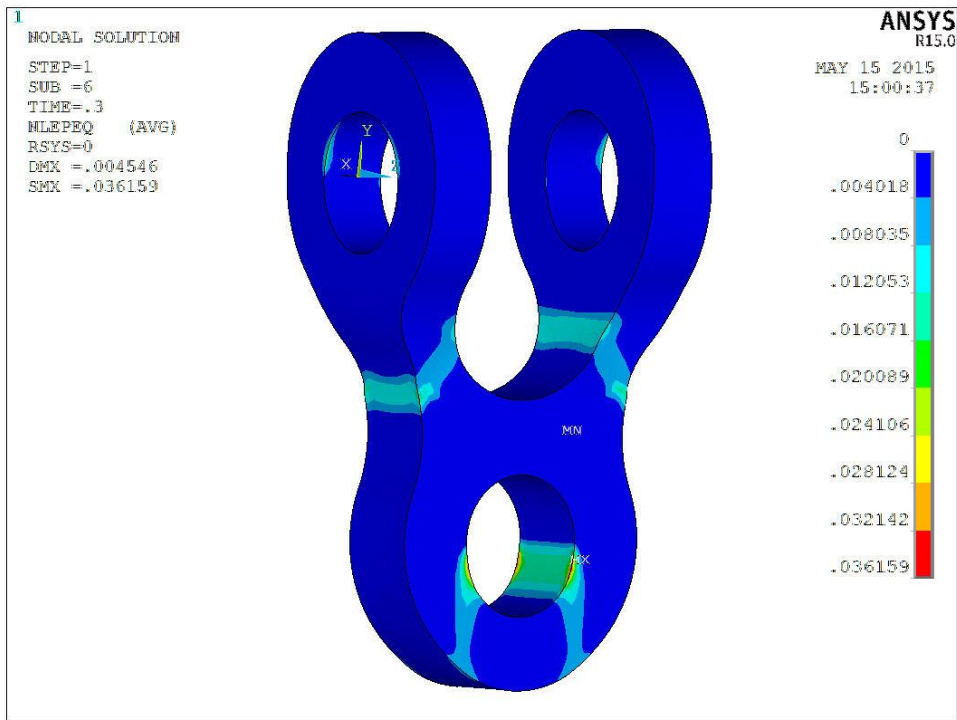
**Figure C - 5: The equivalent plastic strain result for the new connecting link – MBLx1.55 condition – substep 6**
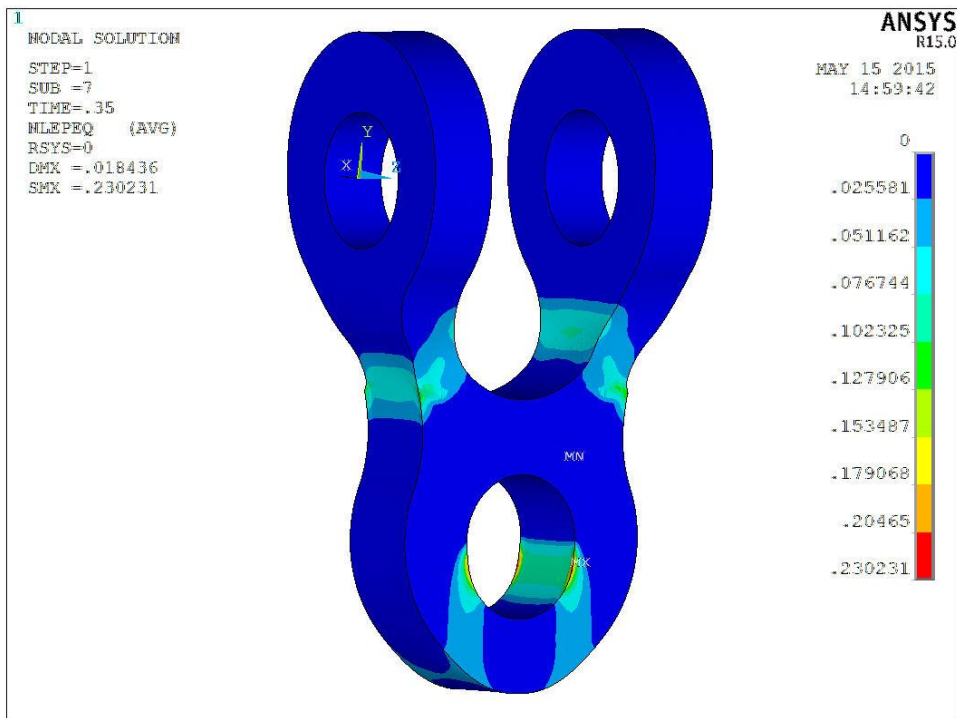


**Figure C - 6: The equivalent plastic strain result for the new connecting link – MBLx1.55 condition – substep 7**

**Appendix D**

**New connecting link without lugs, washers and rings**

**ULS condition**

# Connecting link - ULS condition

Including out of plane slip angle

## 1. Input data

### 1.1 Material and material properties

R3S

$f_y := 490MPa$      Yield strength

$f_u := 770MPa$      Ulimate strength

### 1.2 Load and material factors, ULS, Ref. [1]

$\gamma_f := 1.3$      Load factor

$\gamma_M := 1.15$      Material factor

$\gamma_d := \gamma_f \cdot \gamma_M = 1.495$      Design factor

### 1.3 Loads

$P := 6700kN$      Max. tension towards socket

$\alpha := 5.0deg$      OOP slip angle (in mooring)

$$F_2 := \frac{(P \cdot \cos(\alpha) \cdot 270mm + P \cdot \sin(\alpha) \cdot 700mm)}{540mm} = 4094 \cdot kN$$      Max. tension in connection towards turret

### 1.4 Geometry

Ref. Figure D - 1, and Appendix F Figure F - 1 for geometry details.

$h_{OP} := 135mm$    $b_{NR} := 236mm$    $t_{tu} := 140mm$    $d_{tu} := 270mm$    $d_{IDbushing} := 260mm$

$h_{NQ} := 138mm$    $b_{BF} := 207mm$    $t_{so} := 200mm$    $d_{so} := 265mm$    $d_{IDbushing1} := 245mm$

$h_{CD} := 153mm$

$h_{BE} := 158mm$

tu = Pinholes towards turret

so = Pinhole towards socket

$A_{n.OP} := 2t_{tu} \cdot h_{OP} = 3.78 \times 10^4 \cdot mm^2$      Cross section area through OP.

$A_{n.NQ} := 2t_{tu} \cdot h_{NQ} = 3.86 \times 10^4 \cdot mm^2$      Cross section area through NQ.

$A_{v.NR} := 2t_{tu} \cdot b_{NR} = 6.61 \times 10^4 \cdot mm^2$      Cross section area through NR.

$A_{n.CD} := 2 \cdot t_{so} \cdot h_{CD} = 6.12 \times 10^4 \cdot mm^2$      Cross section area through CD.

$A_{n.BE} := 2 \cdot t_{so} \cdot h_{BE} = 6.32 \times 10^4 \cdot mm^2$      Cross section area through BE.

$A_{v.BF} := 2 \cdot t_{so} \cdot b_{BF} = 8.28 \times 10^4 \cdot mm^2$      Cross section area through BF.
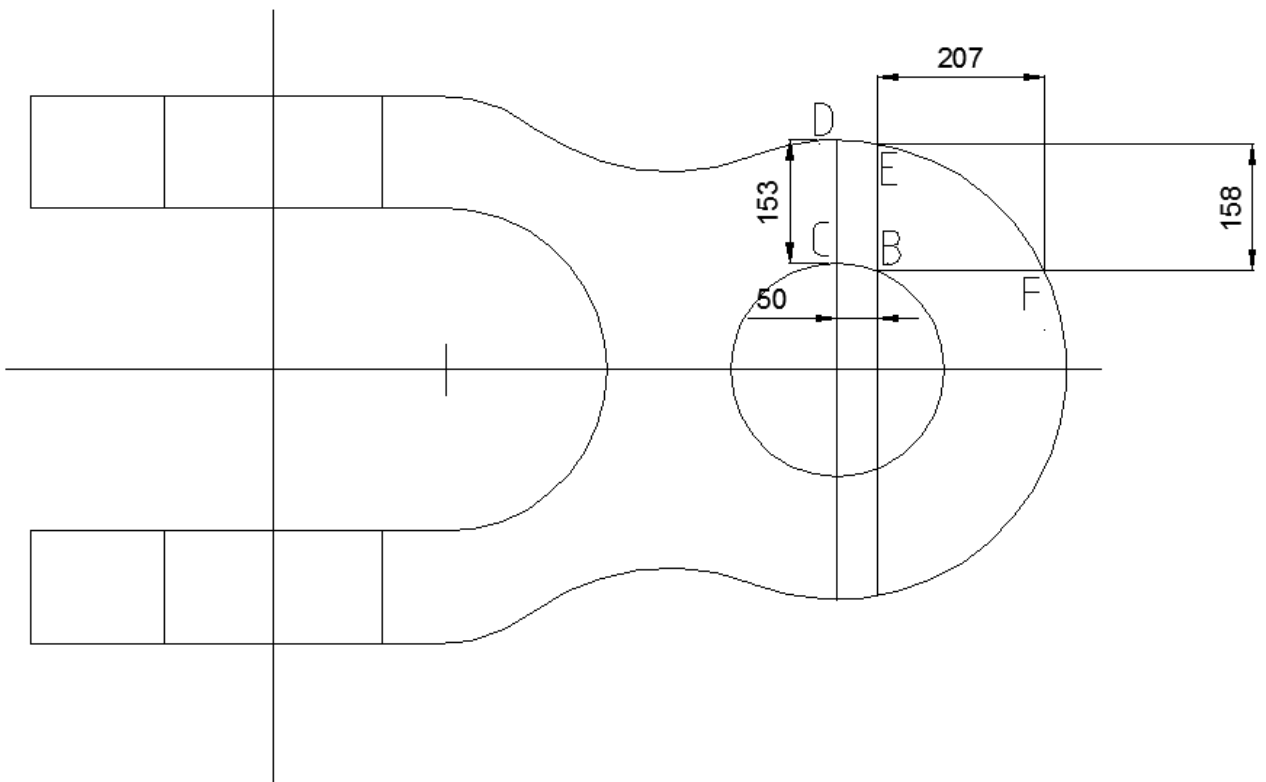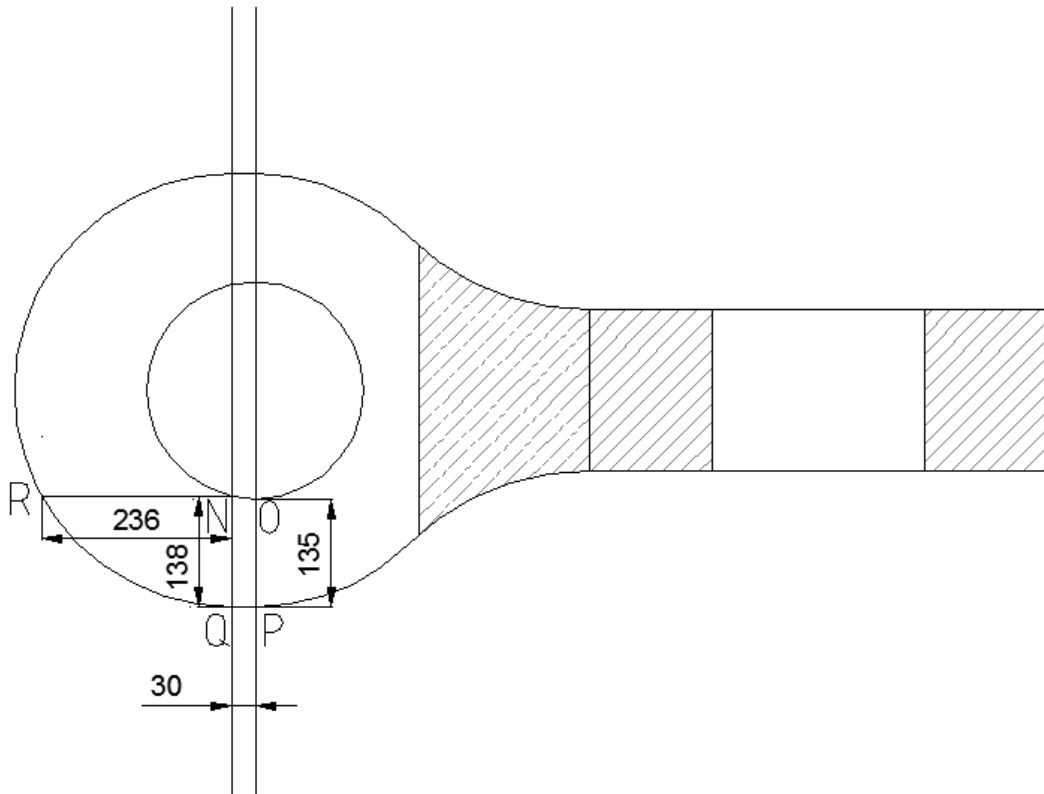
**Figure D - 1: New connecting link (schematic sketch)**

## 2. Design resistance

$$\sigma_d := \frac{f_y}{\gamma_d} = 327.76 \cdot MPa$$

Permissible normal stress, ULS

$$\tau_d := \frac{f_y}{\gamma_d \cdot \sqrt{3}} = 189.23 \cdot MPa$$

Permissible shear stress, ULS

## 3. Connection towards turret

### 3.1 Tensile stress section OP

$$\sigma_{t.tu} := \frac{F_2}{A_{n.OP}} = 108.31 \cdot MPa$$

$$UR_{t.tu} := \frac{\sigma_{t.tu}}{\sigma_d} = 0.33$$

### 3.2 Equivalent stress in point N

$$\sigma_{N.tu} := \frac{F_2}{A_{n.NQ}} = 105.96 \cdot MPa$$

$$\tau_{N.tu} := \frac{F_2}{A_{v.NR}} = 61.96 \cdot MPa$$

$$\sigma_{eqv.tu} := \sqrt{\sigma_{N.tu}^2 + 3 \cdot \tau_{N.tu}^2} = 150.81 \cdot MPa$$

$$UR_{eqv.tu} := \frac{\sigma_{eqv.tu}}{\sigma_d} = 0.46$$

Maximum principal stress:

$$\sigma_{x.tu} := \sigma_{N.tu} \qquad \sigma_{y.tu} := 0 \qquad \tau_{xy.tu} := \tau_{N.tu}$$

$$\sigma_{1.tu} := \frac{\sigma_{x.tu} + \sigma_{y.tu}}{2} + \sqrt{\left(\frac{\sigma_{x.tu} - \sigma_{y.tu}}{2}\right)^2 + \tau_{xy.tu}^2} = 134.5 \cdot MPa$$

### 3.3 Pin hole pressure

Cosine distributed load. Max. at θ = 0 deg.

$$\theta := 0 deg$$

$$\sigma_{b.tu} := \frac{4F_2}{\pi \cdot d_{tu} \cdot t_{tu}} \cdot \cos(\theta) = 137.91 \cdot MPa$$

$$UR_{b.tu} := \frac{\sigma_{b.tu}}{\sigma_d} = 0.42$$

### 3.4 Pin hole pressure (Bearing)

$$\sigma_{bd} := 320 MPa \qquad \text{Maximum Permissible Stress (deva.bm 362/9P Bearing)}$$

$$\frac{3}{}$$

$$\sigma_{b.tu1} := \frac{4F_2}{\pi \cdot d_{IDbushing} \cdot t_{tu}} \cdot \cos(\theta) = 143.21 \cdot MPa$$

$$UR_{b.tu1} := \frac{\sigma_{b.tu1}}{\sigma_{bd}} = 0.45$$

## 4. Connection towards socket

### 4.1 Tensile stress section CD

$$\sigma_{t.so} := \frac{P}{A_{n.CD}} = 109.48 \cdot MPa \qquad\qquad UR_{t.so} := \frac{\sigma_{t.so}}{\sigma_d} = 0.33$$

### 4.2 Equivalent stress in point B

$$\sigma_{B.so} := \frac{P}{A_{n.BE}} = 106.01 \cdot MPa$$

$$\tau_{B.so} := \frac{P}{A_{v.BF}} = 80.92 \cdot MPa$$

$$\sigma_{eqv.so} := \sqrt{\sigma_{B.so}^2 + 3 \cdot \tau_{B.so}^2} = 175.73 \cdot MPa \qquad\qquad UR_{eqv.so} := \frac{\sigma_{eqv.so}}{\sigma_d} = 0.54$$

Maximum principal stress:

$$\sigma_{x.so} := \sigma_{B.so} \qquad \sigma_{y.so} := 0 \qquad \tau_{xy.so} := \tau_{B.so}$$

$$\sigma_{1.so} := \frac{\sigma_{x.so} + \sigma_{y.so}}{2} + \sqrt{\left(\frac{\sigma_{x.so} - \sigma_{y.so}}{2}\right)^2 + \tau_{xy.so}^2} = 149.74 \cdot MPa$$

### 4.3 Pin hole pressure

Cosine distributed load. Max. at θ = 0 deg.

$$\theta := 0deg$$

$$\sigma_{b.so} := \frac{4P}{\pi \cdot d_{so} \cdot t_{so}} \cdot \cos(\theta) = 160.96 \cdot MPa \qquad\qquad UR_{b.so} := \frac{\sigma_{b.so}}{\sigma_d} = 0.49$$

### 4.4 Pin hole pressure (Bearing)

$$\sigma_{bd1} := 280MPa \quad \text{Maximum Permissible Stress (Orkot TXM Bearing)}$$

$$\sigma_{b.so1} := \frac{4P}{\pi \cdot d_{IDbushing1} \cdot t_{so}} \cdot \cos(\theta) = 174.1 \cdot MPa \qquad\qquad UR_{b.so1} := \frac{\sigma_{b.so1}}{\sigma_{bd1}} = 0.62$$

## 5. Utilization ratio

$$UR_{max} := max\left(UR_{t.tu}, UR_{eqv.tu}, UR_{b.tu}, UR_{t.so}, UR_{eqv.so}, UR_{b.so}\right) \qquad \boxed{UR_{max} = 0.54}$$

## 6. Output to Mechanical Transfer Function

Maximum principal stress:

$$\sigma_1 := max\left(\sigma_{1.tu}, \sigma_{1.so}\right) = 149.74 \cdot MPa$$

99
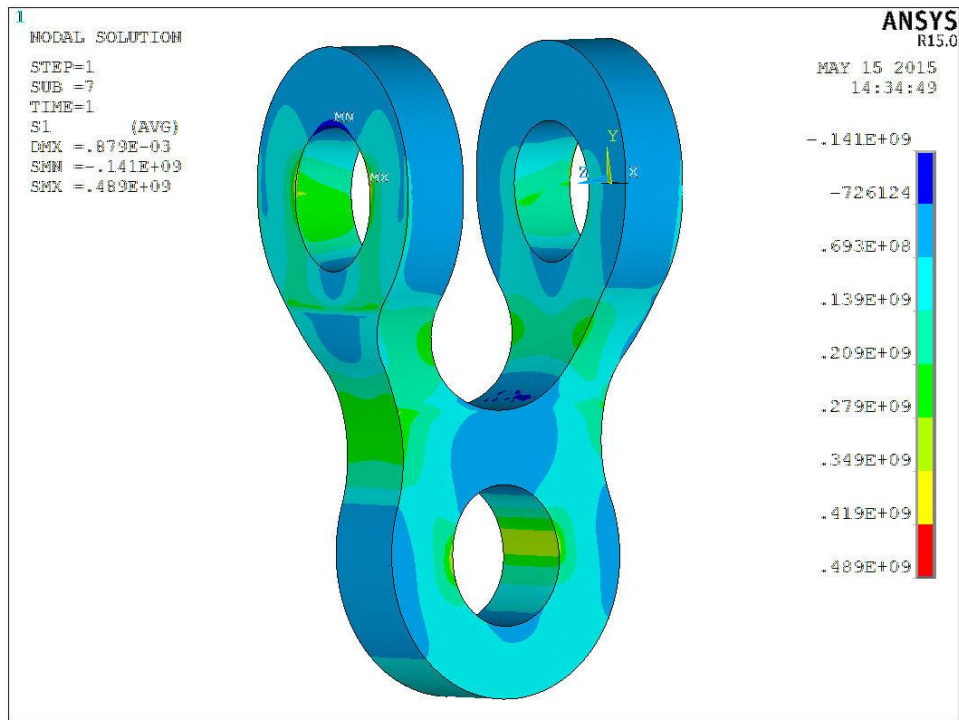
**Figure D - 2: Maximum principal stress in the new connecting link without lugs, washers and rings – ULS condition.**
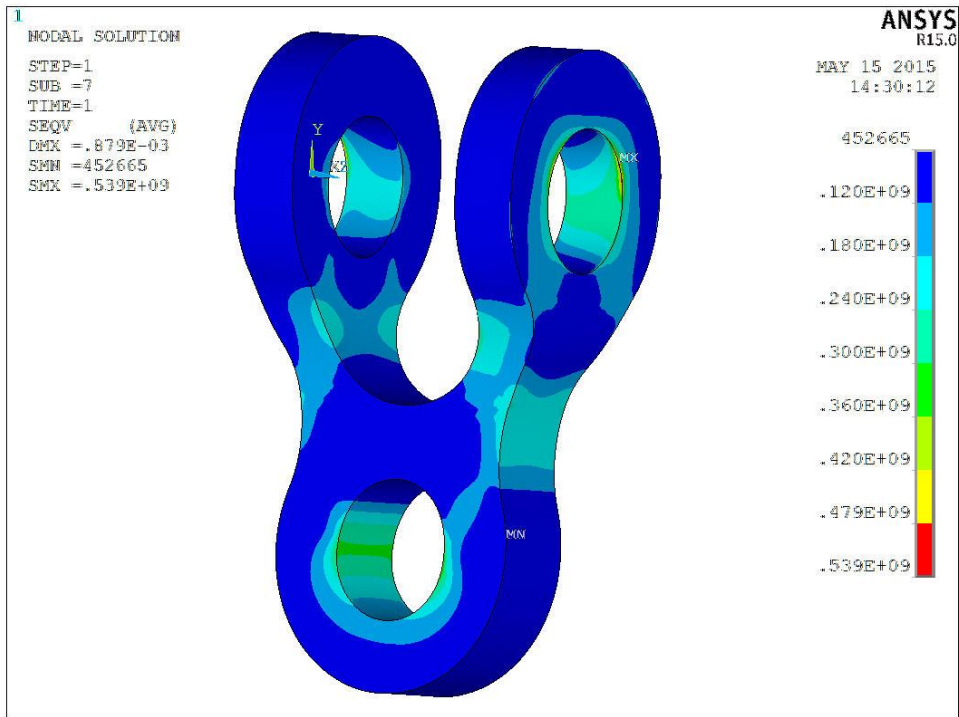


**Figure D - 3: The von Mises stress result for the new connecting link without lugs, washers and rings – ULS condition.**

**Appendix E**

**New connecting link without lugs, washers and rings**

**Fatigue calculations**

# Fatigue calculation - Gina Krog FSO

**HS**      **ULS Intact Buoy**

**New Connecting Link**

**INPUT**

| Hot Spot | Thickness [mm] | | Transf Function (MTF) [Mpa/kN] | SN Class |
|---|---|---|---|---|
| **1a** | 200 | | **0,0730** | C 3 |

| Constants for S-N-curves, structure in sea water, cathodic protection | | | | Hotspot | HS |
|---|---|---|---|---|---|
| **Class** | **C** | | | Thickness | 200 |
| $Log_{10}a$ | 12,192 | 16,320 | | Thickn Correc | 1,366040 |
| m | 3 | 5 | | | |
| k | 0,15 | 0,15 | | | |
| SCF | 1,00 | 1,00 | | | |

**RESULT SUMMARY**

| | Damage |
|---|---|
| **Connected** | 0,000124 |
| **Fatigue Life** | **8065** years |

**CONNECTED CONDITION**

| Load Range [kN] | Tension Range $\Delta T$ [kN] | Annual no. of cycles $n_i$ | Hot spot stress range $\Delta\sigma = \Delta T \times MTF$ | $m*Log(\sigma\ (t/t_{ref})^k)$ N<10^6 | $m*Log(\sigma\ (t/t_{ref})^k)$ N>10^6 | lg N N<10^6 | lg N N>10^6 | Annual Damage $n_i/N$ |
|---|---|---|---|---|---|---|---|---|
| 0-100 | 50 | 1409732,66 | 3,6 | 2,09 | 3,49 | 10,10 | 12,83 | 2,077E-07 |
| 100-200 | 100 | 267000,68 | 7,3 | 3,00 | 4,99 | 9,20 | 11,33 | 1,259E-06 |
| 200-300 | 150 | 82049,49 | 10,9 | 3,52 | 5,87 | 8,67 | 10,45 | 2,938E-06 |
| 300-400 | 200 | 32680,51 | 14,6 | 3,90 | 6,50 | 8,29 | 9,82 | 4,931E-06 |
| 400-500 | 250 | 14780,84 | 18,2 | 4,19 | 6,98 | 8,00 | 9,34 | 6,806E-06 |
| 500-600 | 300 | 7194,82 | 21,9 | 4,43 | 7,38 | 7,76 | 8,94 | 8,244E-06 |
| 600-700 | 350 | 3676,72 | 25,5 | 4,63 | 7,71 | 7,56 | 8,61 | 9,105E-06 |
| 700-800 | 400 | 1962,18 | 29,2 | 4,80 | 8,00 | 7,39 | 8,32 | 9,474E-06 |
| 800-900 | 450 | 1087,2 | 32,8 | 4,96 | 8,26 | 7,24 | 8,06 | 9,459E-06 |
| 900-1000 | 500 | 621,14 | 36,5 | 5,09 | 8,49 | 7,10 | 7,83 | 9,152E-06 |
| 1000-1100 | 550 | 364,14 | 40,1 | 5,22 | 8,70 | 6,97 | 7,62 | 8,641E-06 |
| 1100-1200 | 600 | 218,32 | 43,8 | 5,33 | 8,88 | 6,86 | 7,44 | 8,005E-06 |
| 1200-1300 | 650 | 133,42 | 47,4 | 5,43 | 9,06 | 6,76 | 7,26 | 7,299E-06 |
| 1300-1400 | 700 | 82,81 | 51,1 | 5,53 | 9,22 | 6,66 | 7,10 | 6,562E-06 |
| 1400-1500 | 750 | 51,99 | 54,7 | 5,62 | 9,37 | 6,57 | 6,95 | 5,817E-06 |
| 1500-1600 | 800 | 32,87 | 58,4 | 5,71 | 9,51 | 6,49 | 6,81 | 5,078E-06 |
| 1600-1700 | 850 | 20,85 | 62,0 | 5,78 | 9,64 | 6,41 | 6,68 | 4,362E-06 |
| 1700-1800 | 900 | 13,22 | 65,7 | 5,86 | 9,76 | 6,33 | 6,56 | 3,681E-06 |
| 1800-1900 | 950 | 8,35 | 69,3 | 5,93 | 9,88 | 6,26 | 6,44 | 3,046E-06 |
| 1900-2000 | 1000 | 5,25 | 73,0 | 6,00 | 9,99 | 6,20 | 6,33 | 2,475E-06 |
| 2000-2100 | 1050 | 3,28 | 76,6 | 6,06 | 10,10 | 6,13 | 6,22 | 1,974E-06 |
| 2100-2200 | 1100 | 2,03 | 80,3 | 6,12 | 10,20 | 6,07 | 6,12 | 1,542E-06 |
| 2200-2300 | 1150 | 1,25 | 83,9 | 6,18 | 10,30 | 6,01 | 6,02 | 1,185E-06 |
| 2300-2400 | 1200 | 0,76 | 87,6 | 6,23 | 10,39 | 5,96 | 5,93 | 8,365E-07 |

| | | | | | | | | |
|---|---|---|---|---|---|---|---|---|
| 2400-2500 | 1250 | 0,46 | 91,2 | 6,29 | 10,48 | 5,91 | 5,84 | 5,722E-07 |
| 2500-2600 | 1300 | 0,27 | 94,9 | 6,34 | 10,56 | 5,85 | 5,76 | 3,778E-07 |
| 2600-2700 | 1350 | 0,16 | 98,5 | 6,39 | 10,65 | 5,80 | 5,67 | 2,507E-07 |
| 2700-2800 | 1400 | 0,09 | 102,2 | 6,43 | 10,72 | 5,76 | 5,60 | 1,573E-07 |
| 2800-2900 | 1450 | 0,05 | 105,8 | 6,48 | 10,80 | 5,71 | 5,52 | 9,709E-08 |
| 2900-3000 | 1500 | 0,03 | 109,5 | 6,52 | 10,87 | 5,67 | 5,45 | 6,449E-08 |
| 3000-3100 | 1550 | 0,02 | 113,1 | 6,57 | 10,95 | 5,62 | 5,37 | 4,744E-08 |
| 3100-3200 | 1600 | 0,01 | 116,8 | 6,61 | 11,01 | 5,58 | 5,31 | 2,609E-08 |
| 3200-3300 | 1650 | 0,01 | 120,4 | 6,65 | 11,08 | 5,54 | 5,24 | 2,861E-08 |
| 3300-3400 | 1700 | 0 | 124,1 | 6,69 | 11,15 | 5,50 | 5,17 | 0,000E+00 |
| 3400-3500 | 1750 | 0 | 127,7 | 6,73 | 11,21 | 5,47 | 5,11 | 0,000E+00 |
| 3500-3600 | 1800 | 0 | 131,4 | 6,76 | 11,27 | 5,43 | 5,05 | 0,000E+00 |
| 3600-3700 | 1850 | 0 | 135,0 | 6,80 | 11,33 | 5,39 | 4,99 | 0,000E+00 |
| 3700-3800 | 1900 | 0,0 | 138,7 | 6,83 | 11,39 | 5,36 | 4,93 | 0,000E+00 |
| 3800-3900 | 1950 | 0,0 | 142,3 | 6,87 | 11,44 | 5,33 | 4,88 | 0,000E+00 |
| 3900-4000 | 2000 | 0 | 146,0 | 6,90 | 11,50 | 5,29 | 4,82 | 0,000E+00 |
| 4000-4100 | 2050 | 0 | 149,6 | 6,93 | 11,55 | 5,26 | 4,77 | 0,000E+00 |
| 4100-4200 | 2100 | 0 | 153,3 | 6,96 | 11,60 | 5,23 | 4,72 | 0,000E+00 |
| 4200-4300 | 2150 | 0 | 156,9 | 6,99 | 11,66 | 5,20 | 4,66 | 0,000E+00 |
| 4300-4400 | 2200 | 0 | 160,6 | 7,02 | 11,71 | 5,17 | 4,61 | 0,000E+00 |
| 4400-4500 | 2250 | 0 | 164,2 | 7,05 | 11,75 | 5,14 | 4,57 | 0,000E+00 |
| 4500-4600 | 2300 | 0 | 167,9 | 7,08 | 11,80 | 5,11 | 4,52 | 0,000E+00 |
| 4600-4700 | 2350 | 0 | 171,5 | 7,11 | 11,85 | 5,08 | 4,47 | 0,000E+00 |
| 4700-4800 | 2400 | 0 | 175,2 | 7,14 | 11,89 | 5,06 | 4,43 | 0,000E+00 |
| 4800-4900 | 2450 | 0 | 178,8 | 7,16 | 11,94 | 5,03 | 4,38 | 0,000E+00 |
| 4900-5000 | 2500 | 0 | 182,5 | 7,19 | 11,98 | 5,00 | 4,34 | 0,000E+00 |
| 1000-1020 | 505 | 1,1 | 36,9 | 5,11 | 8,51 | 7,09 | 7,81 | 1,703E-08 |
| 1020-1040 | 515 | 1,0 | 37,6 | 5,13 | 8,55 | 7,06 | 7,77 | 1,708E-08 |
| 1040-1060 | 525 | 0,9 | 38,3 | 5,16 | 8,59 | 7,04 | 7,73 | 1,692E-08 |
| 1060-1080 | 535 | 0,8 | 39,0 | 5,18 | 8,64 | 7,01 | 7,68 | 1,653E-08 |
| 1080-1100 | 545 | 0,7 | 39,8 | 5,21 | 8,68 | 6,99 | 7,64 | 1,587E-08 |
| 1100-1120 | 555 | 0,6 | 40,5 | 5,23 | 8,71 | 6,96 | 7,61 | 1,490E-08 |
| 1120-1140 | 565 | 0,5 | 41,2 | 5,25 | 8,75 | 6,94 | 7,57 | 1,357E-08 |
| 1140-1160 | 575 | 0,5 | 42,0 | 5,28 | 8,79 | 6,92 | 7,53 | 1,482E-08 |
| 1160-1180 | 585 | 0,4 | 42,7 | 5,30 | 8,83 | 6,89 | 7,49 | 1,292E-08 |
| 1180-1200 | 595 | 0,3 | 43,4 | 5,32 | 8,87 | 6,87 | 7,45 | 1,055E-08 |
| 1200-1220 | 605 | 0,3 | 44,2 | 5,34 | 8,90 | 6,85 | 7,42 | 1,147E-08 |
| 1220-1240 | 615 | 0,3 | 44,9 | 5,36 | 8,94 | 6,83 | 7,38 | 1,244E-08 |
| 1240-1260 | 625 | 0,2 | 45,6 | 5,38 | 8,97 | 6,81 | 7,35 | 8,993E-09 |
| 1260-1280 | 635 | 0,2 | 46,3 | 5,40 | 9,01 | 6,79 | 7,31 | 9,736E-09 |
| 1280-1300 | 645 | 0,2 | 47,1 | 5,42 | 9,04 | 6,77 | 7,28 | 1,053E-08 |
| 1300-1320 | 655 | 0,2 | 47,8 | 5,44 | 9,07 | 6,75 | 7,25 | 1,137E-08 |
| 1320-1340 | 665 | 0,1 | 48,5 | 5,46 | 9,11 | 6,73 | 7,21 | 6,132E-09 |
| 1340-1360 | 675 | 0,1 | 49,3 | 5,48 | 9,14 | 6,71 | 7,18 | 6,607E-09 |
| 1360-1380 | 685 | 0,1 | 50,0 | 5,50 | 9,17 | 6,69 | 7,15 | 7,111E-09 |
| 1380-1400 | 695 | 0,1 | 50,7 | 5,52 | 9,20 | 6,67 | 7,12 | 7,646E-09 |
| 1400-1420 | 705 | 0,1 | 51,5 | 5,54 | 9,23 | 6,65 | 7,09 | 8,212E-09 |
| 1420-1440 | 715 | 0,1 | 52,2 | 5,56 | 9,27 | 6,63 | 7,05 | 8,811E-09 |
| 1440-1460 | 725 | 0,1 | 52,9 | 5,58 | 9,30 | 6,61 | 7,02 | 9,444E-09 |
| 1460-1480 | 735 | 0,1 | 53,6 | 5,59 | 9,32 | 6,60 | 7,00 | 1,011E-08 |
| 1480-1500 | 745 | 0,1 | 54,4 | 5,61 | 9,35 | 6,58 | 6,97 | 1,082E-08 |
| 1500-1520 | 755 | 0 | 55,1 | 5,63 | 9,38 | 6,56 | 6,94 | 0,000E+00 |
| 1520-1540 | 765 | 0 | 55,8 | 5,65 | 9,41 | 6,54 | 6,91 | 0,000E+00 |
| 1540-1560 | 775 | 0 | 56,6 | 5,66 | 9,44 | 6,53 | 6,88 | 0,000E+00 |

| | | | | | | | | |
|---|---|---|---|---|---|---|---|---|
| 1560-1580 | 785 | 0 | 57,3 | 5,68 | 9,47 | 6,51 | 6,85 | 0,000E+00 |
| 1580-1600 | 795 | 0 | 58,0 | 5,70 | 9,50 | 6,49 | 6,82 | 0,000E+00 |
| 1600-1620 | 805 | 0 | 58,8 | 5,71 | 9,52 | 6,48 | 6,80 | 0,000E+00 |
| 1620-1640 | 815 | 0 | 59,5 | 5,73 | 9,55 | 6,46 | 6,77 | 0,000E+00 |
| 1640-1660 | 825 | 0 | 60,2 | 5,75 | 9,58 | 6,45 | 6,74 | 0,000E+00 |
| 1660-1680 | 835 | 0 | 60,9 | 5,76 | 9,60 | 6,43 | 6,72 | 0,000E+00 |
| 1680-1700 | 845 | 0 | 61,7 | 5,78 | 9,63 | 6,42 | 6,69 | 0,000E+00 |
| 1700-1720 | 855 | 0 | 62,4 | 5,79 | 9,65 | 6,40 | 6,67 | 0,000E+00 |
| 1720-1740 | 865 | 0 | 63,1 | 5,81 | 9,68 | 6,38 | 6,64 | 0,000E+00 |
| 1740-1760 | 875 | 0 | 63,9 | 5,82 | 9,70 | 6,37 | 6,62 | 0,000E+00 |
| | | 1821734,98 | | | | | | 1,24E-04 |

# Fatigue calculation - Heidrun

**HS**    **ULS Intact Buoy**

**New Connecting Link**

**INPUT**

| Hot Spot | Thickness [mm] | | Transf Function (MTF) [Mpa/kN] | SN Class |
|---|---|---|---|---|
| **HS** | 200 | | **0,0730** | C 3 |

| Constants for S-N-curves, structure in sea water, cathodic protection | | | | Hotspot | HS |
|---|---|---|---|---|---|

| Class | C | |
|---|---|---|
| $Log_{10}a$ | 12,192 | 16,320 |
| m | 3 | 5 |
| k | 0,15 | 0,15 |
| SCF | 1,00 | 1,00 |

| | |
|---|---|
| Hotspot | HS |
| Thickness | 200 |
| Thickn Correc | 1,366040 |

**RESULT SUMMARY**

| | Damage |
|---|---|
| **Connected** | 0,002523 |
| **Fatigue Life** | **396** years |

**CONNECTED CONDITION**

| Load Range [kN] | Tension Range $\Delta T$ [kN] | Annual no. of cycles $n_i$ | Hot spot stress range $\Delta\sigma = \dfrac{\Delta T}{MTF}$ | $m*Log(\sigma\,(t/t_{ref})^k)$ $N<10^6$ | $m*Log(\sigma\,(t/t_{ref})^k)$ $N>10^6$ | lg N $N<10^6$ | lg N $N>10^6$ | Annual Damage $n_i/N$ |
|---|---|---|---|---|---|---|---|---|
| 1 | 81 | 333048,00 | 5,9 | 2,72 | 4,54 | 9,47 | 11,78 | 5,475E-07 |
| 2 | 162 | 107246,10 | 11,8 | 3,62 | 6,04 | 8,57 | 10,28 | 5,642E-06 |
| 3 | 243 | 31590,60 | 17,7 | 4,15 | 6,92 | 8,04 | 9,40 | 1,262E-05 |
| 4 | 324 | 12614,20 | 23,6 | 4,53 | 7,55 | 7,66 | 8,77 | 2,124E-05 |
| 5 | 405 | 7085,80 | 29,6 | 4,82 | 8,03 | 7,37 | 8,29 | 3,640E-05 |
| 6 | 486 | 4495,30 | 35,5 | 5,06 | 8,43 | 7,14 | 7,89 | 5,747E-05 |
| 7 | 567 | 2941,60 | 41,4 | 5,26 | 8,76 | 6,94 | 7,56 | 8,128E-05 |
| 8 | 648 | 1956,30 | 47,3 | 5,43 | 9,05 | 6,76 | 7,27 | 1,054E-04 |
| 9 | 729 | 1321,30 | 53,2 | 5,58 | 9,31 | 6,61 | 7,01 | 1,283E-04 |
| 10 | 810 | 905,10 | 59,1 | 5,72 | 9,54 | 6,47 | 6,78 | 1,488E-04 |
| 11 | 891 | 624,10 | 65,0 | 5,85 | 9,74 | 6,35 | 6,58 | 1,652E-04 |
| 12 | 972 | 433,50 | 70,9 | 5,96 | 9,93 | 6,23 | 6,39 | 1,773E-04 |
| 13 | 1053 | 302,80 | 76,9 | 6,06 | 10,11 | 6,13 | 6,21 | 1,848E-04 |
| 14 | 1134 | 212,90 | 82,8 | 6,16 | 10,27 | 6,03 | 6,05 | 1,882E-04 |
| 15 | 1215 | 151,10 | 88,7 | 6,25 | 10,42 | 5,94 | 5,90 | 1,726E-04 |
| 16 | 1296 | 108,20 | 94,6 | 6,33 | 10,56 | 5,86 | 5,76 | 1,500E-04 |
| 17 | 1377 | 78,30 | 100,5 | 6,41 | 10,69 | 5,78 | 5,63 | 1,302E-04 |
| 18 | 1458 | 57,20 | 106,4 | 6,49 | 10,81 | 5,70 | 5,51 | 1,129E-04 |
| 19 | 1539 | 42,20 | 112,3 | 6,56 | 10,93 | 5,63 | 5,39 | 9,798E-05 |
| 20 | 1620 | 31,30 | 118,2 | 6,62 | 11,04 | 5,57 | 5,28 | 8,476E-05 |
| 21 | 1701 | 23,30 | 124,1 | 6,69 | 11,15 | 5,50 | 5,17 | 7,304E-05 |
| 22 | 1782 | 17,40 | 130,1 | 6,75 | 11,25 | 5,44 | 5,07 | 6,271E-05 |
| 23 | 1863 | 13,10 | 136,0 | 6,81 | 11,34 | 5,39 | 4,98 | 5,395E-05 |
| 24 | 1944 | 9,80 | 141,9 | 6,86 | 11,44 | 5,33 | 4,88 | 4,586E-05 |

| | | | | | | | | |
|---|---|---|---|---|---|---|---|---|
| 25 | 2025 | 7,40 | 147,8 | 6,92 | 11,53 | 5,28 | 4,79 | 3,914E-05 |
| 26 | 2106 | 5,60 | 153,7 | 6,97 | 11,61 | 5,23 | 4,71 | 3,332E-05 |
| 27 | 2187 | 4,20 | 159,6 | 7,02 | 11,69 | 5,18 | 4,63 | 2,798E-05 |
| 28 | 2268 | 3,20 | 165,5 | 7,06 | 11,77 | 5,13 | 4,55 | 2,378E-05 |
| 29 | 2349 | 2,40 | 171,4 | 7,11 | 11,85 | 5,08 | 4,47 | 1,981E-05 |
| 30 | 2430 | 1,80 | 177,4 | 7,15 | 11,92 | 5,04 | 4,40 | 1,645E-05 |
| 31 | 2511 | 1,40 | 183,3 | 7,20 | 11,99 | 5,00 | 4,33 | 1,412E-05 |
| 32 | 2592 | 1,00 | 189,2 | 7,24 | 12,06 | 4,96 | 4,26 | 1,109E-05 |
| 33 | 2673 | 0,80 | 195,1 | 7,28 | 12,13 | 4,91 | 4,19 | 9,731E-06 |
| 34 | 2754 | 0,60 | 201,0 | 7,32 | 12,19 | 4,88 | 4,13 | 7,982E-06 |
| 35 | 2835 | 0,40 | 206,9 | 7,35 | 12,26 | 4,84 | 4,06 | 5,805E-06 |
| 36 | 2916 | 0,30 | 212,8 | 7,39 | 12,32 | 4,80 | 4,00 | 4,738E-06 |
| 37 | 2997 | 0,20 | 218,7 | 7,43 | 12,38 | 4,77 | 3,94 | 3,429E-06 |
| 38 | 3078 | 0,20 | 224,6 | 7,46 | 12,43 | 4,73 | 3,89 | 3,715E-06 |
| 39 | 3159 | 0,10 | 230,6 | 7,49 | 12,49 | 4,70 | 3,83 | 2,008E-06 |
| 40 | 3240 | 0,10 | 236,5 | 7,53 | 12,55 | 4,66 | 3,77 | 2,166E-06 |
| | | 505339,2 | | | | | | 2,52E-03 |

# Fatigue calculation - Mariner

**HS**  **ULS Intact Buoy**

**New Connecting Link**

**INPUT**

| Hot Spot | Thickness<br><br>[mm] | | Transf Function (MTF)<br><br>[Mpa/kN] | SN Class |
|---|---|---|---|---|
| **HS** | 200 | | **0,0730** | C<br>3 |

| **Constants for S-N-curves, structure in sea water, cathodic protection** | | |
|---|---|---|
| **Class** | **C** | |
| $Log_{10}a$ | 12,192 | 16,320 |
| m | 3 | 5 |
| k | 0,15 | 0,15 |
| SCF | 1,00 | 1,00 |

| Hotspot | HS |
|---|---|
| Thickness | 200 |
| Thickn Correc | 1,366040 |

**RESULT SUMMARY**

| | **Damage** | |
|---|---|---|
| **Connected** | 0,000098 | |
| **Fatigue Life** | **10252** | years |

**CONNECTED CONDITION**

| Load Range [kN] | Tension Range $\Delta T$ [kN] | Annual no. of cycles $n_i$ | Hot spot stress range $\Delta\sigma = $ MTF $\Delta T$ x | $m*Log(\sigma (t/t_{ref})^k)$ $N<10^6$ | $m*Log(\sigma (t/t_{ref})^k)$ $N>10^6$ | lg N $N<10^6$ | lg N $N>10^6$ | Annual Damage $n_i/N$ |
|---|---|---|---|---|---|---|---|---|
| 0-50 | 25 | 957933,81 | 1,8 | 1,19 | 1,98 | 11,00 | 14,34 | 4,411E-09 |
| 50-100 | 50 | 507591,59 | 3,6 | 2,09 | 3,49 | 10,10 | 12,83 | 7,479E-08 |
| 100-150 | 75 | 217414,59 | 5,5 | 2,62 | 4,37 | 9,57 | 11,95 | 2,433E-07 |
| 150-200 | 100 | 110619,52 | 7,3 | 3,00 | 4,99 | 9,20 | 11,33 | 5,216E-07 |
| 200-250 | 125 | 60981,6 | 9,1 | 3,29 | 5,48 | 8,91 | 10,84 | 8,775E-07 |
| 250-300 | 150 | 36190,14 | 10,9 | 3,52 | 5,87 | 8,67 | 10,45 | 1,296E-06 |
| 300-350 | 175 | 22603,49 | 12,8 | 3,73 | 6,21 | 8,47 | 10,11 | 1,749E-06 |
| 350-400 | 200 | 14611,67 | 14,6 | 3,90 | 6,50 | 8,29 | 9,82 | 2,205E-06 |
| 400-450 | 225 | 9699,63 | 16,4 | 4,05 | 6,75 | 8,14 | 9,57 | 2,637E-06 |
| 450-500 | 250 | 6575,18 | 18,2 | 4,19 | 6,98 | 8,00 | 9,34 | 3,028E-06 |
| 500-550 | 275 | 4530,39 | 20,1 | 4,31 | 7,19 | 7,88 | 9,13 | 3,360E-06 |
| 550-600 | 300 | 3162,87 | 21,9 | 4,43 | 7,38 | 7,76 | 8,94 | 3,624E-06 |
| 600-650 | 325 | 2233,48 | 23,7 | 4,53 | 7,55 | 7,66 | 8,77 | 3,818E-06 |
| 650-700 | 350 | 1593,6 | 25,5 | 4,63 | 7,71 | 7,56 | 8,61 | 3,946E-06 |
| 700-750 | 375 | 1147,81 | 27,4 | 4,72 | 7,86 | 7,47 | 8,46 | 4,013E-06 |
| 750-800 | 400 | 833,72 | 29,2 | 4,80 | 8,00 | 7,39 | 8,32 | 4,025E-06 |
| 800-850 | 425 | 610,06 | 31,0 | 4,88 | 8,14 | 7,31 | 8,18 | 3,988E-06 |
| 850-900 | 450 | 449,24 | 32,8 | 4,96 | 8,26 | 7,24 | 8,06 | 3,909E-06 |
| 900-950 | 475 | 332,62 | 34,7 | 5,03 | 8,38 | 7,17 | 7,94 | 3,792E-06 |
| 950-1000 | 500 | 247,43 | 36,5 | 5,09 | 8,49 | 7,10 | 7,83 | 3,646E-06 |
| 1000-1050 | 525 | 184,81 | 38,3 | 5,16 | 8,59 | 7,04 | 7,73 | 3,475E-06 |
| 1050-1100 | 550 | 138,55 | 40,1 | 5,22 | 8,70 | 6,97 | 7,62 | 3,288E-06 |
| 1100-1150 | 575 | 104,22 | 42,0 | 5,28 | 8,79 | 6,92 | 7,53 | 3,089E-06 |
| 1150-1200 | 600 | 78,67 | 43,8 | 5,33 | 8,88 | 6,86 | 7,44 | 2,884E-06 |

| | | | | | | | | |
|---|---|---|---|---|---|---|---|---|
| 1200-1250 | 625 | 59,6 | 45,6 | 5,38 | 8,97 | 6,81 | 7,35 | 2,680E-06 |
| 1250-1300 | 650 | 45,32 | 47,4 | 5,43 | 9,06 | 6,76 | 7,26 | 2,479E-06 |
| 1300-1350 | 675 | 34,61 | 49,3 | 5,48 | 9,14 | 6,71 | 7,18 | 2,287E-06 |
| 1350-1400 | 700 | 26,56 | 51,1 | 5,53 | 9,22 | 6,66 | 7,10 | 2,105E-06 |
| 1400-1450 | 725 | 20,49 | 52,9 | 5,58 | 9,30 | 6,61 | 7,02 | 1,935E-06 |
| 1450-1500 | 750 | 15,89 | 54,7 | 5,62 | 9,37 | 6,57 | 6,95 | 1,778E-06 |
| 1500-1550 | 775 | 12,4 | 56,6 | 5,66 | 9,44 | 6,53 | 6,88 | 1,635E-06 |
| 1550-1600 | 800 | 9,74 | 58,4 | 5,71 | 9,51 | 6,49 | 6,81 | 1,505E-06 |
| 1600-1650 | 825 | 7,7 | 60,2 | 5,75 | 9,58 | 6,45 | 6,74 | 1,388E-06 |
| 1650-1700 | 850 | 6,12 | 62,0 | 5,78 | 9,64 | 6,41 | 6,68 | 1,280E-06 |
| 1700-1750 | 875 | 4,91 | 63,9 | 5,82 | 9,70 | 6,37 | 6,62 | 1,187E-06 |
| 1750-1800 | 900 | 3,96 | 65,7 | 5,86 | 9,76 | 6,33 | 6,56 | 1,103E-06 |
| 1800-1850 | 925 | 3,21 | 67,5 | 5,89 | 9,82 | 6,30 | 6,50 | 1,025E-06 |
| 1850-1900 | 950 | 2,62 | 69,3 | 5,93 | 9,88 | 6,26 | 6,44 | 9,559E-07 |
| 1900-1950 | 975 | 2,15 | 71,2 | 5,96 | 9,94 | 6,23 | 6,38 | 8,932E-07 |
| 1950-2000 | 1000 | 1,78 | 73,0 | 6,00 | 9,99 | 6,20 | 6,33 | 8,393E-07 |
| 2000-2050 | 1025 | 1,47 | 74,8 | 6,03 | 10,05 | 6,16 | 6,27 | 7,842E-07 |
| 2050-2100 | 1050 | 1,23 | 76,6 | 6,06 | 10,10 | 6,13 | 6,22 | 7,402E-07 |
| 2100-2150 | 1075 | 1,03 | 78,5 | 6,09 | 10,15 | 6,10 | 6,17 | 6,972E-07 |
| 2150-2200 | 1100 | 0,86 | 80,3 | 6,12 | 10,20 | 6,07 | 6,12 | 6,531E-07 |
| 2200-2250 | 1125 | 0,73 | 82,1 | 6,15 | 10,25 | 6,04 | 6,07 | 6,203E-07 |
| 2250-2300 | 1150 | 0,61 | 83,9 | 6,18 | 10,30 | 6,01 | 6,02 | 5,785E-07 |
| 2300-2350 | 1175 | 0,52 | 85,8 | 6,21 | 10,34 | 5,99 | 5,98 | 5,373E-07 |
| 2350-2400 | 1200 | 0,44 | 87,6 | 6,23 | 10,39 | 5,96 | 5,93 | 4,843E-07 |
| 2400-2450 | 1225 | 0,38 | 89,4 | 6,26 | 10,43 | 5,93 | 5,89 | 4,449E-07 |
| 2450-2500 | 1250 | 0,32 | 91,2 | 6,29 | 10,48 | 5,91 | 5,84 | 3,981E-07 |
| 2500-2550 | 1275 | 0,27 | 93,1 | 6,31 | 10,52 | 5,88 | 5,80 | 3,564E-07 |
| 2550-2600 | 1300 | 0,23 | 94,9 | 6,34 | 10,56 | 5,85 | 5,76 | 3,218E-07 |
| 2600-2650 | 1325 | 0,2 | 96,7 | 6,36 | 10,60 | 5,83 | 5,72 | 2,963E-07 |
| 2650-2700 | 1350 | 0,17 | 98,5 | 6,39 | 10,65 | 5,80 | 5,67 | 2,664E-07 |
| 2700-2750 | 1375 | 0,14 | 100,4 | 6,41 | 10,68 | 5,78 | 5,64 | 2,318E-07 |
| 2750-2800 | 1400 | 0,12 | 102,2 | 6,43 | 10,72 | 5,76 | 5,60 | 2,097E-07 |
| 2800-2850 | 1425 | 0,1 | 104,0 | 6,46 | 10,76 | 5,73 | 5,56 | 1,843E-07 |
| 2850-2900 | 1450 | 0,09 | 105,8 | 6,48 | 10,80 | 5,71 | 5,52 | 1,748E-07 |
| 2900-2950 | 1475 | 0,07 | 107,7 | 6,50 | 10,84 | 5,69 | 5,48 | 1,431E-07 |
| 2950-3000 | 1500 | 0,06 | 109,5 | 6,52 | 10,87 | 5,67 | 5,45 | 1,290E-07 |
| 3000-3050 | 1525 | 0,05 | 111,3 | 6,55 | 10,91 | 5,65 | 5,41 | 1,129E-07 |
| 3050-3100 | 1550 | 0,04 | 113,1 | 6,57 | 10,95 | 5,62 | 5,37 | 9,487E-08 |
| 3100-3150 | 1575 | 0,04 | 115,0 | 6,59 | 10,98 | 5,60 | 5,34 | 9,954E-08 |
| 3150-3200 | 1600 | 0,03 | 116,8 | 6,61 | 11,01 | 5,58 | 5,31 | 7,827E-08 |
| 3200-3250 | 1625 | 0,03 | 118,6 | 6,63 | 11,05 | 5,56 | 5,27 | 8,199E-08 |
| 3250-3300 | 1650 | 0,02 | 120,4 | 6,65 | 11,08 | 5,54 | 5,24 | 5,722E-08 |
| 3300-3350 | 1675 | 0,02 | 122,2 | 6,67 | 11,11 | 5,52 | 5,21 | 5,986E-08 |
| 3350-3400 | 1700 | 0,01 | 124,1 | 6,69 | 11,15 | 5,50 | 5,17 | 3,129E-08 |
| 3400-3450 | 1725 | 0,01 | 125,9 | 6,71 | 11,18 | 5,49 | 5,14 | 3,269E-08 |
| 3450-3500 | 1750 | 0,01 | 127,7 | 6,73 | 11,21 | 5,47 | 5,11 | 3,414E-08 |
| 3500-3550 | 1775 | 0,01 | 129,5 | 6,74 | 11,24 | 5,45 | 5,08 | 3,562E-08 |
| | | 1960135,06 | | | | | | 9,75E-05 |

| Curve | lg a | m | lga | m | κ | SCF |
|-------|------|---|------|---|------|------|
| B1 | 14,917 | 4 | 17,146 | 5 | 0,00 | 1,00 |
| B2 | 14,685 | 4 | 16,856 | 5 | 0,00 | 1,00 |
| C | 12,192 | 3 | 16,320 | 5 | 0,15 | 1,00 |
| C1 | 12,049 | 3 | 16,081 | 5 | 0,15 | 1,00 |
| C2 | 11,901 | 3 | 15,835 | 5 | 0,15 | 1,00 |
| D | 11,764 | 3 | 15,606 | 5 | 0,20 | 1,00 |
| E | 11,610 | 3 | 15,350 | 5 | 0,20 | 1,13 |
| F | 11,455 | 3 | 15,091 | 5 | 0,25 | 1,27 |
| F1 | 11,299 | 3 | 14,832 | 5 | 0,25 | 1,43 |
| F3 | 11,146 | 3 | 14,576 | 5 | 0,25 | 1,61 |
| G | 11,998 | 3 | 14,330 | 5 | 0,25 | 1,80 |
| W1 | 10,861 | 3 | 14,101 | 5 | 0,25 | 2,00 |
| W2 | 10,707 | 3 | 13,845 | 5 | 0,25 | 2,25 |
| W3 | 10,570 | 3 | 13,617 | 5 | 0,25 | 2,50 |
| T | 11,764 | 3 | | 5 | 0,25 | 1,00 |

**Appendix F**

**Drawings of the new connecting link**
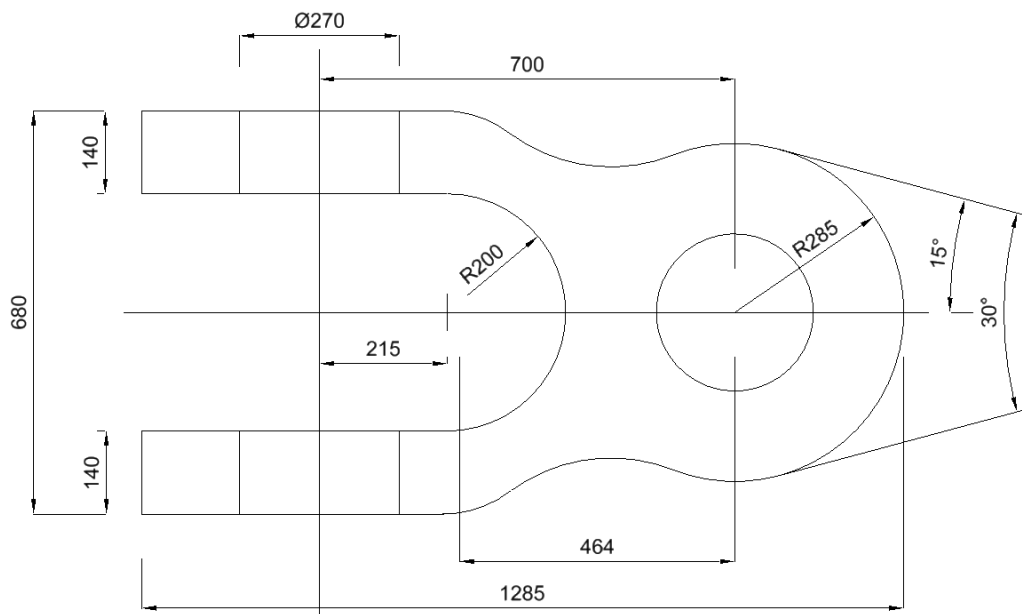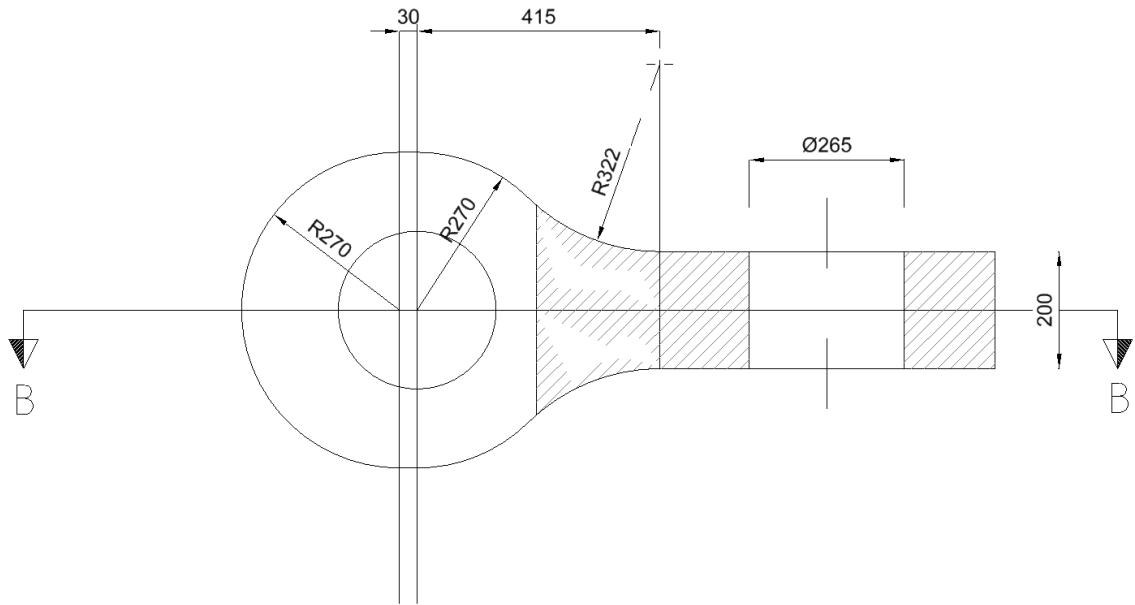
**Figure F - 1: The geometry of the new connecting link – eye-bar and top view.**

**Appendix G**

**New connecting link with lugs, washers and rings**

**Bearing wear assessment calculations**

# Wear Calculation Mooring Bearing Connections

## 1908 Gina Krog STL - Connecting Link

**Location:** **Towards Turret**

Vertical rotations

**Bearing data**

| | | | |
|---|---|---|---|
| Type: | DEVA BM 362 / 9P | | |
| ID | 260 | mm | Inner Diameter |
| s | 280 | mm | Width (2x140mm) |
| O | 817 | mm | Circumference |
| Ap | 72800 | mm | Area |
| delta | 25 % | Skew load effect on lugs | 1,25 |

**Results**

| | | |
|---|---|---|
| Total annual wear | 0,030 | mm |
| Total after 10 years | 0,30 | mm |
| Max mean bearing pressure | **17,55** | MPa |

| Case | Tension [kN] | Rotations yearly | Annual sliding length [m] | Mean bearing pressure [Mpa] | Wear factor K [$10^{-15}$m$^3$/Nm] | Annual wear [mm] |
|---|---|---|---|---|---|---|
| 1 | 1022 | 12943 | 10572,02 | 17,55 | 0,16 | 0,030 |

**Location:** **Towards Socket**

| | | |
|---|---|---|
| Type | ORKOT TXM | |
| ID | 245 | mm |
| s | 200 | mm |
| O | 770 | mm |
| Ap | 49000 | mm |

**Results**

| | | |
|---|---|---|
| Total annual wear | 0,050 | mm |
| Total after 10 years | 0,50 | mm |
| Max mean bearing pressure | **20,86** | MPa |

| Case | Tension [kN] | Rotations yearly | Annual sliding length [m] | Mean bearing pressure [Mpa] | Wear factor K [$10^{-15}$m$^3$/Nm] | Annual wear [mm] |
|---|---|---|---|---|---|---|
| 1 | 1022 | 1015 | 781,24 | 20,86 | 3,05 | 0,050 |

**Appendix H**

**New connecting link with lugs, washers and rings**
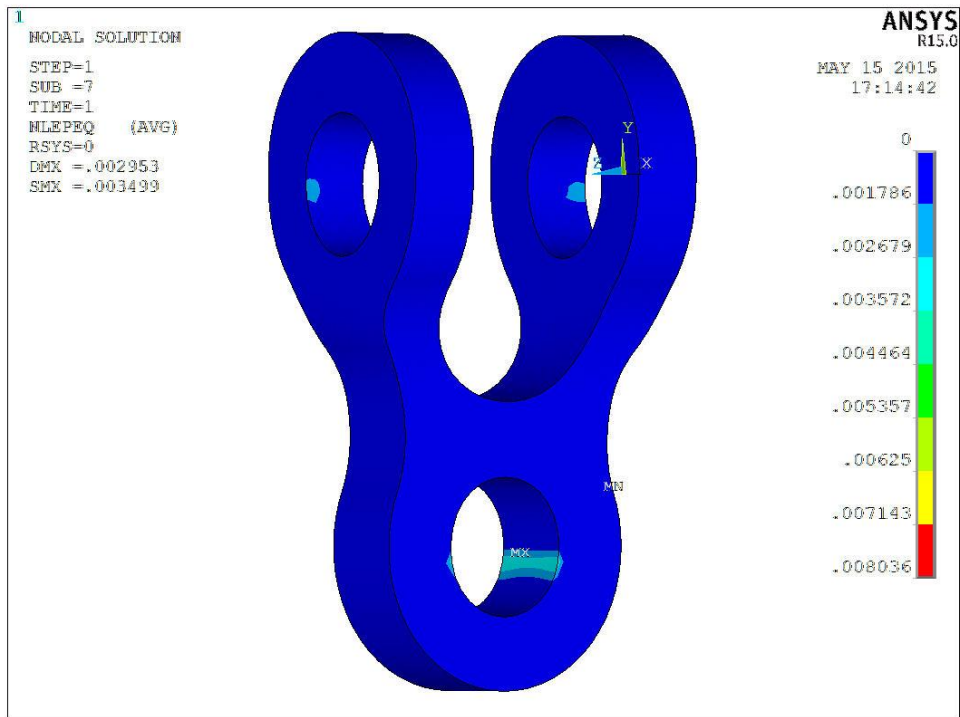
**MBL condition**

**Figure H - 1: The equivalent plastic strain result for the new connecting link with lugs, washers and rings – MBL condition.**
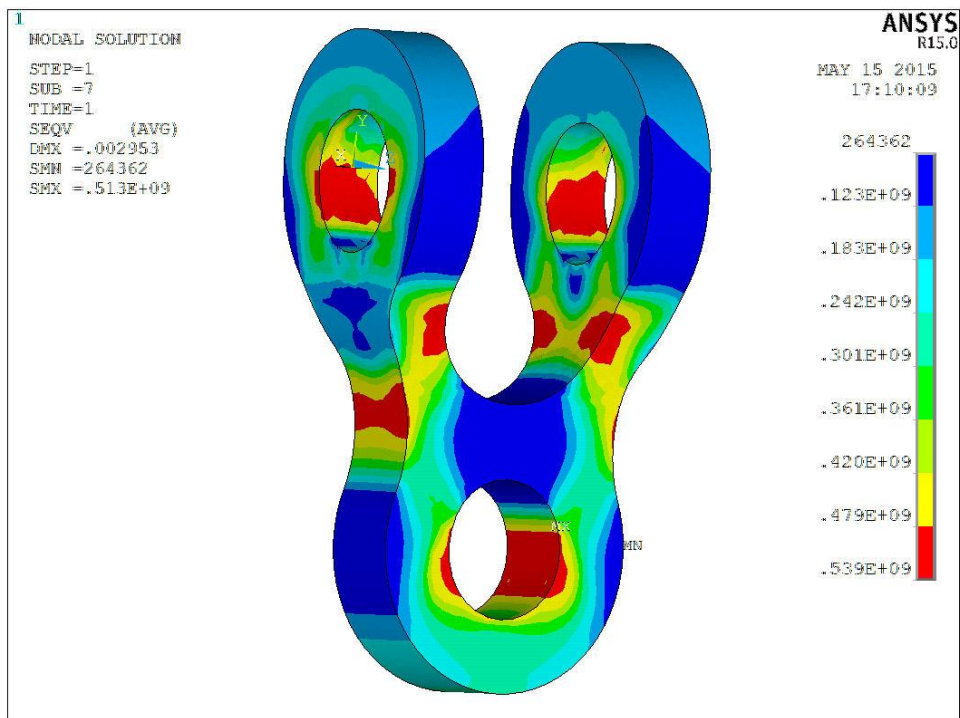


**Figure H - 2: The von Mises result for the new connecting link with lugs, washers and rings – MBL condition.**
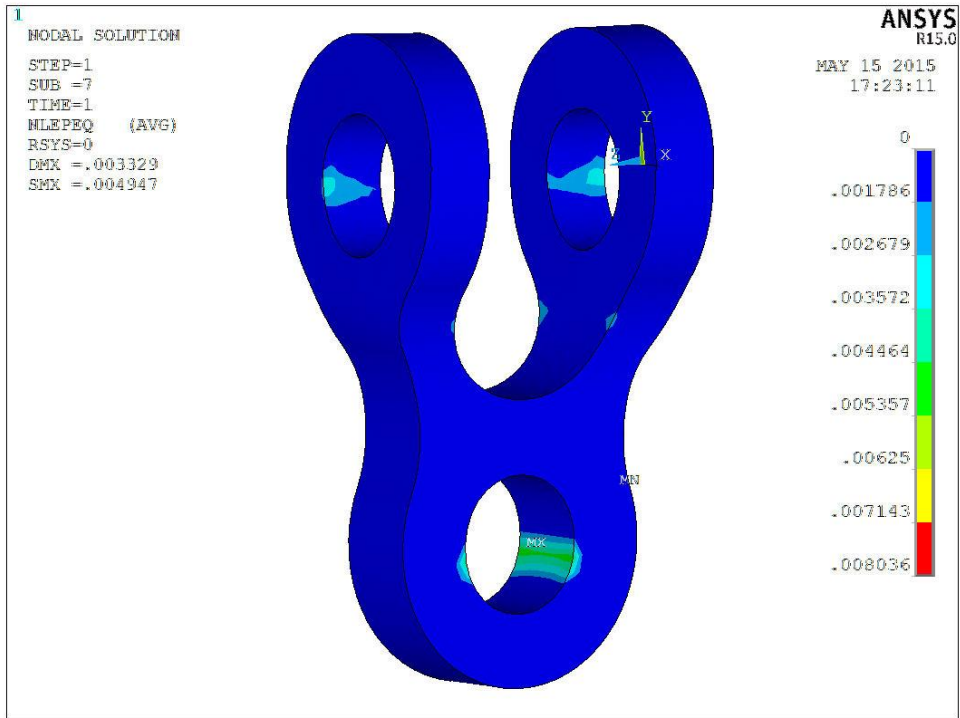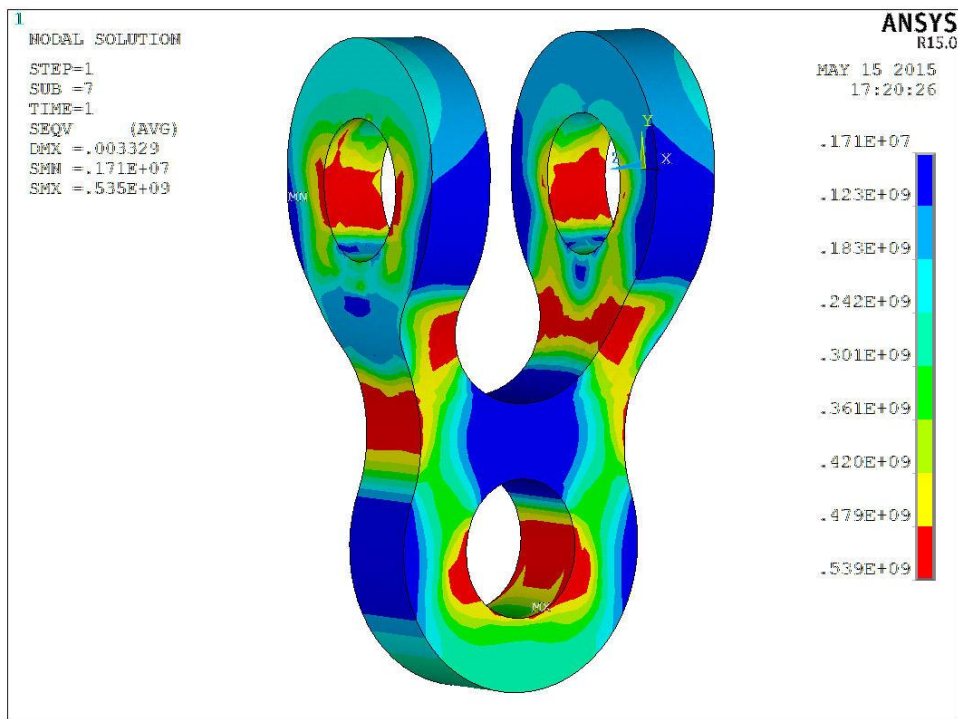
**Figure H - 3: The equivalent plastic strain result for the new connecting link with lugs, washers and rings – MBLx1.1 condition.**



**Figure H - 4: The von Mises result for the new connecting link with lugs, washers and rings – MBLx1.1 condition.**

**Appendix I**

**New connecting link with lugs, washers and rings**
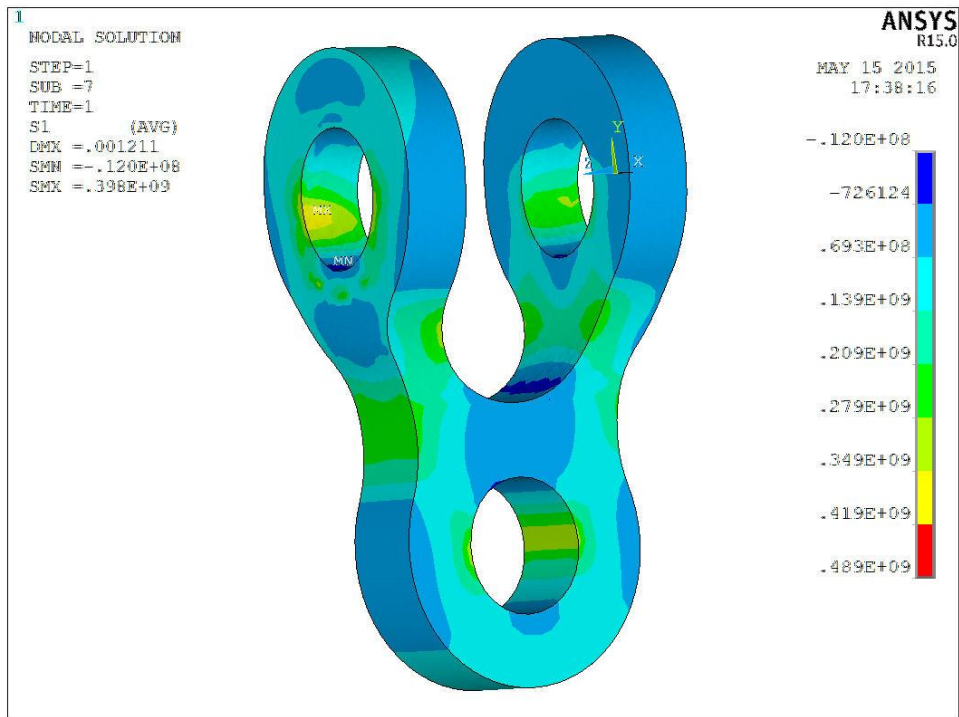
**ULS condition**

**Figure I - 1: Maximum principal stress in the new connecting link with lugs, washers and rings – ULS condition.**
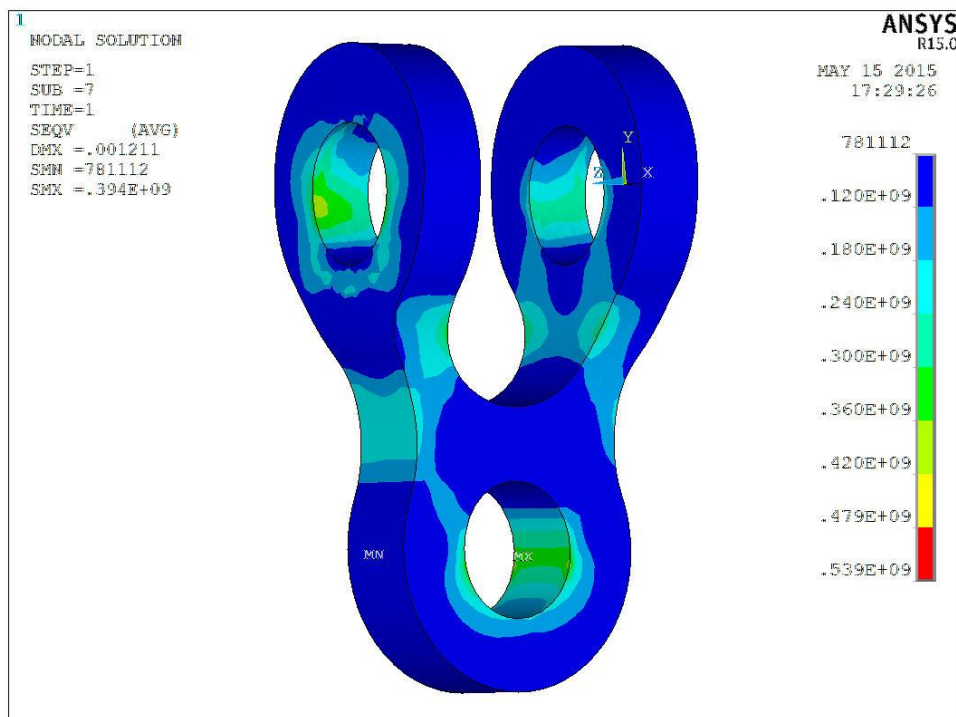


**Figure I - 2: The von Mises stress result in the new connecting link with lugs, washers and rings – ULS condition.**

**Appendix J**

**The results for the verification of the mesh applied**
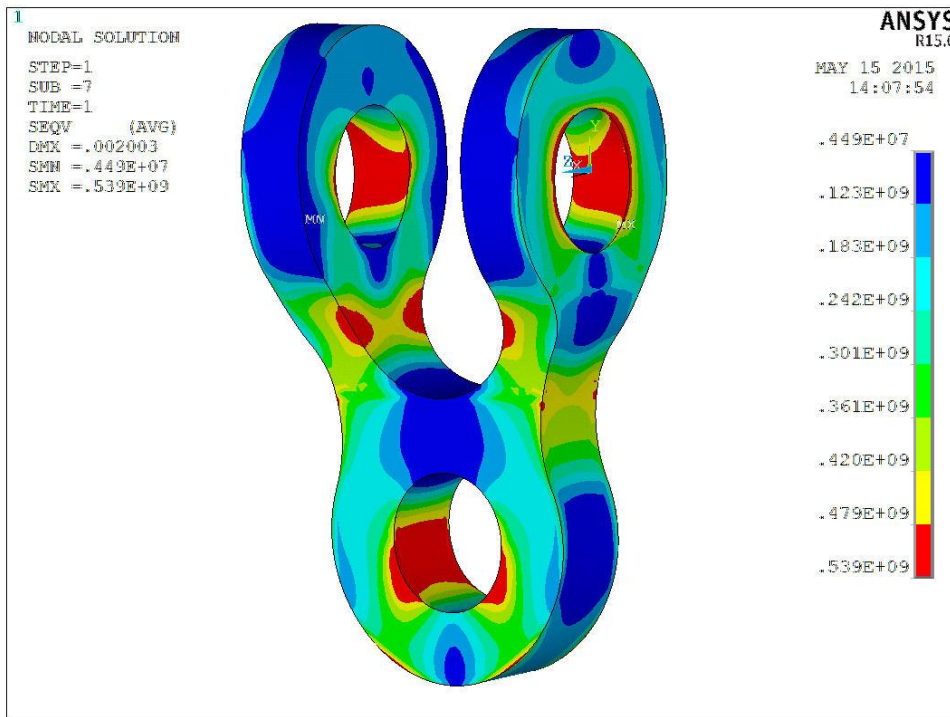
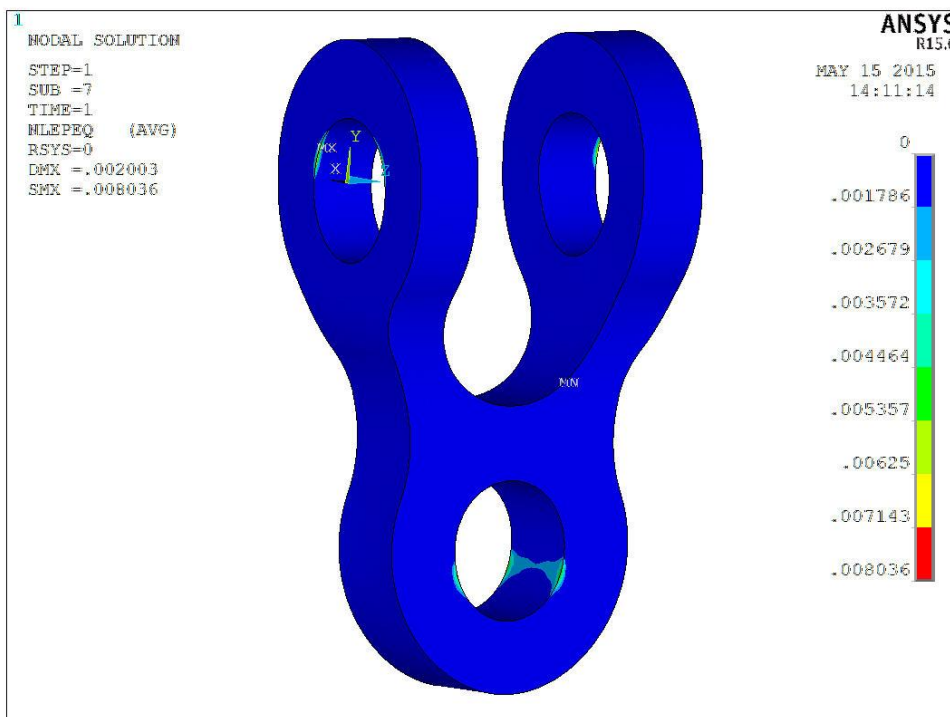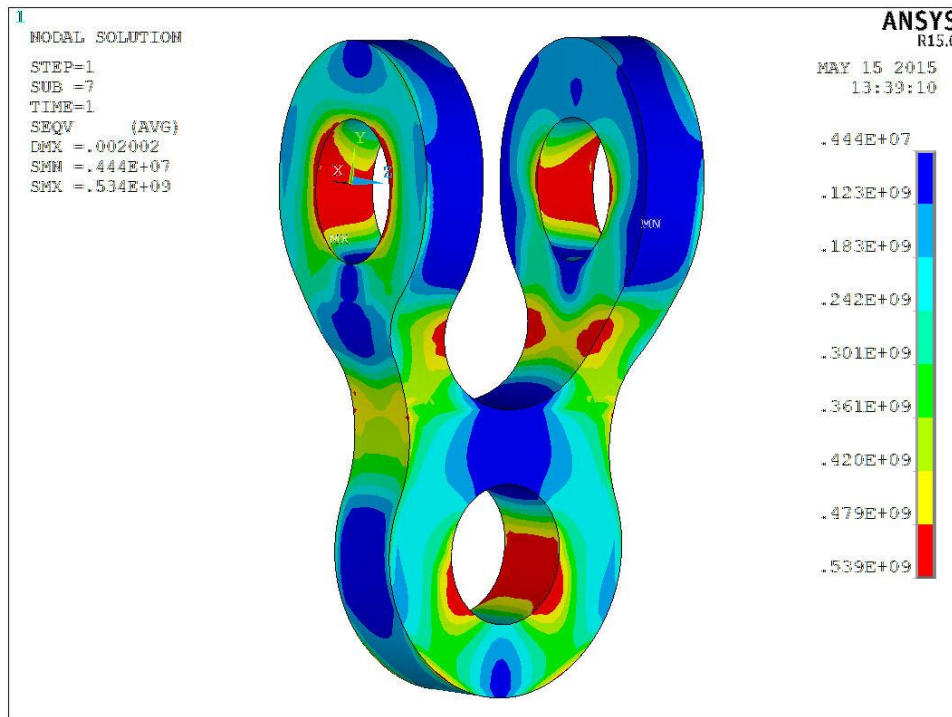**Figure J - 1: The von Mises stress result for the model with element size = 15 mm**



**Figure J - 2: The equivalent plastic strain result for the model with element size = 15 mm**

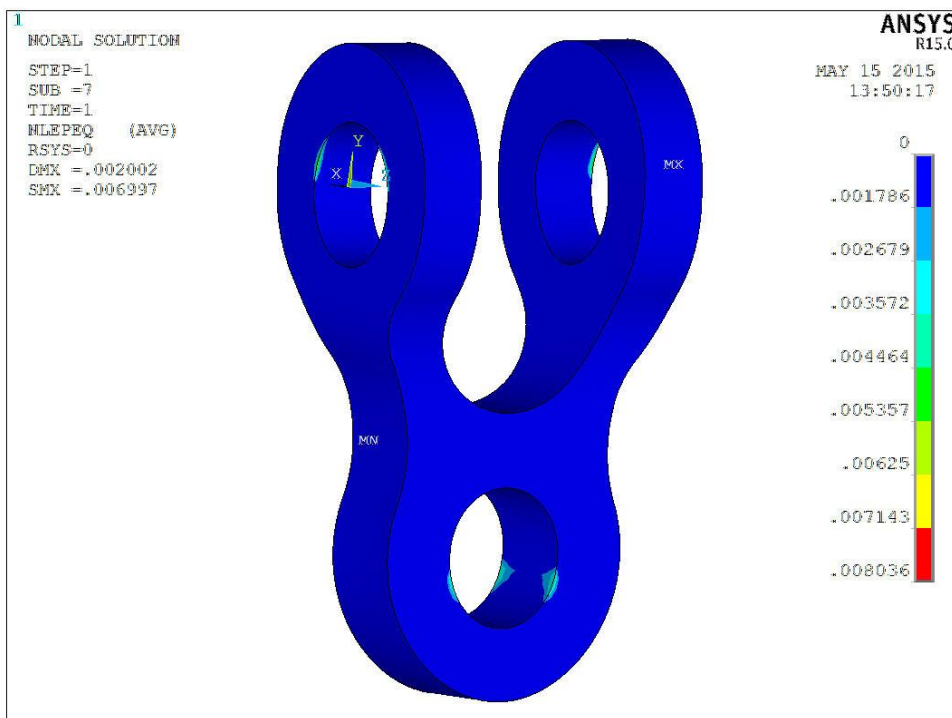**Figure J - 3: The von Mises stress result for the model with element size = 20 mm**



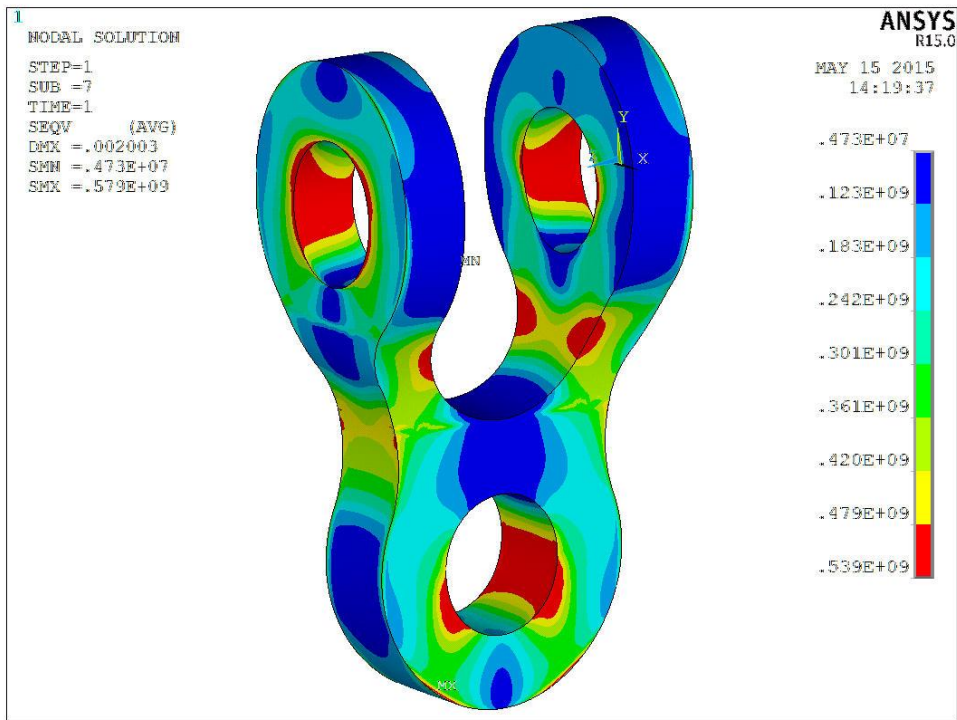**Figure J - 4: The equivalent plastic strain result for the model with element size = 20 mm**

121

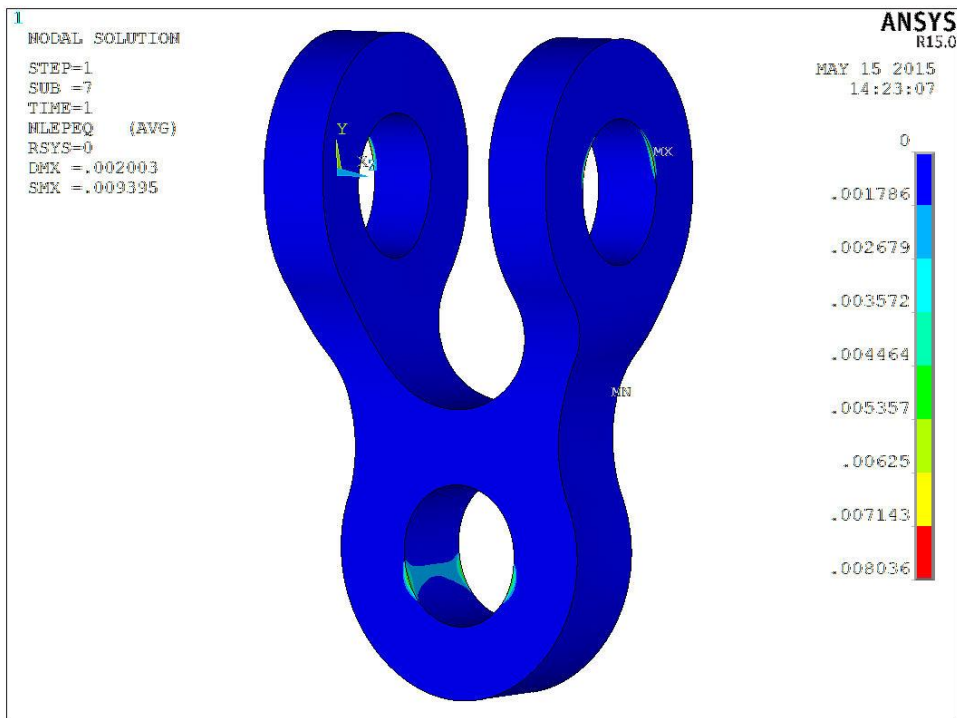**Figure J - 5: The von Mises stress result for the model with element size = 10 mm**



**Figure J - 6: The equivalent plastic strain result for the model with element size = 10 mm**